# Deep Brine Aquifers in the Palo Duro Basin:
## Regional Flow and Geochemical Constraints

by
R. L. Bassett and M. E. Bentley

1983

## BUREAU OF ECONOMIC GEOLOGY

QAe4027

Report of Investigations No. 130

# Deep Brine Aquifers in the Palo Duro Basin:
Regional Flow and Geochemical Constraints

by
R. L. Bassett and M. E. Bentley

assisted by
E. A. Duncan
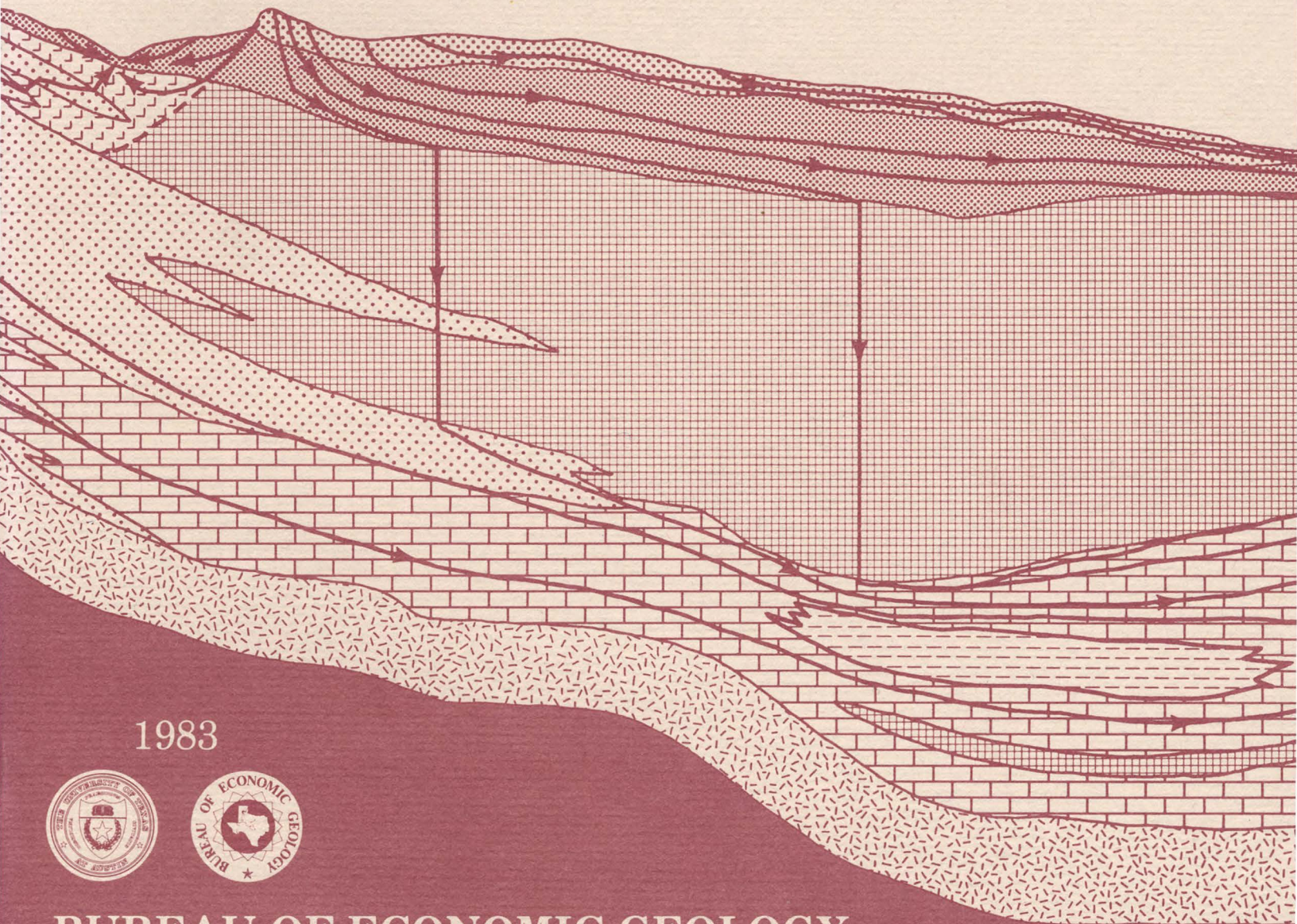
1983

## BUREAU OF ECONOMIC GEOLOGY

W. L. Fisher, Director
The University of Texas at Austin
Austin, Texas 78712

# CONTENTS

## Figures

# Tables

# ABSTRACT

Geologic characterization of evaporite deposits as potential host rocks for burial of radioactive waste must include hydrogeologic investigations at both local and regional scales. The Palo Duro and Dalhart Basins of Texas contain candidate salt deposits that are underlain by shelf carbonates and fan-delta sandstones. These basins are ancient intracratonic elements exhibiting regional eastward flow in the deep brine aquifers. Pressures in these aquifers are "subnormal"; however, the major component of flow appears to be parallel to bedding, owing to the low permeability of the overlying evaporite strata in the central part of the basin.

Salinity values computed from geophysical logs or obtained from chemical analyses indicate only small aberrations from a regional average salinity for brines in carbonate rocks and sandstones of Late Pennsylvanian and Early Permian age. Brine composition is derived by reaction with the host rock, obtaining salinity primarily from evaporite facies and, at present, apparently follows the calcite phase boundary. Brines may also be near equilibrium with anhydrite except in regions where sulfate reduction has generated hydrogen sulfide. Evidence of ion exchange is tenuous; however, clastic sediments predominate in the western part of the basin, early in the flow path, and a significant reduction in the molar ratio of sodium to chloride is observed in many samples. Substantial outgassing of carbon dioxide ($CO_2$) and oxidation of ferrous iron appear to have occurred as the samples were collected by industry during wildcat drilling. Mass transfer computer programs have been used to determine the most probable in situ brine composition. Support for the validity of the computed equilibrium state is the correlation between the values of partial pressure of carbon dioxide ($P_{CO_2}$) calculated for the brines and the $P_{CO_2}$ observed in adjacent natural gas reservoirs.

*Keywords: aquifers, computer modeling, drill-stem-test analysis, Early Permian, geochemistry, hydrogeology, Late Pennsylvanian, nuclear waste, Palo Duro Basin, Permian Basin, Texas*

# INTRODUCTION

Locating and characterizing geologic sites for burial of high-level commercial radioactive waste entails a multidisciplinary approach. The Bureau of Economic Geology (BEG) of The University of Texas at Austin is responsible for investigating all aspects of the geology and hydrology of the Palo Duro and Dalhart Basins of Texas. The results will be used by the U.S. Department of Energy (DOE) to determine if these basins are suitable for disposal of nuclear waste in Permian salt formations. Predictions of the long-term behavior of a mined geologic nuclear waste repository will be based on knowledge of the ground-water hydrology of the environment surrounding the proposed site. Transportation by ground water is by far the most likely mechanism by which radionuclides could reach the biosphere from an underground repository. The physical and hydrologic framework of the region is established by integrating the results of studies in stratigraphy, structure, economic resources, surface processes, geochemistry, and hydrology.

Recently the hydrogeology of deep, saline aquifers has received increased attention from researchers investigating a variety of topics, including petroleum migration and entrapment, disposal of liquid wastes, desalinization, origins of oil field brines, and regional fluid flow. Consequently, a number of benchmark papers describe regional hydrogeologic systems, such as the investigation of the San Juan Basin (Berry, 1958), the Permian Basin (McNeal, 1965), the Paradox Basin (Hanshaw and Hill, 1969), the Western Canada sedimentary basin (Hitchon, 1969a, b; Hitchon and Hayes, 1971; Tóth, 1978), the Australian Surat Basin (Hitchon and Hayes, 1971), and the Illinois Basin (Bond, 1972).

1

Geochemical studies such as those by Hitchon (1963a, b, c), White (1965), Clayton and others (1966), Rittenhouse (1967), Carpenter and Miller (1969), Collins (1975), and Carpenter (1978) have been pivotal in describing water/rock interactions in deep formation brines.

Emerging from many of these studies is the concept that the potential distribution, and therefore flow, in mature compacted basins may be significantly determined by the surface topography and resultant configuration of the top of the saturated zone (Tóth, 1978). This conclusion indicates that strata usually considered to be impermeable may actually permit vertical and cross-formational flow sufficient to transmit fluid pressure from shallow to much deeper flow systems. These studies also suggest that brines are actively reacting with host rocks in sedimentary basins. Depending on the nature of the basin fill (for example, whether the fill is evaporite, carbonate, or clastic), the host rock actively modifies the composition of the brine as it moves along the flow path.

Hydrologic interpretation of the Palo Duro and Dalhart Basins is limited by the same constraints that qualify these basins as potential repository sites, specifically, the low well density and the low resource potential. Petroleum exploration activities provide the primary, if not the exclusive, source of pressure measurements for the deep aquifers, as well as the chemical determinations of formation brines.

Exploration for hydrocarbons in the Palo Duro and Dalhart Basins historically has been nonproductive; consequently, the amount of subsurface data is severely limited. Hydrologic conclusions are drawn both from wildcat well data available for the basins of interest and from information obtained from the basin margins and adjacent basins that are petroliferous. This report describes the first phases in a regional study of deep ground-water hydraulics and dominant geological constraints on brine compositions. Particular emphasis is placed on the Wolfcamp carbonate aquifers of Early Permian age. Information derived from these and other geological investigations is being further refined with data from additional drilling and will be presented elsewhere (Bassett and Bentley, in press). Nevertheless, preliminary characterization is needed now to evaluate these basins as candidates for waste isolation. The Palo Duro Basin is the focus of this investigation. Detailed discussion of the Dalhart Basin is deferred owing to the sparse data base and the fact that the hydrogeology of the two basins can be treated independently.

## HYDROGEOLOGIC FRAMEWORK

The Palo Duro and Dalhart Basins are shallow intracratonic basins, two of the several subbasins composing the larger Permian Basin. The Palo Duro Basin is asymmetrical; the greatest thickness of sediment (about 10,000 ft [3,050 m]) occurs just north of the Matador Arch (fig. 1). The extreme hydrologic inhomogeneity of the basins results from long-lived cycles of different styles of sedimentation. Relatively permeable formations are vertically separated by a thick interval of middle and Upper Permian evaporites and fine-grained red beds that effectively divides the sedimentary sequence into deep and shallow flow systems.

The relation between stratigraphic and hydrogeologic divisions (Tóth, 1978) is shown in table 1. The hydrogeologic elements were designated according to their relative water-conducting or water-retarding character. Several of the hydrogeologic elements are composed of generally permeable lithologies (sandstone, dolomite) interbedded with mudstone; in this case the appellation of "aquifer" or "aquitard" was based on the properties of the more permeable strata. For this report, hydrogeologic units (table 1) are composed of one or more of the hydrogeologic elements. Thus, the units represent assemblages of vertically contiguous strata that have different primary lithologies but the same general hydraulic properties. The permeabilities shown in table 1 are representative values derived from the literature or determined in this study by analysis of drill-stem tests.

The apparent upper stratigraphic limit of the deep-basin brine aquifers coincides with the top of the Wolfcamp (Lower Permian) dolomite (table 1). Most of the pre-Leonardian deep-basin brine aquifer is composed of open-marine platform carbonates and fluvial-deltaic arkosic sandstones
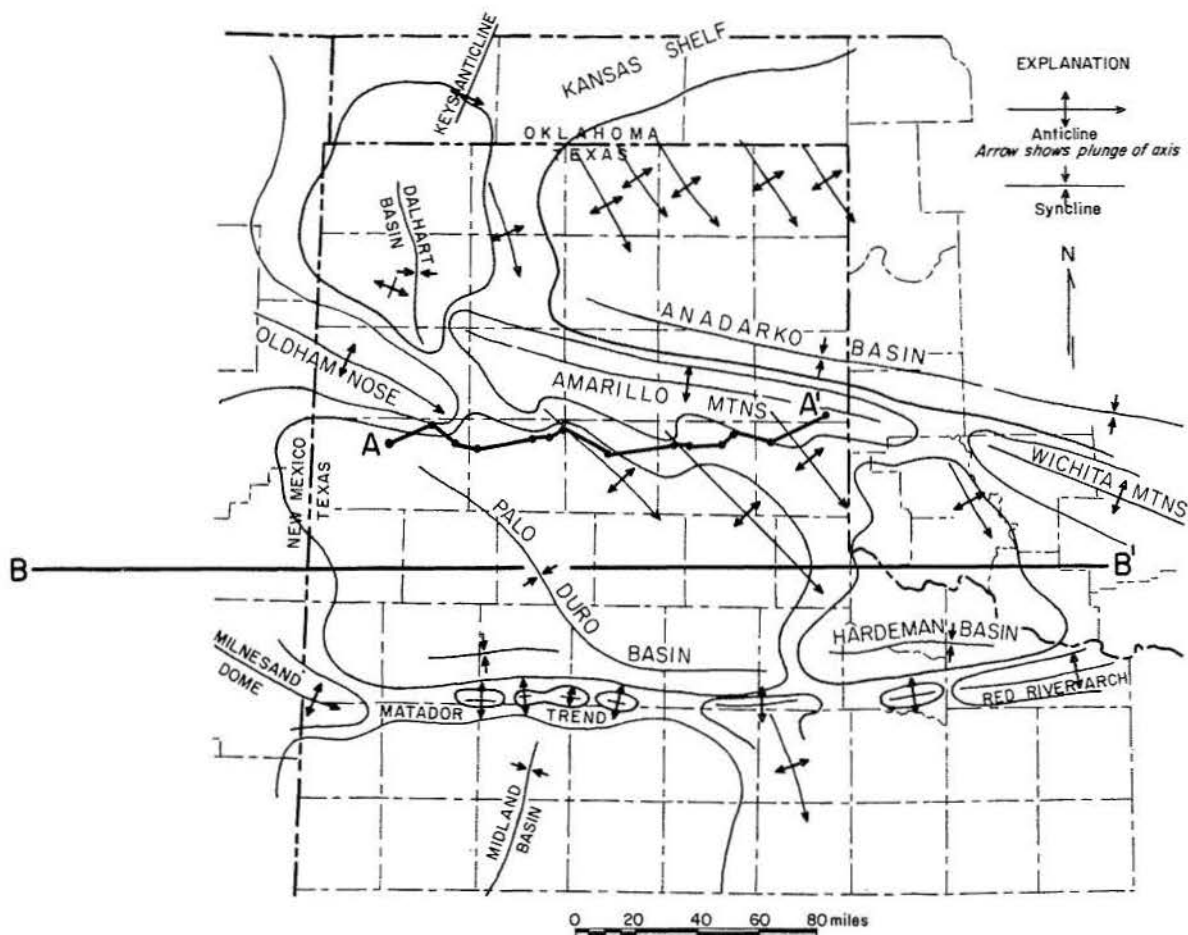
**Figure 1.** *Location of study area and cross sections (see figs. 5 and 8). Structural elements of the Texas Panhandle from Nicholson (1960).*

(granite wash) interbedded with mudstone. No major lithic change marks the Pennsylvanian-Permian boundary; throughout this time the nature and location of different depositional environments was strongly influenced by syndepositional tectonism that was actively shaping the basin. The distribution of sandstone aquifers was controlled by erosion of faulted granitic and gabbroic Precambrian basement highlands that formed the basin boundaries (figs. 1 and 2). Fan-delta sandstones emanate from major sediment-source areas such as the Amarillo Uplift to the north and the Oldham Nose and Sierra Grande Uplift to the northwest (figs. 1 and 3). Other deltaic deposits extend into the basin from the northeast; those were supplied by sediments eroded in the Wichita Mountains of

Oklahoma (Handford and Dutton, 1980). Basinward from these peripheral sandstones and intertonguing with them are shelf carbonates that themselves grade basinward into thicker, more vertically persistent shelf-edge carbonate buildups that bordered the central basin (figs. 2 and 4). As subsidence diminished in late Wolfcamp time, shelf-margin carbonates had prograded across the mud-filled central basin to form a basinwide shelf-carbonate system (fig. 2). Wolfcamp carbonates were eventually deposited over the previously emergent arches and uplifts that mark the boundaries of the basin.

Although tectonic controls produced irregular sedimentation patterns and lateral lithic changes, the deep-basin brine aquifer (table 1) exhibits vertically uniform hydraulic heads and similar

3

*Table 1. Generalized stratigraphic column, depositional environment, and general hydrologic properties, Palo Duro Basin.*

| System | Series | Group | General lithology and depositional setting | Hydrogeologic element | Hydrogeologic unit | Approximate permeability (gpd/ft²) | Relative permeability |
|---|---|---|---|---|---|---|---|
| Quaternary | | | Fluvial and lacustrine clastics | Ogallala · aquifer | Upper aquifer | 200 [a] | 10⁸ |
| Tertiary | | | | | | | |
| Cretaceous | | | Nearshore marine clastics | | | | |
| Triassic | | Dockum | Fluvial deltaic and lacustrine clastics and limestones | Dockum aquifer | | 2-20(?) [b] | 10⁶-10⁷(?) |
| Permian | Ochoa | | Salt, anhydrite, red beds and peritidal dolomite | Evaporite aquitard | Evaporite aquitard | 2 x 10⁻⁶ [c] | 1 |
| | Guadalupe | Artesia | | | | | |
| | | Pease River | | | | | |
| | Leonard | Clear Fork | | | | | |
| | | Wichita | | | | | |
| | Wolfcamp | | Shelf and platform carbonates, basin shale and deltaic sandstones | Wolfcamp carbonate aquifer | Deep-basin brine aquifer | 2 x 10⁻² [d] | 10⁴ |
| Pennsylvanian | | | | Pennsylvanian carbonate aquifer | | | |
| | | | | Upper Paleozoic granite wash aquifer | | | |
| | | | Basin shale aquitard | Basin shale aquitard | | | |
| Mississippian | | | Shelf limestone and chert | Lower Paleozoic carbonate aquifer | | | |
| Ordovician | | Ellenburger | Shelf dolomite | | | | |
| Cambrian | | | Shallow marine (?) sandstone | Lower Paleozoic sandstone aquifer | | | |
| Precambrian | | | Igneous and metamorphic | Basement aquiclude | Basement aquiclude | 0 | 0 |

[a] Cronin and Wells (1960), Myers (1969), Cronin (1961)
[b] Stevens (1980, written communication)
[c] Geotechnical Engineers (1978)
[d] This study

permeabilities (for further discussion, see p. 10); therefore all pre-Leonardian formations were grouped together into a single hydrogeologic unit for this preliminary regional analysis.

Middle and Upper Permian strata consist almost entirely of halite, anhydrite, dolomite, and fine-grained siliciclastic red beds, which grade southward into shallow-marine carbonates in the Midland Basin (Dutton and others, 1979). Together these formations compose the evaporite aquitard (table 1).

Overlying the Permian evaporites and red beds are the fluvial, deltaic, and lacustrine deposits of the Triassic Dockum Group and alluvial deposits of the Tertiary Ogallala Formation (fig. 5; table 1). The Dockum Group records the final stages of filling of the Permian Basin (McGowen and

others, 1979). Hydrogeologic information on Dockum sandstones is limited; wells over the basin tapping these beds have low specific capacities and produce waters that range widely in salinity. In contrast, potable ground water in the overlying Ogallala aquifer has been heavily pumped for agricultural, industrial, and domestic purposes. The Ogallala is an extensive alluvial apron of sand, gravel, and clay that extends eastward from the Rocky Mountains in the form of coalescing alluvial fan lobes (Seni, 1980). The upper part of the Ogallala Formation is cemented with calcium carbonate or "caliche" that forms the resistant "caprock" rim of the Caprock Escarpment along the eastern boundary of the High Plains (fig. 5).

Shallow, fresh ground waters generally move eastward under the influence of the regional
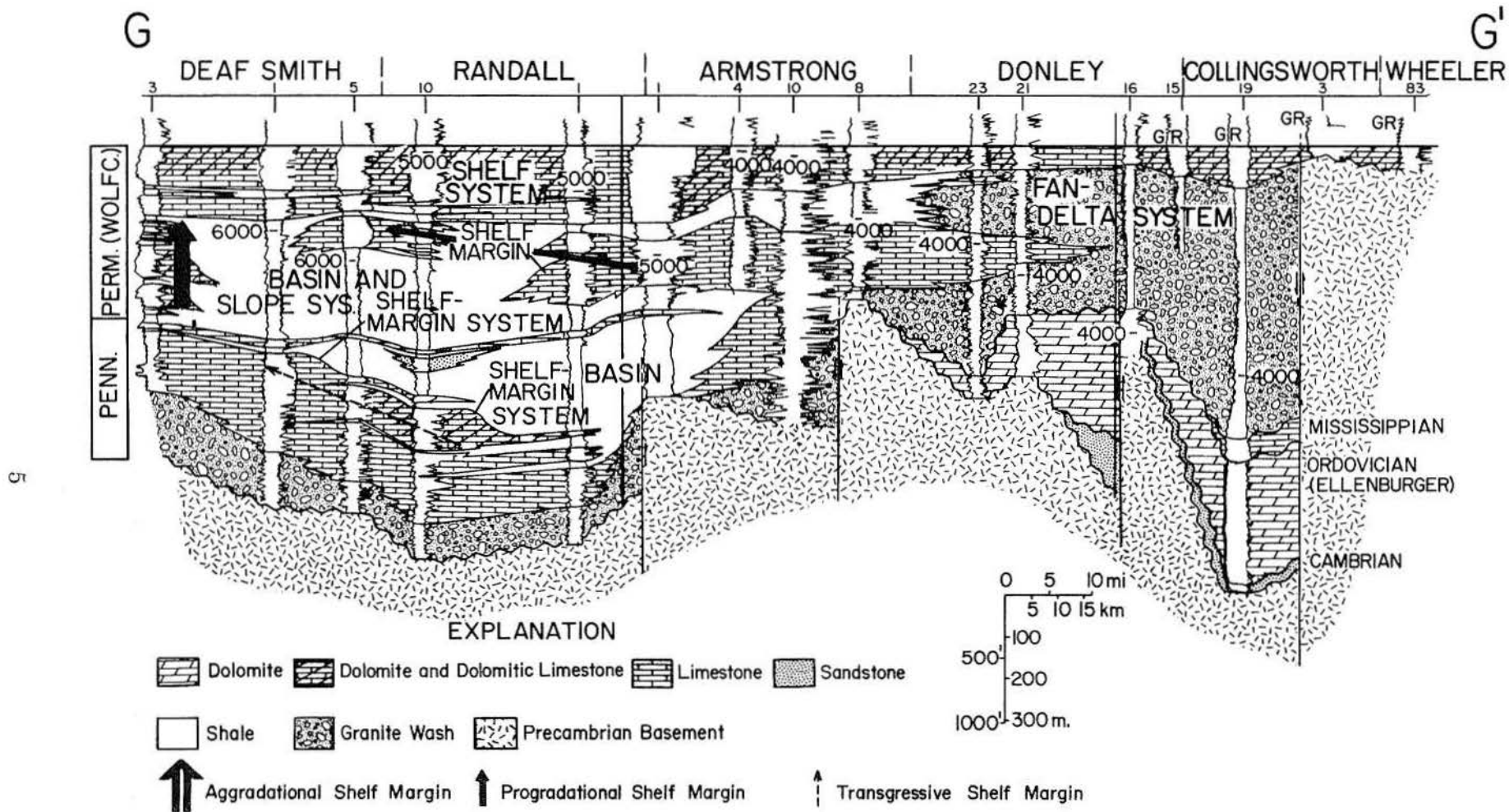
**Figure 2.** *East-west cross section showing stratigraphic framework and depositional systems of Pennsylvanian-Lower Permian strata. Datum is top of Wolfcampian Series. Well logs are gamma ray (GR), spontaneous potential (SP), and resistivity (Res). Depths are in feet. See figure 1 for location (from Handford and Dutton, 1980).*
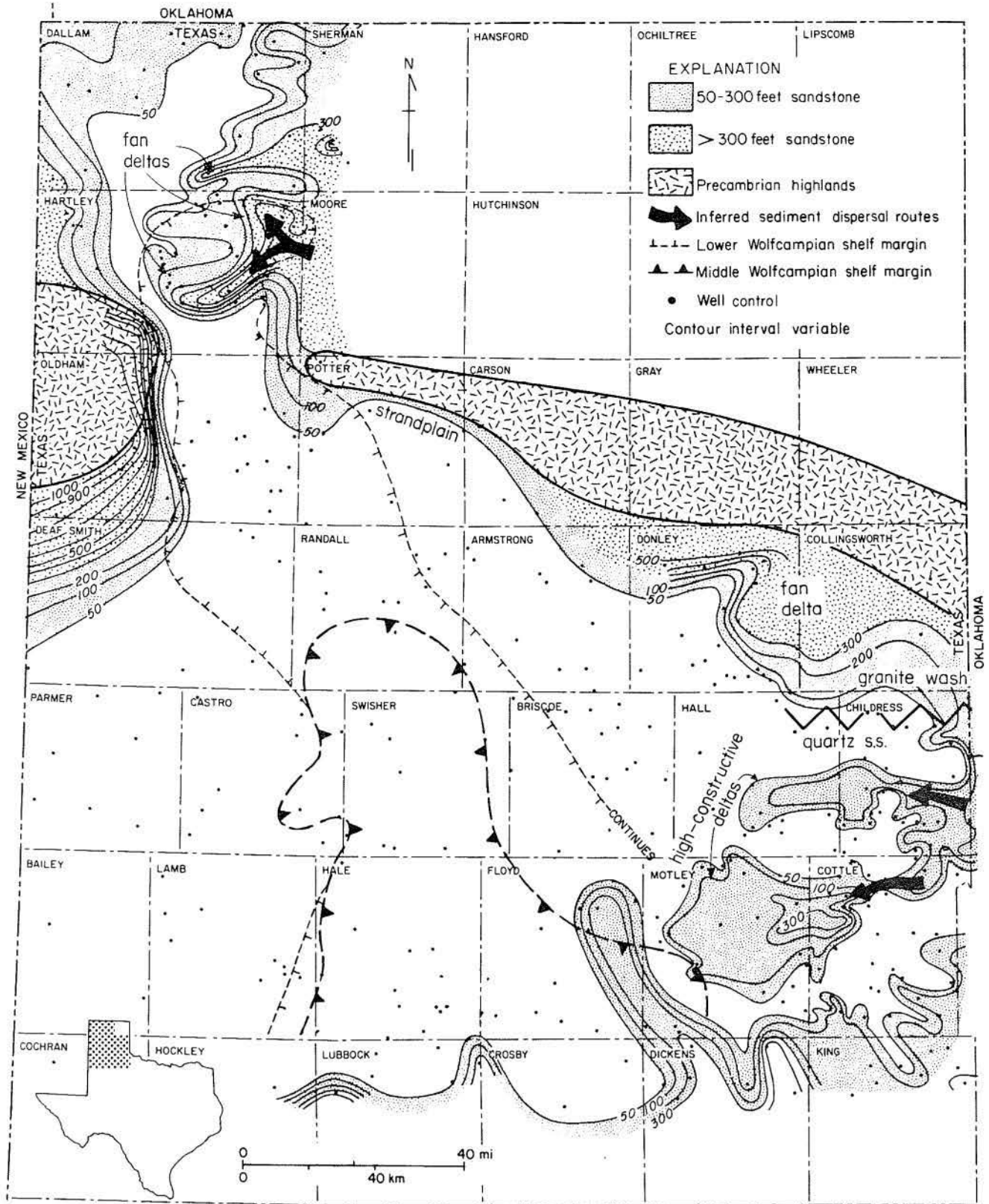
**Figure 3.** Net-sandstone map of Wolfcampian Series (from Dutton and others, 1979).

6
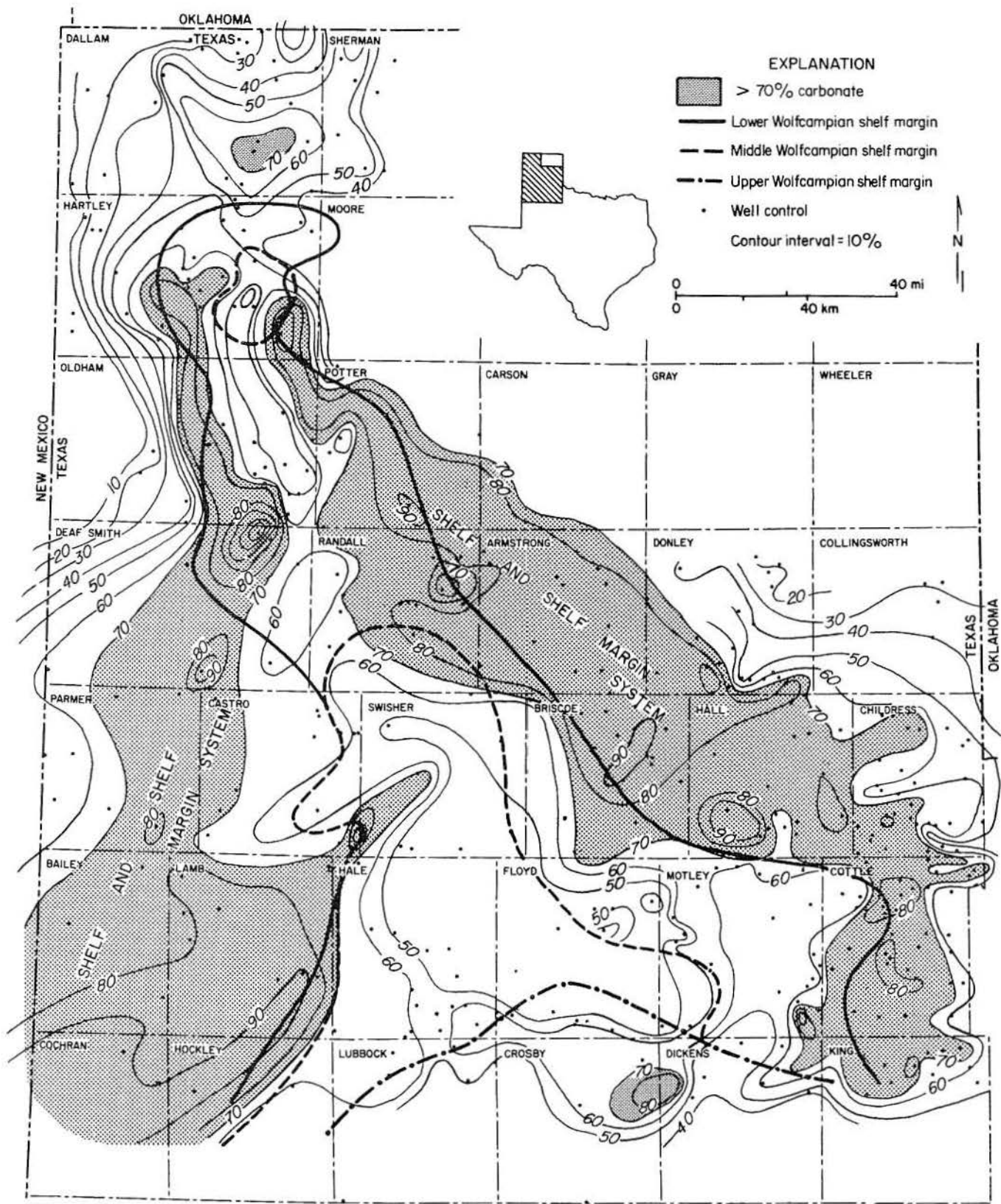
**Figure 4.** *Percent carbonate map of Lower Permian Wolfcamp strata. Position of the shelf margin is shown by dashed line (from Handford, 1980).*
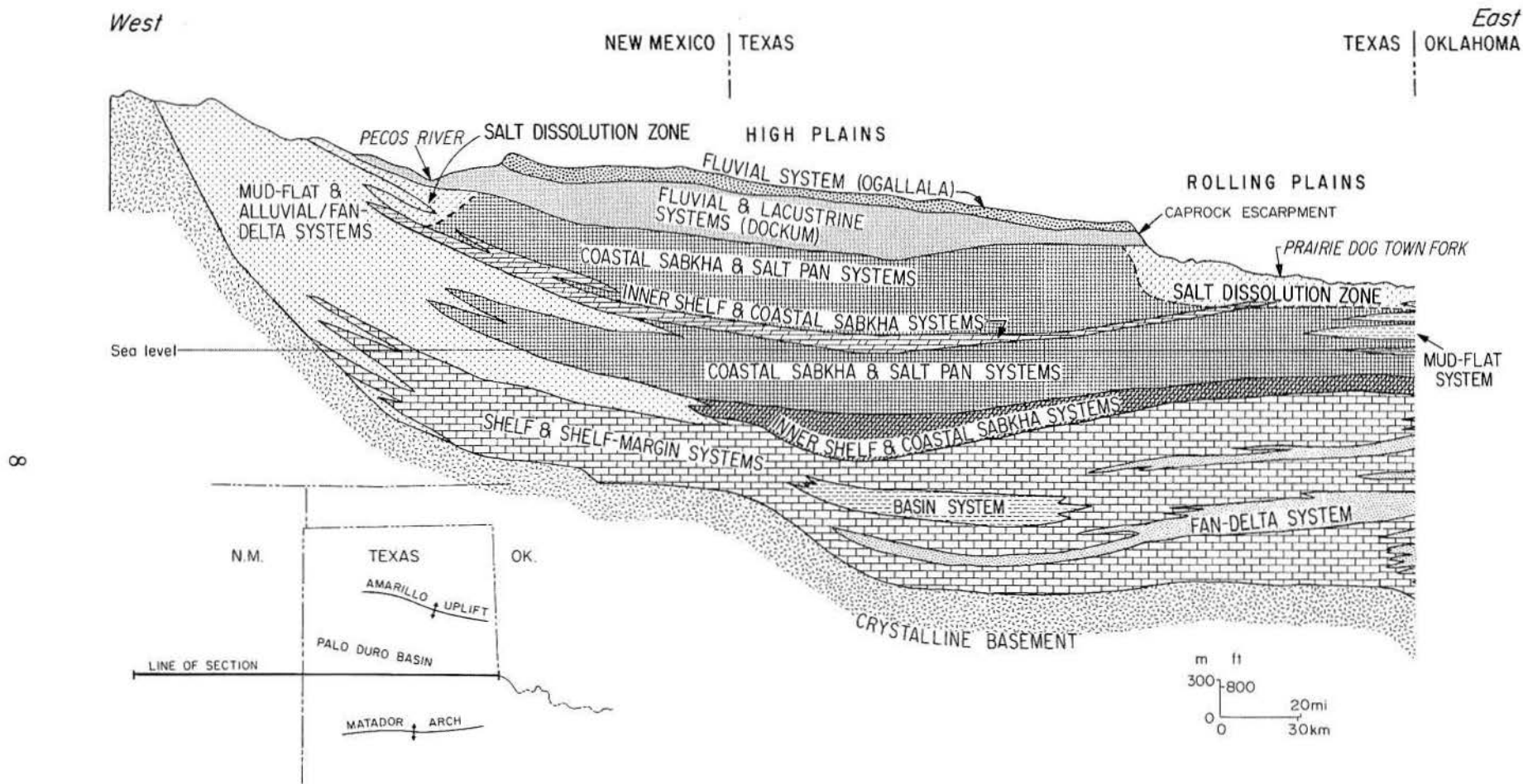
**Figure 5.** *Regional east-west cross section illustrating spatial relations among the major depositional systems in the Palo Duro Basin.*

structural and topographic dip (Cronin and Wells, 1960; Cronin, 1961; Gutentag and Weeks, 1980; Weeks and Gutentag, 1981; Texas Department of Water Resources, in press). Some of this water discharges as springs along the Caprock Escarpment (fig. 5). The middle and Upper Permian evaporite aquitard beds crop out east of the Caprock Escarpment in the Rolling Plains region, and here the weathered sediments yield moderate supplies of water for agriculture. In this Rolling Plains area, dissolution of halite and resultant collapse and disturbance of bedding have enhanced the permeability and porosity of overlying beds (Gustavson and others, 1980a). Salt dissolution, however, has led to formation of saline seeps and springs along eastward-draining stream courses, degrading the quality of surface waters for tens of miles downstream (Allen and others, 1971; Leifeste and others, 1971).

# HYDROLOGY OF THE
_ DEEP-BASIN FLOW SYSTEM _

## Sources of Hydraulic Data

Studies of deep, saline waters typically must rely on a more limited data base than do similar studies of shallow, more extensively developed aquifers because fewer wells are drilled to these depths and because hydraulic measurements are more difficult to obtain. The data used in this study came almost exclusively from the results of drill-stem tests (DST) conducted in petroleum wildcat wells, and from bottom-hole pressures measured in oil fields. Since there is no petroleum production in the central Palo Duro Basin, accurately measured fluid pressures presumably approximate natural pre-stress conditions.

Properly conducted drill-stem tests can yield adequate values of transmissivity, can approximate equilibrium fluid pressure, and, under appropriate conditions, can provide the distance to aquifer boundaries. During a typical drill-stem test, a section of the hole is isolated from the column of drilling mud by packers attached to a string of drill pipe. A valve is opened and formation fluid flows through perforations and into the pipe, typically for 15 minutes to 2 hours. The valve is closed (the formation is "shut in") to

allow recovery of pressure in the formation. The time required for substantially complete pressure recovery is longer if permeability is low or if a large volume of fluid is removed. In many tests, reported final pressures are too low because of incomplete recovery owing to insufficient shut-in time. The calculated head, of course, will also be too low under such conditions. The trend of pressure build-up must be extrapolated to determine true formation-fluid pressure. Other, sometimes large, deviations from true pressures are caused by the mechanical and operational difficulties of drill-stem testing.

The most useful and accurate drill-stem-test information is obtained from the actual pressure/time charts recorded downhole. Proper performance of the test tools can be confirmed by visual inspection of these charts (Black, 1956); the valid records can then be analyzed to determine aquifer characteristics. A few complete pressure/time charts were available; these were analyzed to determine true formation-fluid pressures by extrapolation to infinite time and to obtain representative permeability values.

The pressure/time charts were analyzed according to methods outlined in Matthews and Russell (1967) and Earlougher (1977). Most of the pressure build-up data formed a straight line when plotted in semilog form, as predicted by the Horner (1951) method (appendix A). In many cases, the initial shut-in pressure (ISIP) extrapolated from data from the first shut-in period approximates the final shut-in pressure (FSIP) from the second pressure build-up. If these two pressures are equal, the aquifer tested may be relatively large, or "infinite acting" (Earlougher, 1977). The two principal causes of unequal shut-in pressures are depressuring (depletion) of a small, isolated aquifer by fluid removal and supercharging. Invasion of drilling mud can increase (supercharge) the pressure around the well bore before testing, especially if formation pressures are much lower than the pressure exerted by the column of drilling mud. In the Palo Duro Basin, the fluid pressures are generally less than hydrostatic (subnormal for a given depth), a condition that is conducive to supercharging. Numerous notations on sample logs of lost circulation of mud indicate that the combination of low formation pressures and high mud weight makes mud invasion common. A small number of the analyzed drill-stem tests showed anomalously high pressures

that may be due to supercharging; however, if the first flowing period is longer than five minutes, the supercharged condition is usually rectified. Depletion results in lowered pressures.

The number of derived permeability values is small, given the large volume of rock in the basin. Moreover, the permeability values measured in any given well are greatly dependent on the interval chosen for testing; these decisions are usually based on hydrocarbon shows rather than on other physical criteria such as high porosity indicated by electric logs. The most permeable parts of the deep formations may be untested. These data are summarized in appendix A.

Formation-fluid pressures were converted to an equivalent fresh-water head (specific gravity = 1.0). On the basis of estimates made from values of total dissolved solids (TDS), specific gravity of brines in the Palo Duro Basin ranges from about 1.05 to 1.13. The range of specific gravities is too small to cancel or to reverse the apparent directions of the calculated fresh-water head gradients (Bond, 1972).

The head map for the Wolfcamp aquifer was constructed principally from more than 400 pressure values reported in commercial digitized drill-stem-test summaries; 23 extrapolated pressures controlled the accuracy of the generalized head contours. Inspection or analysis of several pressure/time charts of the same drill-stem tests that reported anomalous pressure values showed that their rejection was justified. The most common errors were (1) insufficient shut-in time, probably owing to very low permeability, (2) clerical error in reporting pressures to the commercial drill-stem-test service, (3) tool failure, or (4) supercharging. Most of the differences between true and reported pressure values were small, low-side deviations apparently caused by slightly insufficient shut-in times. However, since horizontal pressure gradients in the Wolfcamp aquifer are great compared with the latter type of error, the data quality was sufficient to determine general magnitudes of pressures and of the resulting horizontal head gradients.

## Hydrodynamics

Computed fresh-water hydraulic heads in the Wolfcamp carbonate aquifer decline from west to east (fig. 6), reflecting the regional topographic

and structural dip away from the Rocky Mountains. Eastward decline of head values also occurs in brines in both the Midland Basin south of the study area (McNeal, 1965), and in the Midcontinent province to the north (Larson, 1971). At all test points in the Palo Duro Basin, the heads in aquifers below the Wolfcamp are similar. Although vertical leakage across aquitards may be significant owing to the large contact area between formations, locating where leakage may occur is difficult because of low density and unreliable data. Least-squares analysis of pressure and depth data from all uncorrected drill-stem-test reports yielded slopes equivalent to the pressure gradient in static or horizontally flowing typical brines (Bentley, 1981). Therefore, the assumption of predominantly horizontal flow in the basin appears valid.

The 19 calculated permeability values for Wolfcamp carbonates ranged from 0.03 to 44 md, with a mean of 5.3 md and a median of 0.77 md (appendix A, table A-1). Most values are between 0.1 and 10 md (fig. 7), and a value of 2 md was adopted for estimation of flow velocities. The Wolfcamp dolomite locally has higher permeability over the Amarillo Uplift in the Panhandle oil and gas field, where early postdepositional flushing by meteoric waters produced solution cavities sufficiently large to cause drill-bit drops several feet deep (J. Nicholson, personal communication, 1980).

Aside from the regional west-to-east fluid migration pattern, topography appears to exert little control on deep-basin circulation. A major topographic feature in the study area is the Caprock Escarpment (figs. 5 and 8), which has over 1,000 ft (305 m) of relief within a few miles. Head contours (fig. 6) do not correlate with this feature. Beneath the High Plains (west of the escarpment), deep-basin fresh-water heads are approximately 1,200 to 2,200 ft (366 to 671 m) below land surface, and east of the escarpment, heads in the same system occur at the level of the land surface. It is possible that present conditions may be transient and that pressures at depth may be slowly increasing due to hydraulic conditions imposed more recently by the younger, shallow systems.

The Panhandle field gas reservoir is capped by anhydritic limestone that forms the base of the overlying evaporite section. Initial fluid pres-

10
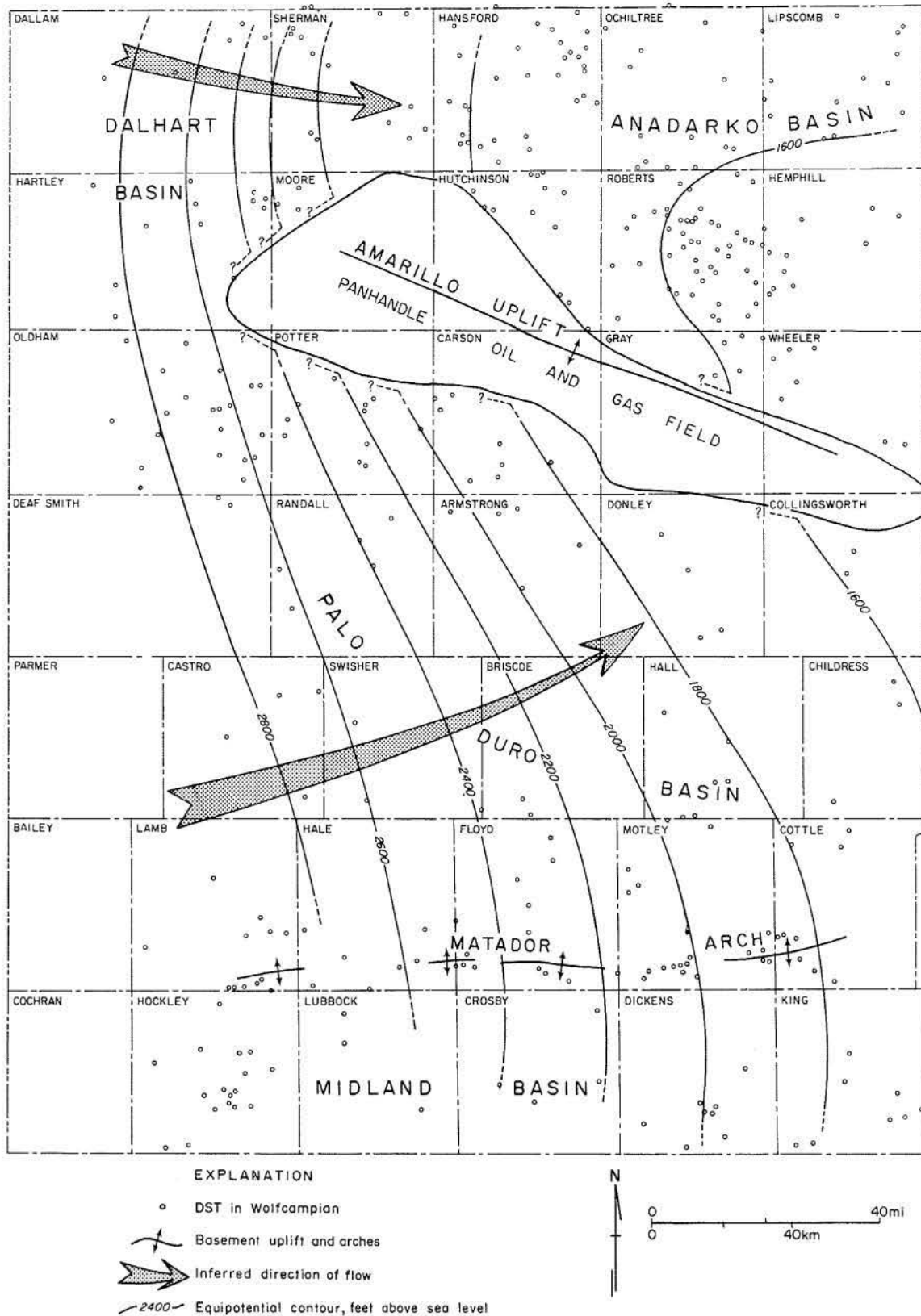
**Figure 6.** *Hydraulic head map, Wolfcamp aquifer, Texas Panhandle. Head contours interpreted from fresh-water head values calculated from uncorrected shut-in pressures. Low head values (1,000 ft) in the Panhandle oil and gas field appear to cut across regional trends and may represent relative hydraulic isolation of eastward-drained porous strata. Well locations not shown in the Panhandle field.*

11
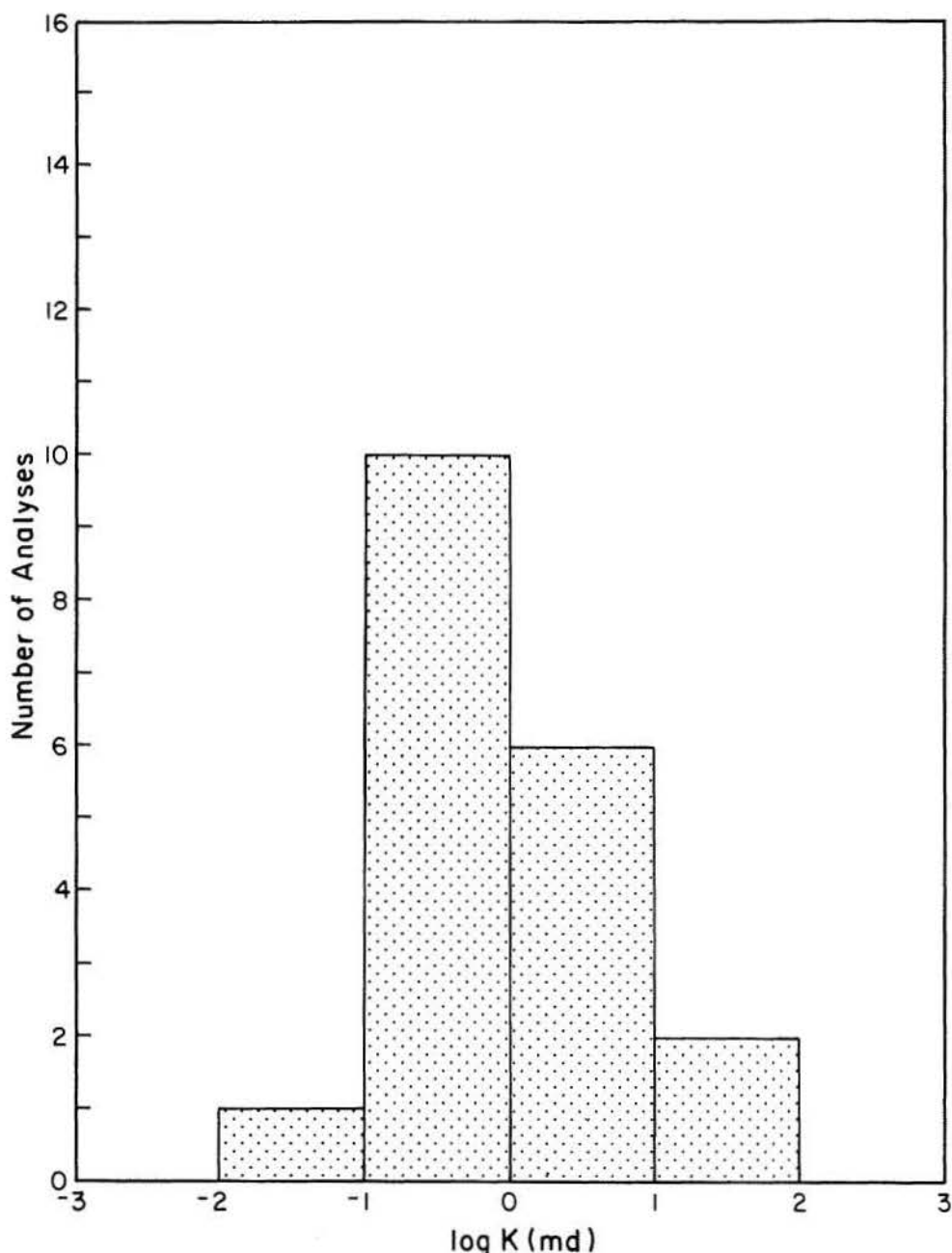
**Figure 7.** *Frequency distribution of the effective permeability in Wolfcamp carbonates determined by analysis of 19 drill-stem-test charts. Data range from 0.03 to 44 md, with a mean of 5.3 md and a median of 0.77 md (see table A-1).*

sure everywhere in the Panhandle field was approximately 435 psi (Rogatz, 1939), which is about 265 psi lower than in the brine-bearing rocks immediately adjacent to the field. This abrupt pressure differential is apparently caused by faults that effectively isolate the reservoir from laterally adjacent parts of the Wolfcamp aquifer.

## COMPOSITION OF DEEP-BASIN BRINES

### Sources of Chemical Data

Chemical compositions of fluids used in this investigation were obtained from petroleum
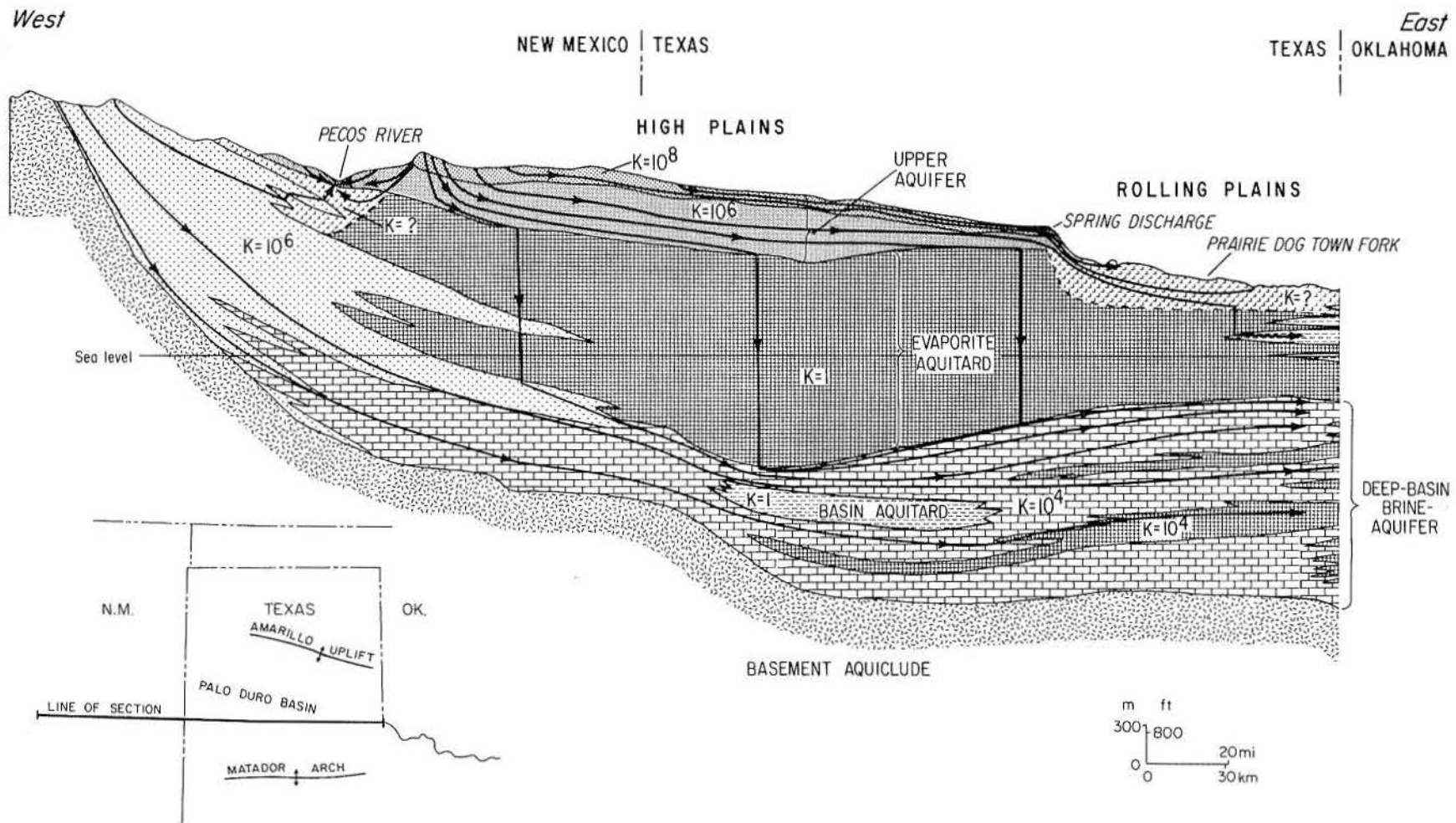
**Figure 8.** Regional east-west section approximately parallel to flow, illustrating the distribution of major hydrogeologic units (table 1) and their corresponding relative permeabilities (k). Flow lines are intended to describe conceptual flow patterns on the basis of head distribution and relative average permeabilities.

companies and from petroleum information companies. These analyses are predominantly from samples that were collected during wildcat drilling programs.

Brine compositions that most nearly represent the composition of the in situ formation fluid are from samples collected after a drill-stem test ended. Most tests of wildcat wells are conducted primarily to determine the presence of hydrocarbons and secondarily to determine reservoir permeability. During the recovery part of the test, fluid derived from a packed-off section passes through perforations in the drill-stem-test tool and enters the drill stem. The more sophisticated drill-stem-test tools contain sample chambers that allow collection of the last brine to leave the formation and enter the tool. More commonly, the sample is collected from the last string of pipe as it is removed from the drill hole after the test.

Samples of more questionable quality may be collected directly from a holding tank of a producing well or from the borehole by bailing. Obviously, such samples are collected under non-ideal conditions, and their usefulness for geochemical interpretation is severely limited. Analysis of minor and trace constituents is seldom done, and any such analysis would certainly be suspect owing to the likelihood of contamination from drilling fluids, hardware, or containment vessels.

Using several thousand chemical analyses from the Palo Duro and Dalhart Basins, we have deleted those for which (1) dilution with drilling fluid is suspected, (2) information indicates that the brine originated from a production or injection well in an enhanced recovery process, (3) either depth or location data are unavailable, or (4) the tested formation is unrelated to this study. The remaining data are subject to three types of error: (1) collection procedure, (2) sample preservation, and (3) analytical procedure.

Chemical compositions of formation brines historically have been found to have limited use by the petroleum industry. The industry requires only approximate information on brine composition to calibrate geophysical logs, to evaluate fluid compatibilities, to evaluate scaling and corrosion, and to make gross correlations of hydraulic connection in reservoirs. Consequently, sampling and preservation techniques generally have been commensurate with the intended use of the data, and the resulting values frequently are ill-suited for analysis of the geochemistry of a system.

Substantial outgassing of volatiles will occur as the fluid is brought to the surface and exposed to atmospheric conditions, unless special precautions are taken to prevent it. Our investigation indicates that formation brines in the region exhibit $CO_2$ partial pressures ($P_{CO_2}$) significantly higher than atmospheric pressure (fig. 9). The consequences of this are outgassing of $CO_2$ from the brine before analysis, elevation in pH, and possibly the precipitation of carbonate minerals in the sample container, as discussed in a subsequent section. The oxidation state of the sample will obviously be altered with the loss of $H_2S$ or the exposure to atmospheric oxygen. It is occasionally noted on reports of analyses that the samples appear rusty; this is most likely caused by ferrous iron oxidation and precipitation of hydrated ferric hydroxides in the sample bottle.

The composition of a brine generally is determined in a laboratory operated by the drilling company or in a commercial laboratory. Results are seldom presented with tabulated cation and anion balances. In addition, our computations reveal that many analyses balance exactly, indicating that one or more constituents are determined by difference. Of the 121 analytical results selected as acceptable for further interpretive work, few include more than major constituents (Na, K, Ca, Mg, $HCO_3$, $SO_4$, and Cl). Moreover, the sodium value commonly represents the sum of both potassium and sodium. Temperature, pH, and a few minor components ($H_2S$, Sr, Br, and Si) rarely are included. The data selected for this study are included in appendix B.

We tried to locate brine-producing petroleum wells within the Palo Duro Basin so that the results of complete analyses of brines could be presented in this study. The majority of oil fields are undergoing or have been subjected to some form of enhanced oil recovery treatment (such as chemical treatments or water flooding through reinjection). Such treatment is common in this region because of naturally low formation pressures. We concluded that successful sampling of representative formation brine was highly unlikely and that the available brine compositions obtained during wildcat exploration programs would be the most useful.

Well density within the basin is extremely sparse. Consequently, few chemical data are available from the central basin area; most are from marginal areas. A location map shows field location and brine-sample sources (fig. 9).

## Geophysical Data and Regional Salinity

Geologists at the BEG used more than 5,000 geophysical logs to interpret the stratigraphic sequences in the Palo Duro and Dalhart Basins (Dutton and others, 1979; Gustavson and others, 1980b). Electric logs are particularly useful for lithologic correlation, and spontaneous potential (SP) logs additionally may be used as an indicator of fluid resistivity (Keys and MacCary, 1971; Schlumberger, 1972). Resistivity of the formation water is measured relative to the resistivity of the borehole fluid, then converted to an equivalent resistivity (or salinity) of a sodium chloride solution. According to Keys and MacCary (1971), at least three assumptions must hold: (1) both fluids must be dominantly sodium chloride; (2) shales must be treated as ideal membranes; and (3) formation fluid and matrix should have a lower resistivity than borehole fluid. If these constraints are satisfied, then the following relation may be used:

$$SP = -K \log (Rm/Rw)$$

SP = deflection in SP log (mV)
K = 60 + 0.133 T
T = temperature at the formation depth (°F)
Rm = resistivity of the borehole fluid (ohm-m)
Rw = resistivity of the formation water (ohm-m)

Brines from the Palo Duro Basin appear to meet the above criteria. Information about drilling fluids tested at the well is given in the header of each log chart. Spontaneous potential logs from Wolfcamp carbonates or granite-wash facies that satisfied the prerequisites of the method were selected for computation. Resistivities (or salinities) were computed and the values converted to TDS as sodium chloride (g/L), then plotted on isopach maps of both Wolfcamp and granite-wash facies (figs. 10 and 11). Formation factors and computed salinities used in those figures are tabulated in appendix C. For comparison,

the values of dissolved solids from actual chemical analyses are also included on the map, and a reasonable similarity is apparent. The maps indicate that there is little need to correct the fresh-water head map for salinity difference (fig. 6), owing to the rather uniform salinity across the Palo Duro Basin. In the Anadarko Basin north of the Amarillo Uplift, higher salinities exist. This anomaly may be explained by the relative hydraulic isolation and long residence times. Hydraulic isolation is evidenced by overpressure in the deep Anadarko Basin east of the mapped area.

## GEOCHEMICAL CONSTRAINTS ON THE BRINE ENVIRONMENT

### Defining Reactions and Chemical Composition

Brines produced from Upper Pennsylvanian and Lower Permian formations in the Palo Duro Basin appear to be part of a continuous system, moving eastward under a gradient of less than 6.3 ft/mi (2 m/km). Lithostratigraphy below the evaporites in this basin is dominated by carbonates (limestone, micritic limestone, dolomite) and substantial intertongued arkosic clastic facies. Because of the regional nature of brine migration, the lateral continuity of carbonate facies, and the long residence and reaction times, it might be expected that the brine composition would reflect the composition of the host rock. Dissolved solids values from chemical determinations and geophysical data are similar; however, we know less about regional variations of individual concentrations.

Typical of sedimentary basins, brine composition is dominated by sodium chloride, and salinity is several times that of seawater. A number of mechanisms have been proposed to describe the evolution of brines, such as membrane filtration, dissolution of evaporites, or mixing with metamorphic or magmatic waters (Berry, 1958; White, 1965; Hanshaw and Bredehoeft, 1968a, b; Carpenter, 1978). Development of salinity in this basin is probably related to the presence of evaporites. Of incidental note is the absence of post-Paleozoic magmatic activity within the basin
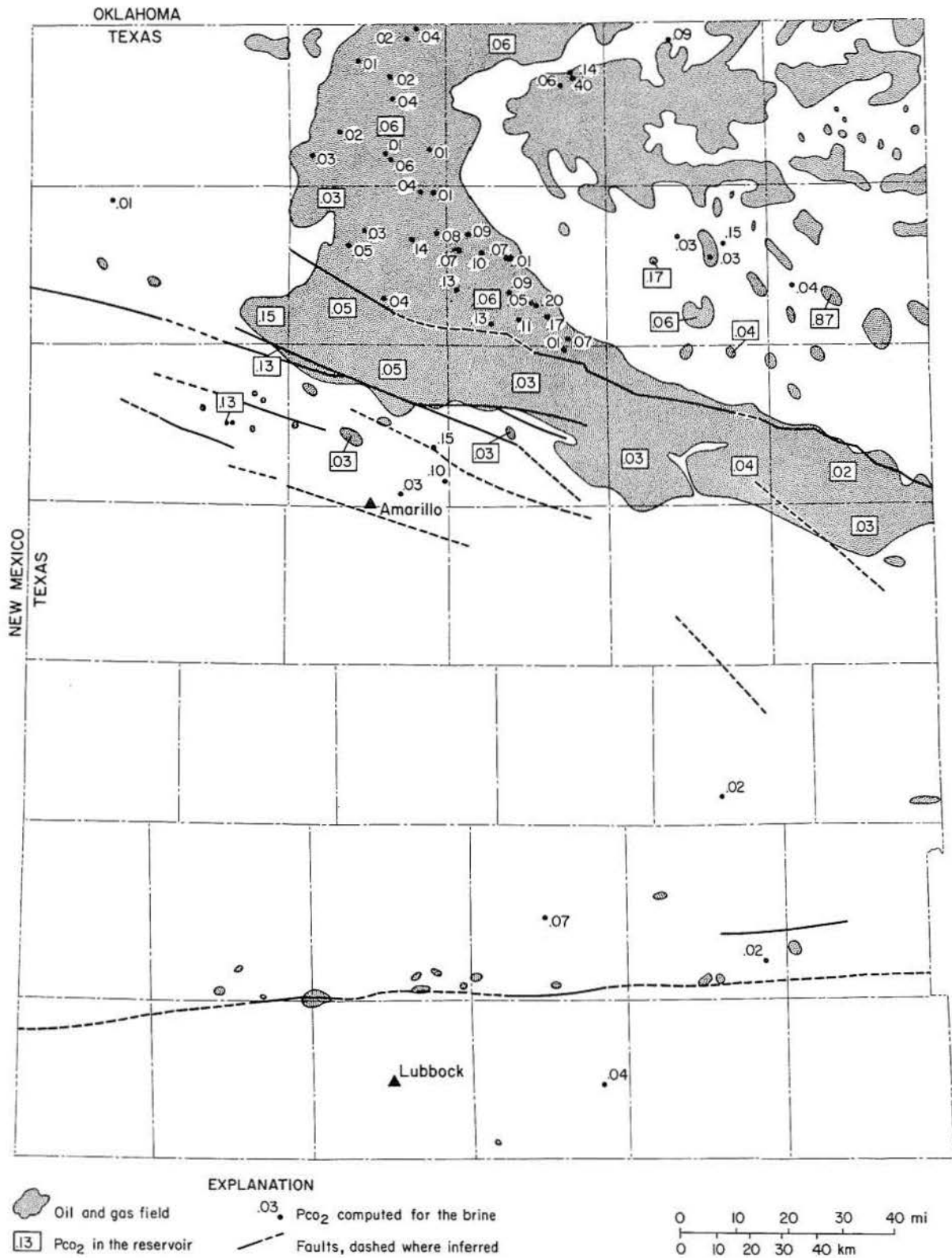
**Figure 9.** Location map showing (1) the $P_{CO_2}$ of oil and gas fields computed from analyses of gas samples (from Moore, 1976), and (2) the $P_{CO_2}$ computed from analytical results obtained from brine in wildcat and production wells. The distribution of oil and gas fields in the Dalhart and Palo Duro Basins is derived from Best (1961), Johnson (1976), Birsa (1977), Panhandle Geological Society (1961), Petroleum Information Corporation (1980), and the map files located at the Texas Railroad Commission. Structure information from A. Goldstein (written communication, 1981).
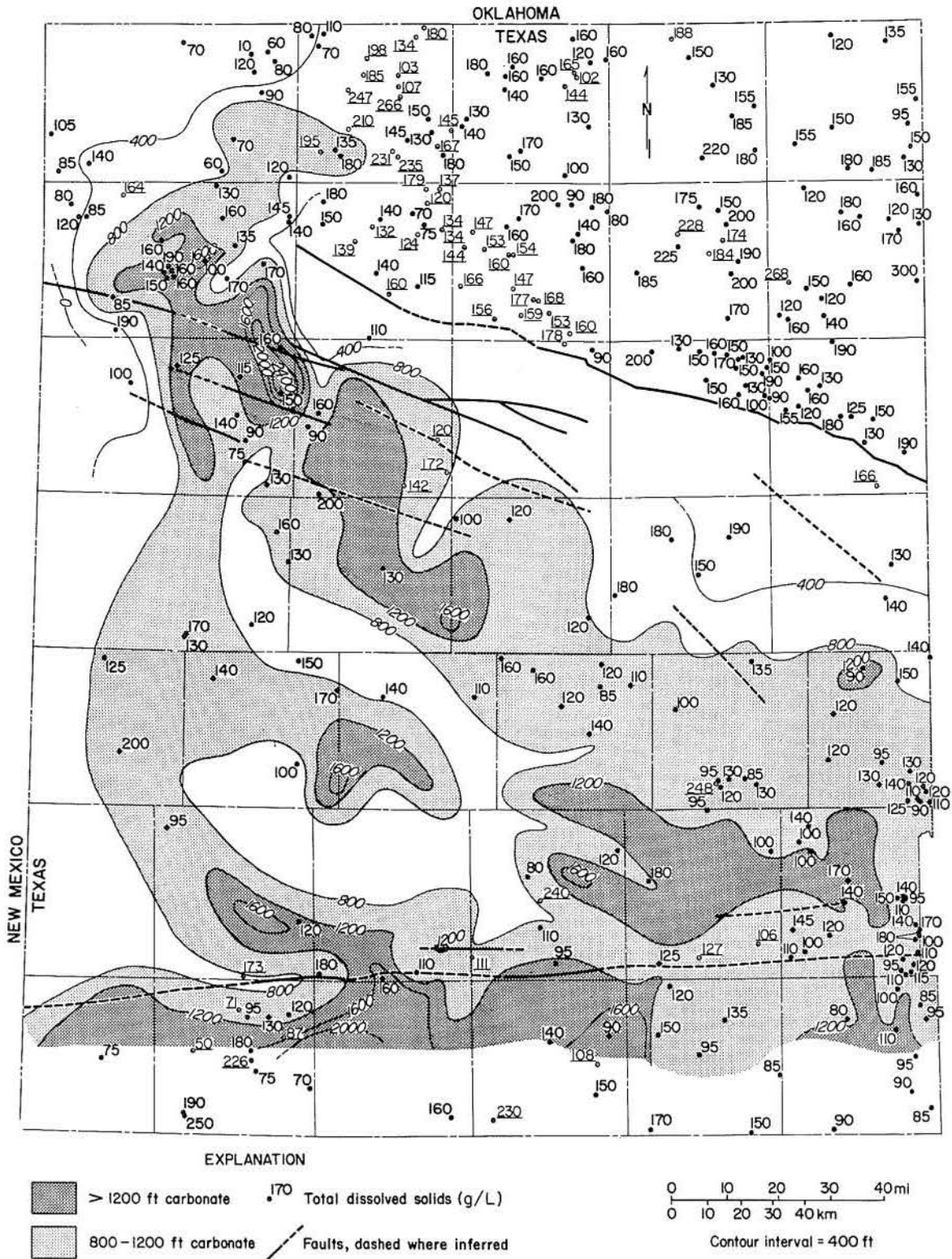
**Figure 10.** Contour lines showing carbonate isoliths for the Wolfcampian-age section of the deep-basin brine aquifer (from C. R. Handford, written communication, 1981). Data points indicate total dissolved solids (g/L) from chemical analyses of the brines (see underlined data, this figure, which are from appendix B, table B-1) or computed from spontaneous potential logs (see appendix C, table C-1). Structure data are from A. Goldstein (written communication, 1981).

17
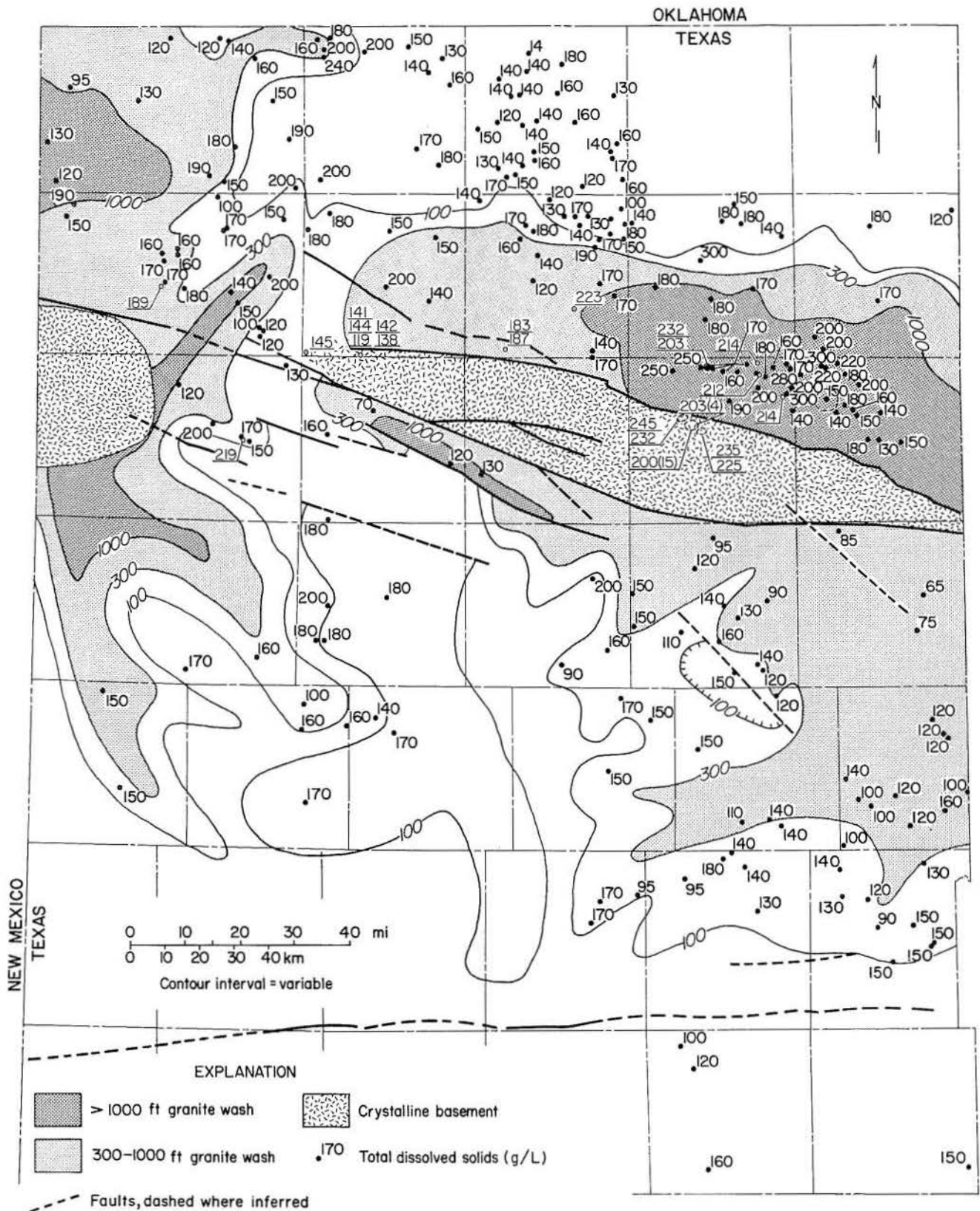
**Figure 11.** Contour lines showing isopachous map of granite wash in the deep-basin brine aquifer (from Dutton, 1982). Data points indicate total dissolved solids (g/L) from chemical analyses of the brines (see underlined data, this figure, which are from appendix B, table B-1) or computed from spontaneous potential logs (see appendix C, table C-2). Structure data are from A. Goldstein (written communication, 1981).

18

and the absence of membrane effects in any detected chemical or head gradients. Mudstones and shales required for membrane filtration are volumetrically of little significance in this basin, which is dominated by chemical precipitates (evaporites), coarse-grained siliciclastic sediments, and carbonates.

Carpenter (1978) suggested that, in sedimentary basins, brine compositions greater than 100,000 mg/L TDS are influenced by evaporite dissolution. The deep formations in the Palo Duro and Dalhart Basins have been overlain by evaporites since Late Permian time. At present, the hydraulic head declines with depth through the evaporite section below the topographically elevated Southern High Plains, and any fluid migrating through this section would be saturated with sodium chloride. Upon discharge from the evaporites, this fluid would mix with brines in the Wolfcamp carbonates (fig. 5). Permeability of the evaporites is extremely low (table 1); consequently, flux through this section must be low. Although some mixing with waters leaking downward from evaporite lithologies has surely occurred, a more reasonable source of the salinity would be from dissolution occurring earlier in the flow history and originating relatively near the recharge areas to the west (figs. 5 and 8).

Ancient salt dissolution zones (originating as early as the Triassic) have been identified near the margins of the basin (Gustavson and others, 1980a). Regional hydraulic gradients during the Triassic are uncertain; however, the Panhandle area was still a topographic low, as evidenced by convergence of sediments from surrounding fluvial to lacustrine sources (McGowen and others, 1980).

During the Late Cretaceous, the Panhandle area was still at or below sea level, and broad carbonate platforms covered the Triassic basin fill. Marine regression accompanied by Laramide tectonism (Late Cretaceous to Paleocene) in New Mexico most likely initiated the ambient regional eastward topographic and hydraulic gradients. Fluids migrating through the deep basin may have entered the system primarily in New Mexico. Owing to the extreme anisotropy between vertical permeability in the evaporites and horizontal permeability in the carbonates (a ratio of 1:10$^6$), most recharge may come from areas where outcropping aquifers are juxtaposed with updip

limits of evaporite beds undergoing dissolution. If hydraulic gradients shown in figure 6 have remained unchanged since the Late Cretaceous, and if permeability and porosity of 2.0 md and 0.5 percent can be considered average for the carbonates (Bentley, 1981), then the fluid from western recharge areas could replace the basinal brines in cycles of about one million years. After the Laramide Orogeny, the entire mass of fluid in Wolfcampian age strata from outcrop to the basin center may have been displaced more than 60 times. Any residual brine from the sabkha deposits would have been displaced early in the development of the regional flow regime. Brines present today in the carbonate rocks and sandstones cannot be connate water. Original fluids have been driven out by the regional flow, and the character of the brines is dominated by dissolution of evaporites early in the flow path and by subsequent modification in transit.

Compositions of both Wolfcamp carbonate (fig. 12) and Pennsylvanian-Permian granite-wash brines (fig. 13) have been plotted on trilinear diagrams. A prominent feature of the pattern is the predominance of sodium chloride. Of the 121 values plotted for Wolfcamp samples, most are aligned along a ray emerging from the Na apex, which indicates a common Mg/Ca ratio.

The slope of the salinity ray of fluids in carbonates (fig. 12) corresponds to a higher Mg/Ca ratio than that of fluids in clastics (fig. 13), suggesting that brines in the granite-wash facies are depleted in magnesium or that the calcium content has been elevated. The sulfate concentration in granite-wash brines is also significantly lower than in Wolfcamp carbonates, commonly by two orders of magnitude. It was noted even in the earliest production reports that fields developed in granite wash, particularly north of the Amarillo Mountains, produce hydrogen sulfide. Sulfate reduction with continued dissolution of anhydrite would in effect elevate calcium and deplete sulfate concentrations.

The data to determine the most likely source of calcium are presently unavailable. It is possible that albitization of intermediate plagioclases in the sandstones and granite washes is contributing substantial calcium to the system. The mechanism will be investigated in detail when new core holes are completed in the basin. Brine samples will be
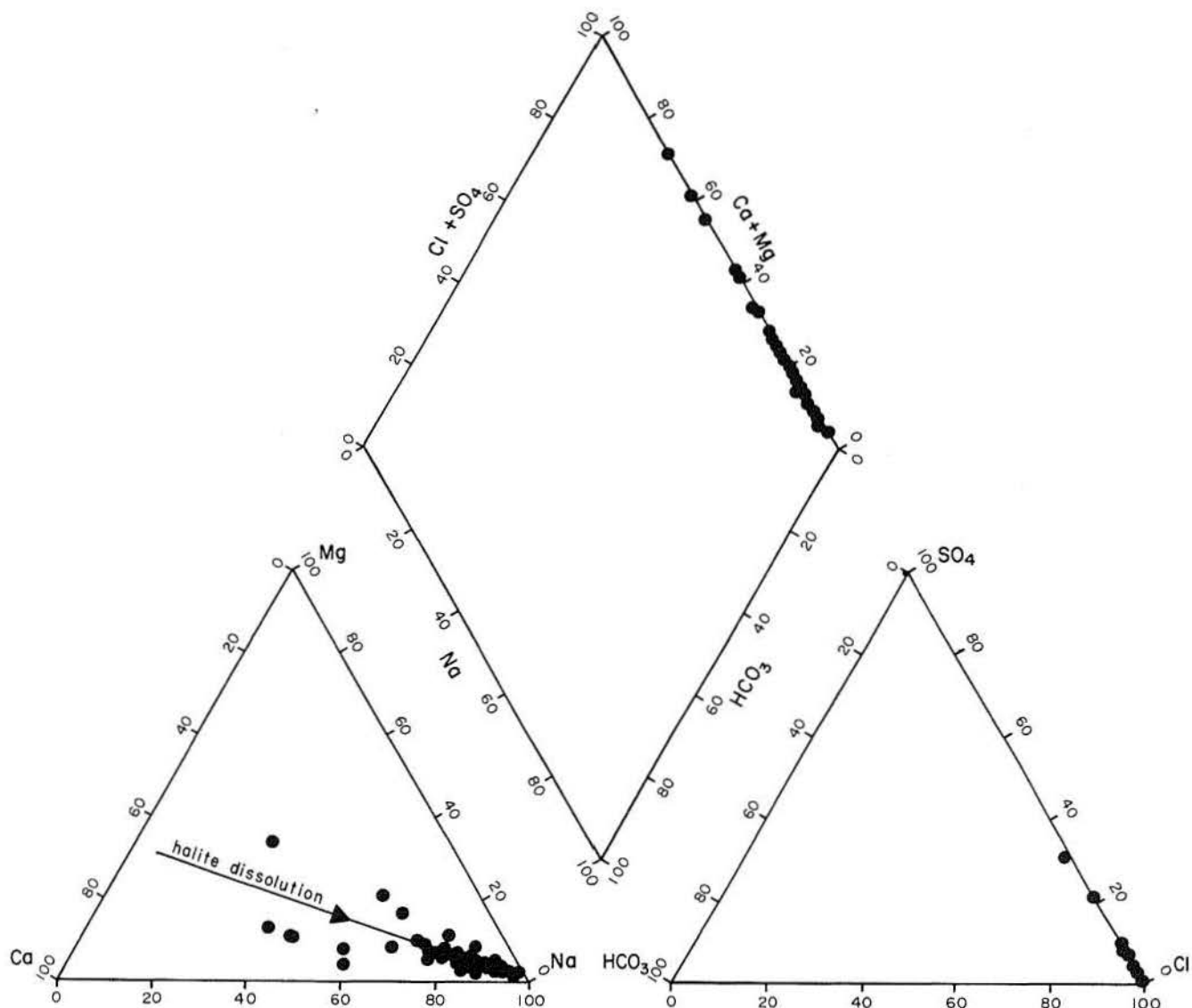
**Figure 12.** *Trilinear diagram illustrating the compositional variation of brine samples from the Permian Wolfcamp carbonate aquifer.*

collected for chemical analysis, and petrographic examination of siliciclastics may provide evidence of albitization if the process is active.

To identify the thermodynamic constraints on brine compositions, we used a computer model, AQ/SALT, which was designed specifically for application to brines. AQ/SALT computes the activity coefficients for components in the brine using the results of analyzed concentrations and then determines the reaction state of the brine with respect to many common minerals in the host rock (Barnes and Clarke, 1980) (see p. 23 for further discussion). Granite-wash and Wolfcamp carbonate brines were computer-processed

separately; the saturation states with respect to halite and anhydrite are illustrated in figures 14 and 15. Wolfcamp carbonate brines cluster relatively near equilibrium with anhydrite and show a significant degree of undersaturation with respect to halite. In contrast, the deeper granite-wash values appear to be shifted away from saturation with anhydrite, most likely in response to sulfate reduction. In addition to the original calibration with solubility data that the model received during development, a test of the accuracy of the model is provided with the two samples. Samples 1 and 2 were collected from Bristol Dry Lake, California, a continental sab-

20
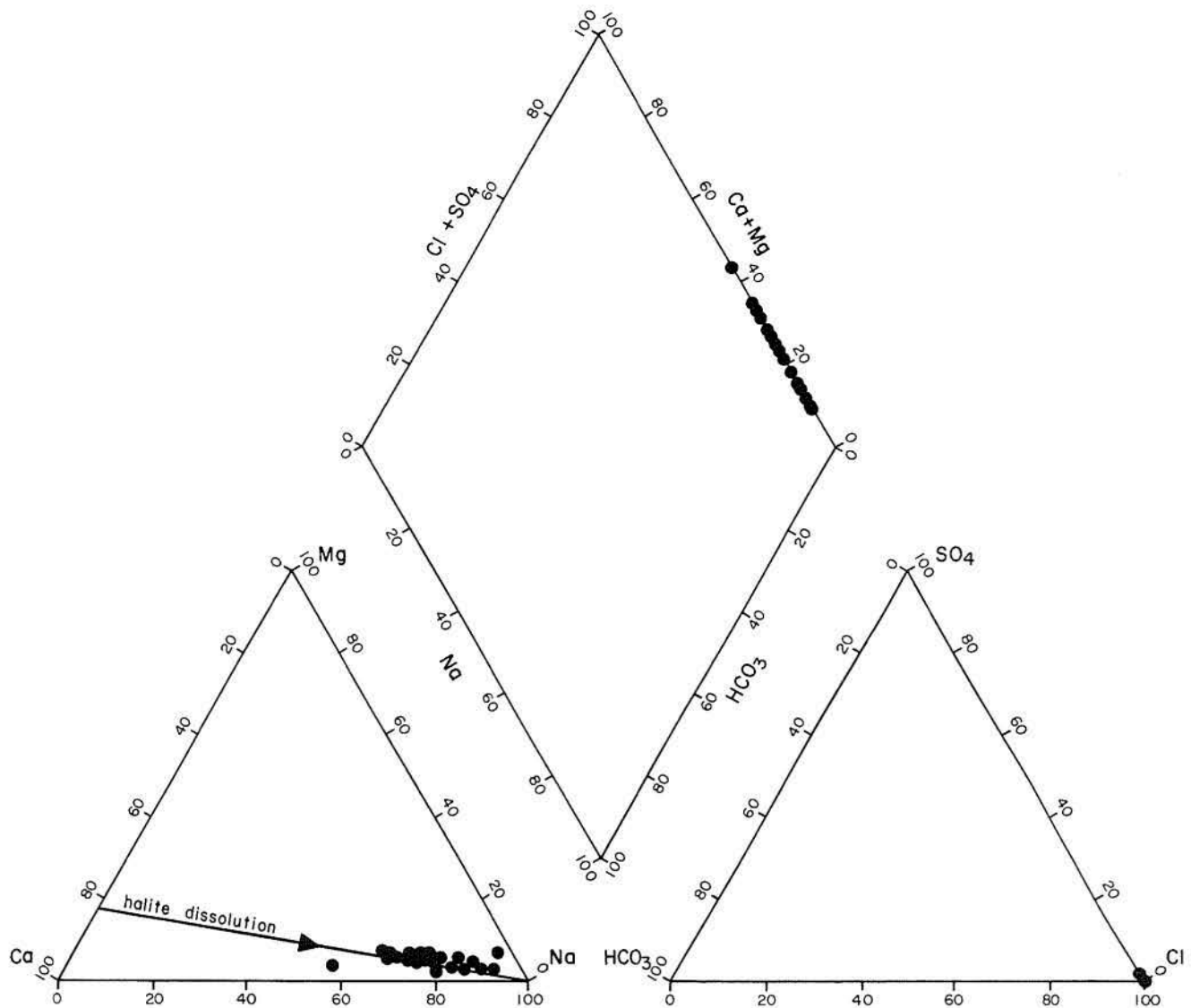
**Figure 13.** *Trilinear diagram illustrating the compositional variation of brine samples from the Pennsylvanian-Permian granite-wash facies.*

kha in which both halite and anhydrite are precipitating. These two brine analyses plot at the point of simultaneous equilibrium with halite and anhydrite (see samples 1 and 2, plotted on figs. 14 and 15).

If the source of sodium and chloride is dissolution of halite early in the flow path or mixing with fluids leaking from the overlying evaporite section, then the ratio of sodium to chloride (mg/L) should be very near the theoretical value of 0.65. Ratios for both brine types are indicating some perturbation from the ideal value (figs. 16 and 17). As might be expected, Wolf-camp carbonate brines, which are shallower and

occur adjacent to the evaporite facies, have compositions that are only slightly offset from the theoretical ratio, whereas the compositional shift for granite-wash brines is more pronounced, probably as a result of ion exchange. Even though the clastic sediments are of marine origin and contain large amounts of exchangeable sodium from equilibrium with seawater, the elevated sodium in these deep basinal brines will continue to drive calcium and magnesium from the clay. Exchange consequently depletes sodium relative to chloride. The sandstone and granite-wash facies are significantly rich in clay minerals, providing substantial ion exchange capacity.
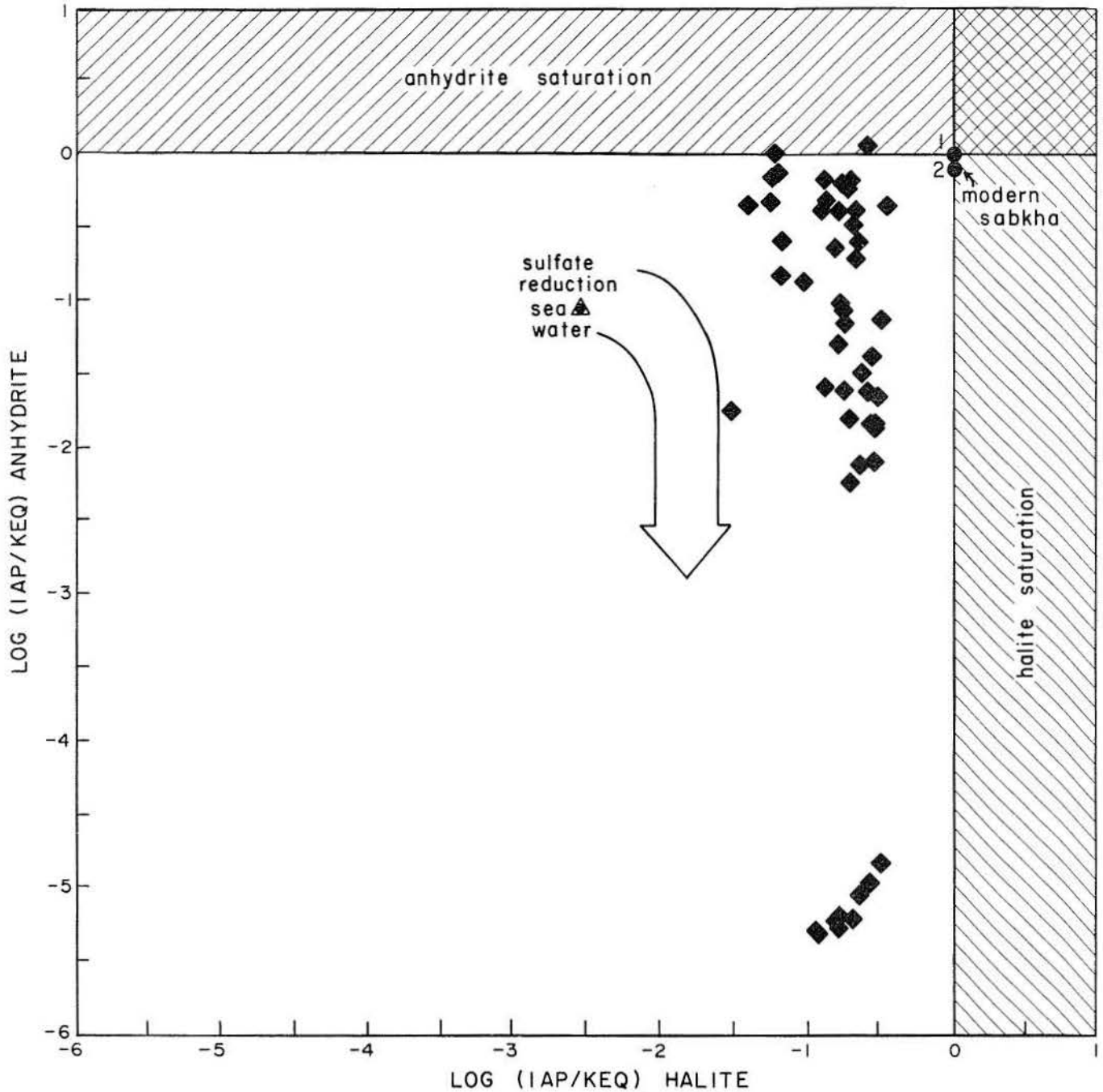
**Figure 14.** *Saturation state of brine samples from the granite-wash facies as computed with AQ/SALT. The arrow indicates the suspected direction of movement away from the anhydrite phase boundary with continued sulfate reduction. However, this is not intended as a quantitative prediction of the actual reaction path.*

The potassium content of brines in the Palo Duro Basin is not accurately known; potassium usually is reported as sodium. The close association of Palo Duro brines with evaporite facies suggests that some of the aberrations in brine composition might reflect the dissolution of minerals other than the common evaporite phases of halite, anhydrite, and dolomite. Unfortunately, there are no known occurrences of any late-stage evaporite minerals in the Texas Panhandle. None were identified in petrographic (Handford and others, in preparation) and X-ray diffraction
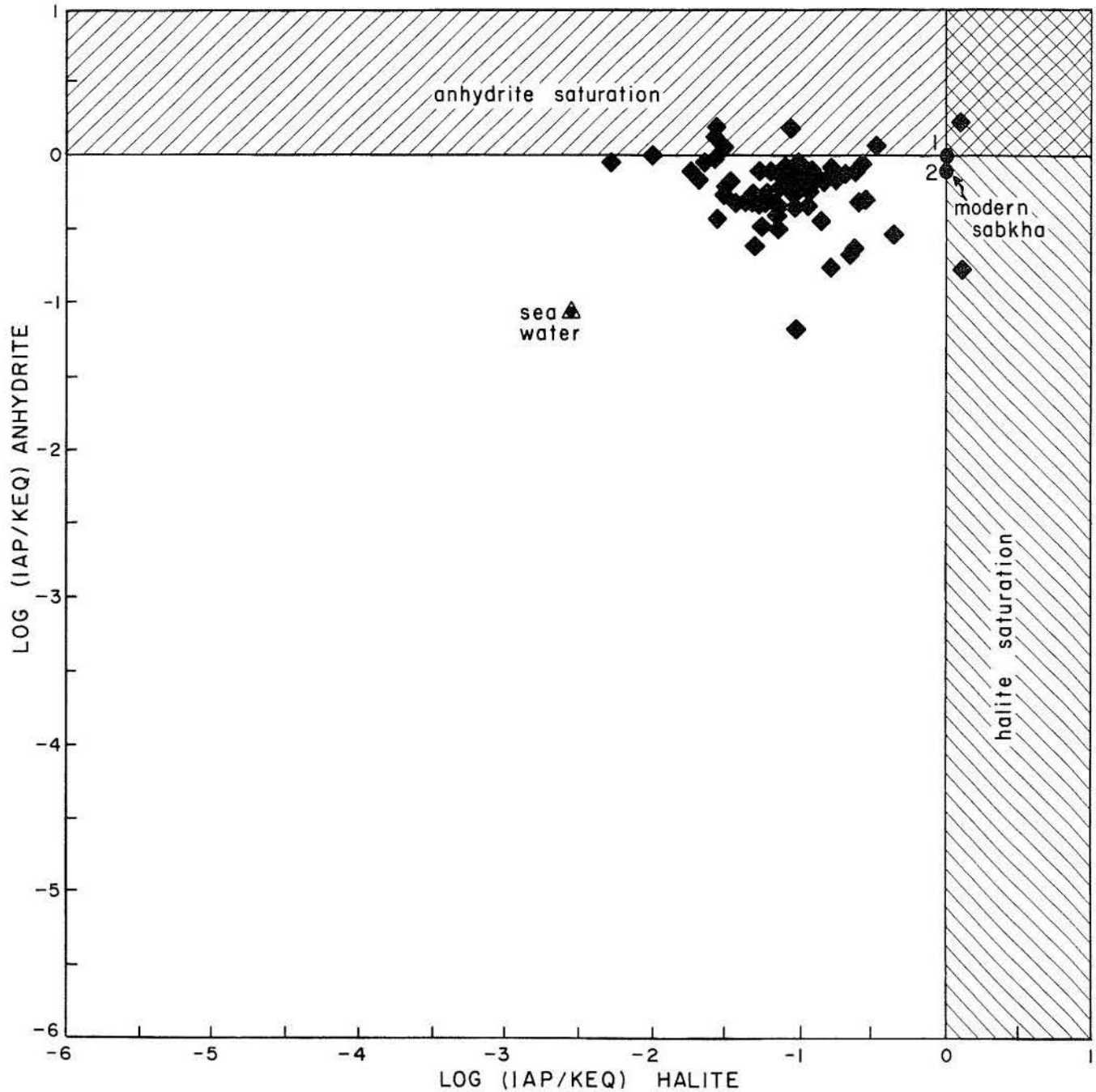
**Figure 15.** *Saturation state of brine samples from Wolfcamp carbonate facies as computed with AQ/SALT.*

(Bassett and Palmer, 1981) studies of 7,700 ft (2,369 m) of continuous core through the salt-bearing section. Potash has not been reported in the Palo Duro or Dalhart Basins; however, potash is mined in New Mexico in the southwestern part of the Permian Basin where the extent of Permian evaporation appears to have reached the stage of potash precipitation.

## Thermodynamic Data and Computations

Equations have recently been formulated that describe ionic behavior in concentrated electrolyte solutions. The fundamental expression by Debye and Hückel (1923) and subsequent extensions
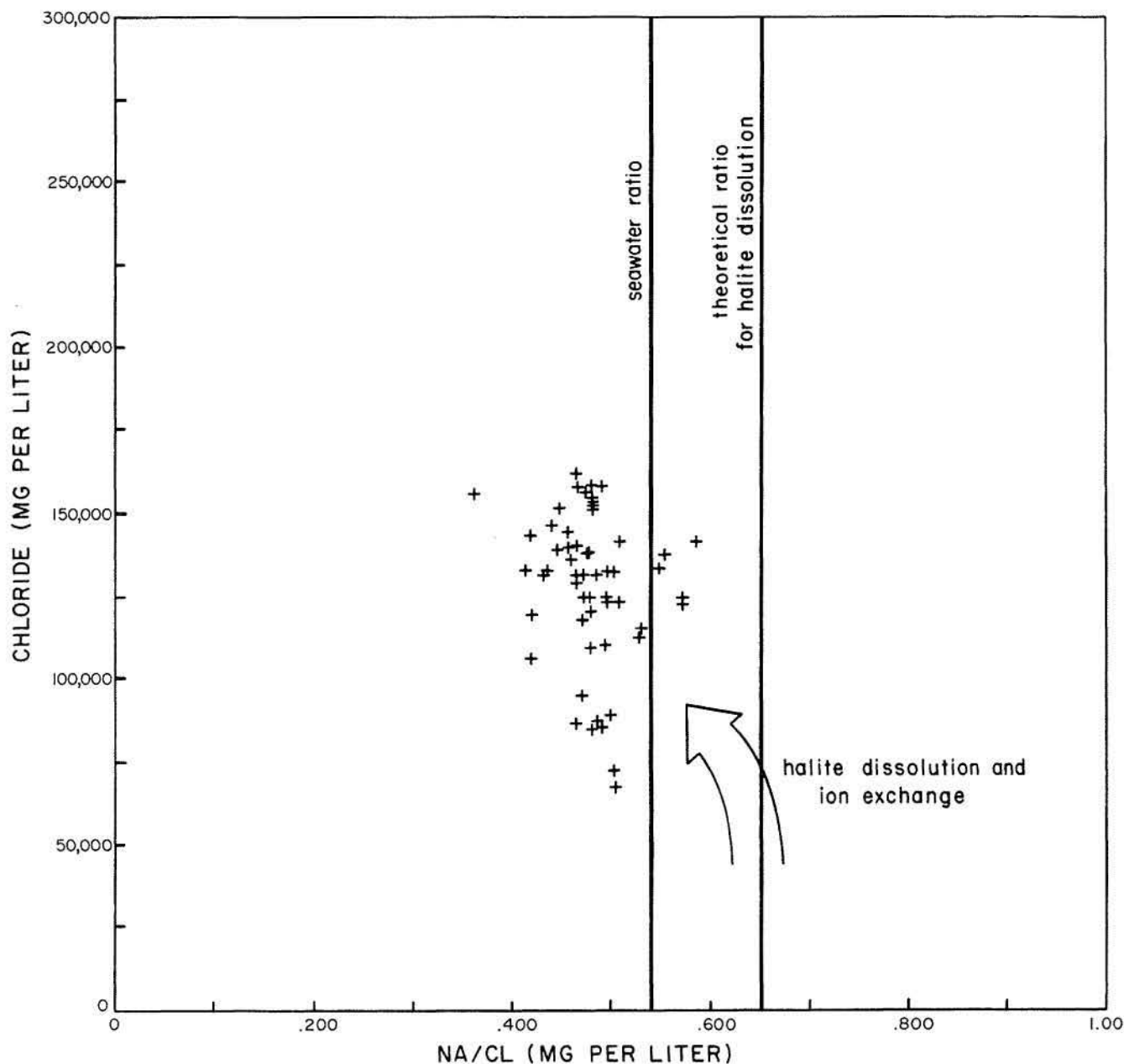
**Figure 16.** *Sodium to chloride ratio in granite-wash facies shifting away from that typical of halite dissolution, followed by ion exchange. Arrow is included to indicate suspected shift, but is not intended as a quantitative prediction of actual reaction path.*

have not performed adequately in the evaluation of concentrated brines, or in the investigation of solubilities of highly soluble minerals. The lack of an accurate mathematical model of short-range interionic forces in the computation of potentials apparently has been a major source of the deviation from experimentally obtained data. Pitzer (1979), Scatchard (1968), and others have developed a rigorous and comprehensive theory for electrolyte solutions that can be approximated by a series of semiempirical equations. The equations, although somewhat cumbersome, especially for mixed electrolyte systems, can be quickly processed by the computer.

A rigorous test of Pitzer's (1979) equations to model mineral solubilities has been conducted by
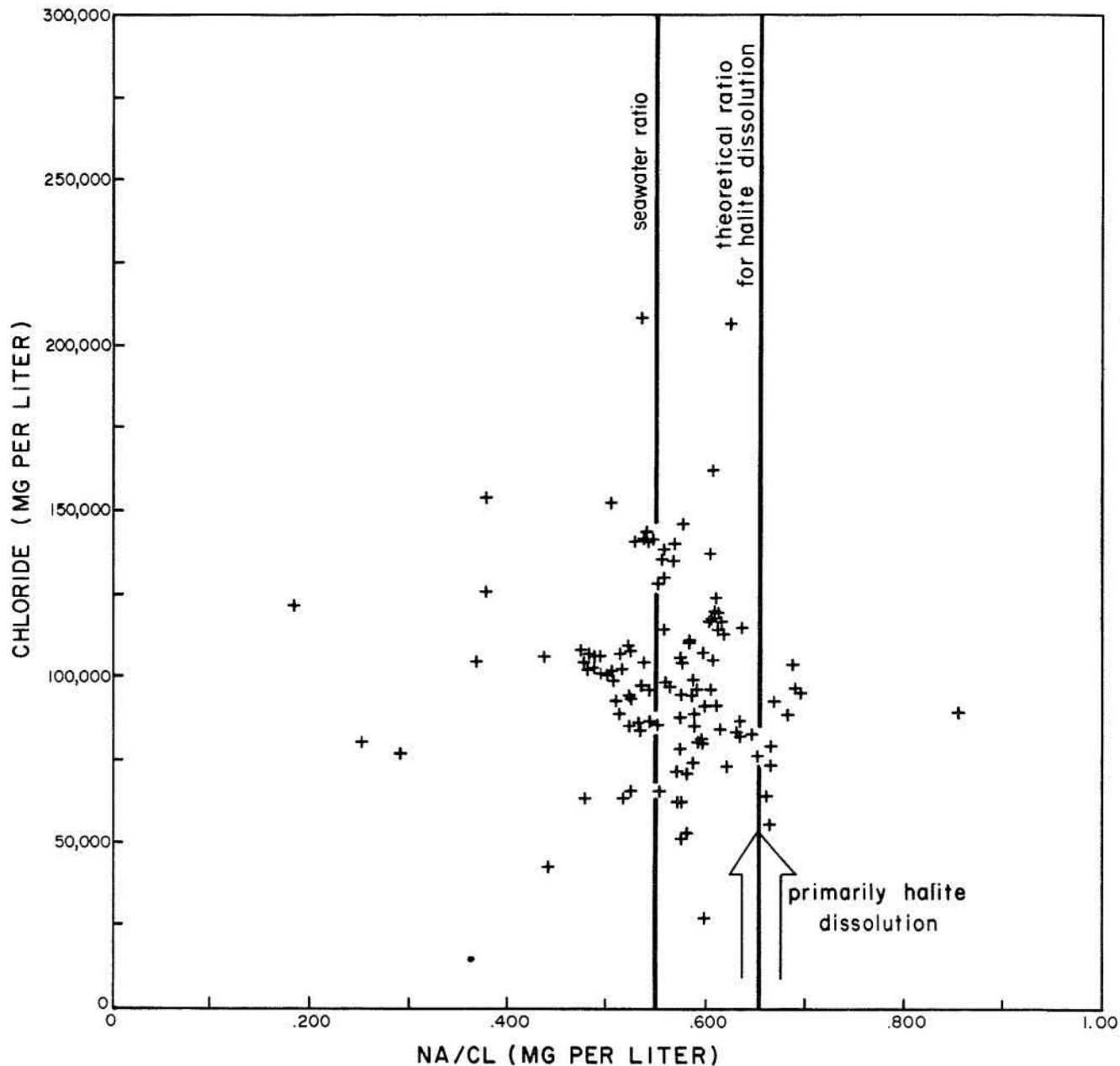
**Figure 17.** *Sodium to chloride ratio in brine samples from Wolfcamp carbonates. Salinity is derived primarily from the overlying evaporites and from evaporite dissolution early in the flow path. Arrows are included to indicate suspected shift, but are not intended as a quantitative prediction of the actual reaction path.*

Harvie and Weare (1980). Their results agreed with published solubility data. Harvie and others (1980) used free energy minimization to compute mineral sequences observed in the Permian Zechstein evaporites.

The computer model AQ/SALT has been developed for applications in studies of radioactive waste disposal and the geochemistry of deep

formation brines. The model employs the computationally more appropriate revision of Pitzer's equations by Harvie and Weare (1980). The model, discussed in more detail elsewhere (Bassett and Griffin, in preparation), will be only briefly mentioned here. AQ/SALT is a table-driven program that can accommodate any number of species and can be readily expanded

as new data and equation parameters become available. The model computes activity coefficients, activities of ions, and the activity of water. Temperature dependence is available for only a few species; however, additional parameterization and expansion is in progress.

By comparing calculated activity products with thermodynamic equilibrium constants, the reaction state of a brine with respect to the minerals of interest can be determined. The model prints out the possible phase assemblages and determines whether they are stable or have the potential to dissolve in the brine.

At present, data are insufficient for application of Pitzer's equations to carbonate species in brines. The approach we used was to interface AQ/SALT and an ion-pairing model, SOLMNEQ (Kharaka and Barnes, 1973), for the carbonate speciation. The extended Debye-Hückel expression used in SOLMNEQ contains a deviation parameter obtained empirically from solutions containing sodium and chloride as the dominant species. This parameter is useful in the high-salinity brines found in the Palo Duro Basin. AQ/SALT has been calibrated with solubility data and seems to fit the data closely. SOLMNEQ was therefore only used to calculate carbonate species. All other activities are more precisely defined by AQ/SALT.

## Mass Transfer in the Carbonate System

The reaction state of Wolfcamp carbonate brines was computed with SOLMNEQ and AQ/SALT using the results of 121 analyses. Subsurface temperatures were calculated using an average geothermal gradient for the basin of $0.611°C/100$ ft (Dutton, 1980). Depth was computed to the midpoint of the reported packer depths. All analyses were received in units of mg/L; consequently, a density correction was required to convert to units of molality. Density is computed assuming that brine weight is equal to the same equivalents of sodium chloride. Of the 121 Wolfcamp carbonate analyses, only 91 had a reported pH value; for the initial computations, only these analyses were processed.

Given the previous assumptions, the models indicate that almost all Wolfcamp carbonate brines are supersaturated with respect to calcite

(fig. 18) and dolomite (fig. 19). Handford (1980) identified dolomite and low-porosity limestone in Lower Permian carbonate shelf and shelf-margin facies on the basis of sample and geophysical logs. The dolomite and limestone contact is regionally discordant, displaying a non-stratal, cross-cutting relationship that suggests shallow and early diagenesis (Handford, 1980). Without core samples for petrographic or stable isotope analyses, a reconstruction of the diagenetic sequence in the carbonate rocks is inconclusive. Porosity, according to SP logs, correlates well with the distribution of dolomite identified on sample logs; consequently, a common mechanism is probably responsible. Except for the shelf-margin dolomite, most dolomitization was focused along the facies boundary between the Wolfcamp carbonate strata and the overlying sabkha-margin anhydritic dolomites. It is likely that as the coastal sabkha environment encroached on the region, magnesium-rich brines formed in areas of evaporation circulated through the buried marine-shelf carbonates.

Dolomite should not be stable in its present environment, even though the brines appear supersaturated (fig. 19). Magnesium to calcium ratios (mg/L) are generally low (<0.3), and salinity is elevated. Magnesium to calcium ratios near 0.5, consistently noted in ground water elsewhere, have been interpreted as representative of the stable two-phase equilibrium between calcite and dolomite at 25°C (Folk and Land, 1975). Dolomitization appears to have been an early process, resulting in local rather than pervasive distribution, and it is unlikely that present-day brines are responsible for continued dolomitization in the basin. Consequently, calcite solubility may be the predominant factor in determining carbonate mass transfer in this brine system.

Outgassing of carbon dioxide at the surface during sample collection is undoubtedly the cause of the apparent supersaturation with respect to carbonate minerals. Two approaches were taken to estimate the in situ partial pressure of carbon dioxide ($P_{CO_2}$) and to determine if calcite was in equilibrium with the brine. The first approach was to seek an analogy between in situ brine $P_{CO_2}$ and the $P_{CO_2}$ in natural gas from nearby producing fields. Second, a mass transfer approach was used, requiring a computer equilibrium model to

26
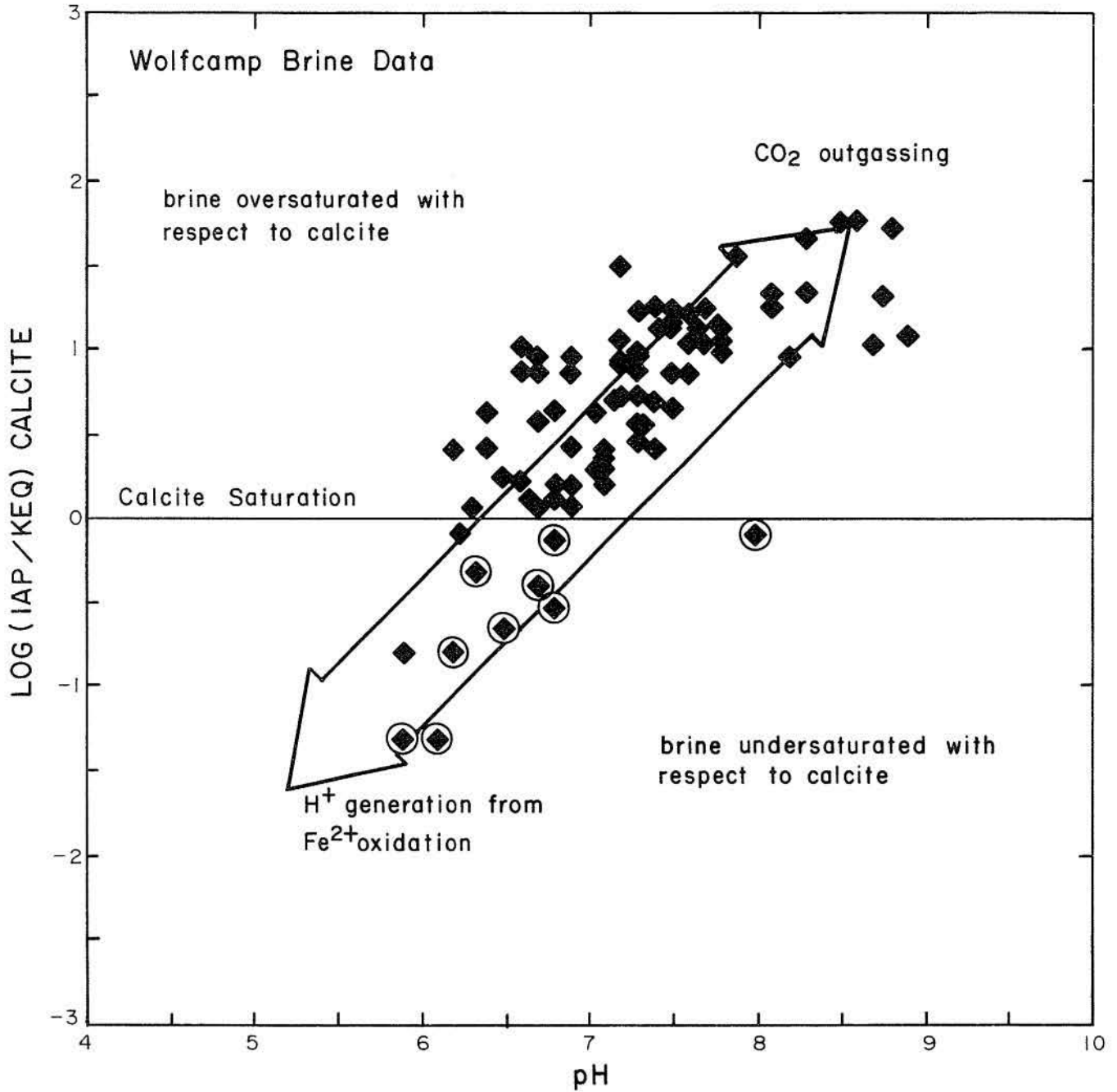
**Figure 18.** *Saturation states computed with AQ/SALT and SOLMNEQ for Wolfcamp carbonate brines, the effect of outgassing of $CO_2$, and the oxidation of dissolved iron. Circled data points represent compositions of fluid from Sherman County.*

simulate the stepwise addition of $CO_2$ back into the sample. The variation in speciation was monitored along the reaction path, and a new in situ pH and $P_{CO_2}$ were computed at the calcite phase boundary.

The Bureau of Mines (U.S. Department of Interior) surveyed worldwide helium potential from 1917 to 1974 by analyzing natural gas samples from 37 states and 23 foreign countries. Numerous oil and gas fields from the Texas
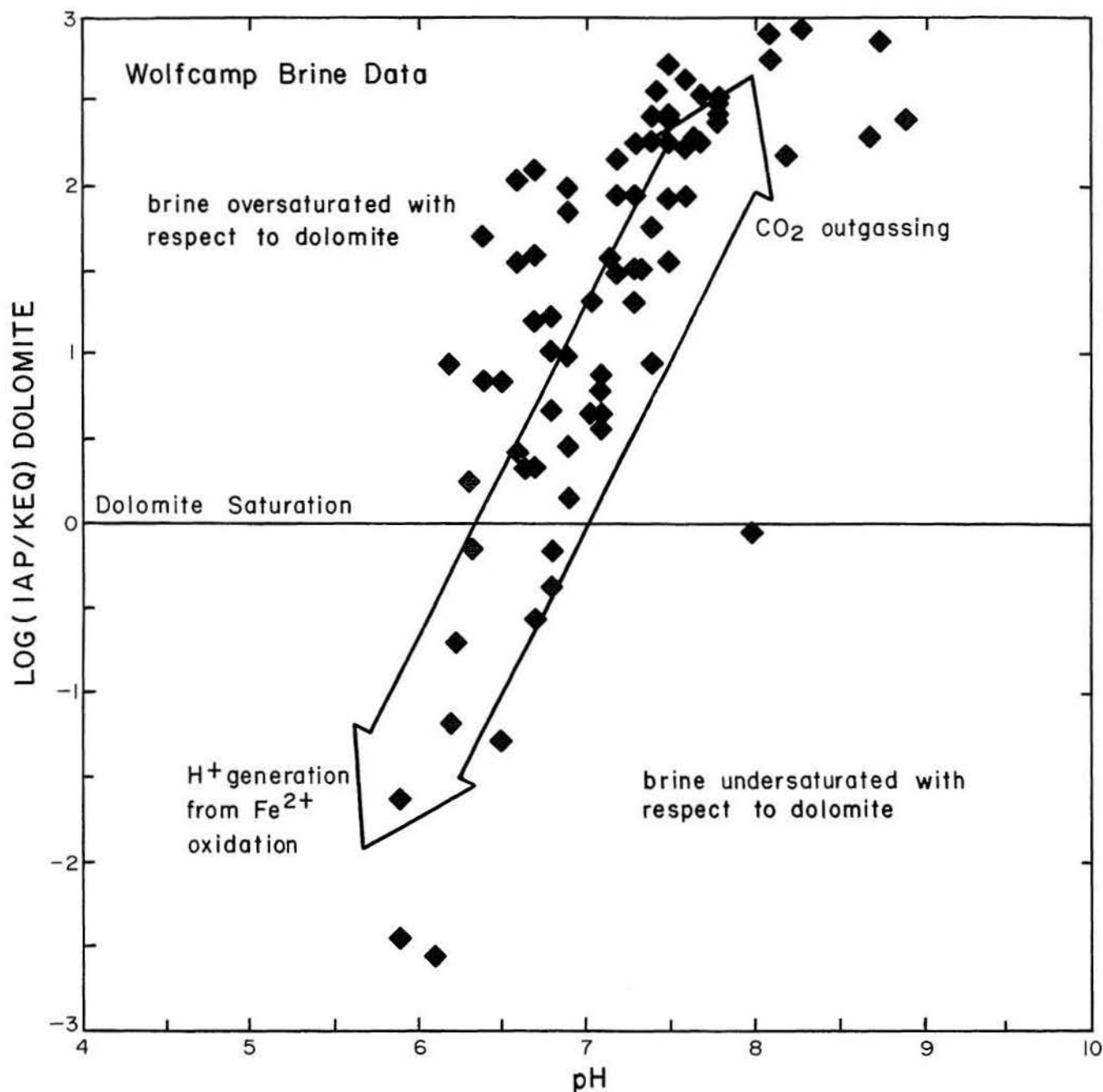
**Figure 19.** *Saturation state of Wolfcamp carbonate brine with respect to dolomite as computed with AQ/SALT and SOLMNEQ.*

Panhandle were included in this study (Moore, 1976). Data on wellhead pressures, depth, and mole percent $CO_2$ from Moore (1976) were used to compute a field $P_{CO_2}$ (atm). Even though substantial variation in wellhead pressures exists among the producing fields, the $P_{CO_2}$ across the region is defined within a relatively narrow range (fig. 20). Without stable isotope data, we assume

that the $CO_2$ is derived from within the basin during hydrocarbon maturation. The fields are too deep to be associated with biogenic methane (Hunt, 1979), and there is certainly no evidence of carbonate decomposition attending volcanic intrusion. It seems doubtful that $CO_2$ pressures would be so uniform across the basin (figs. 9 and 20) were there not some buffering mechanism. We
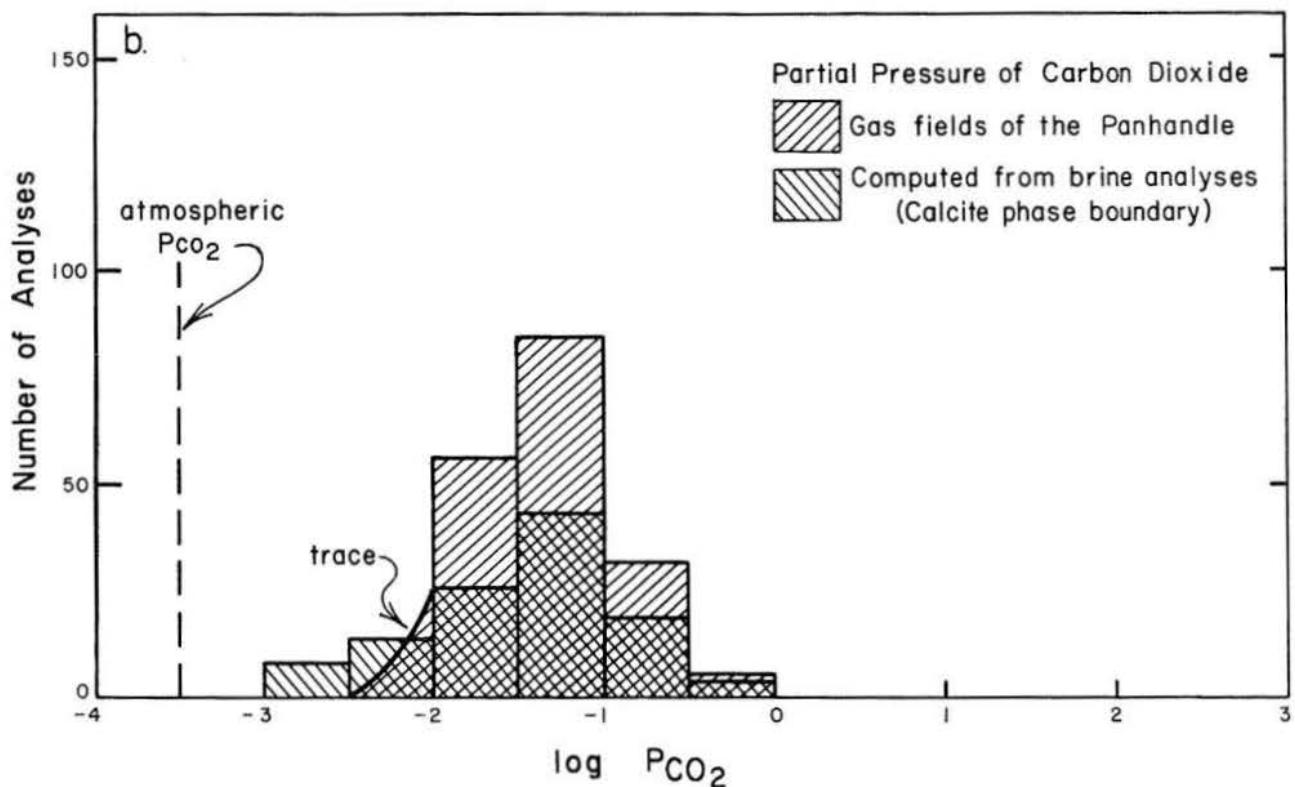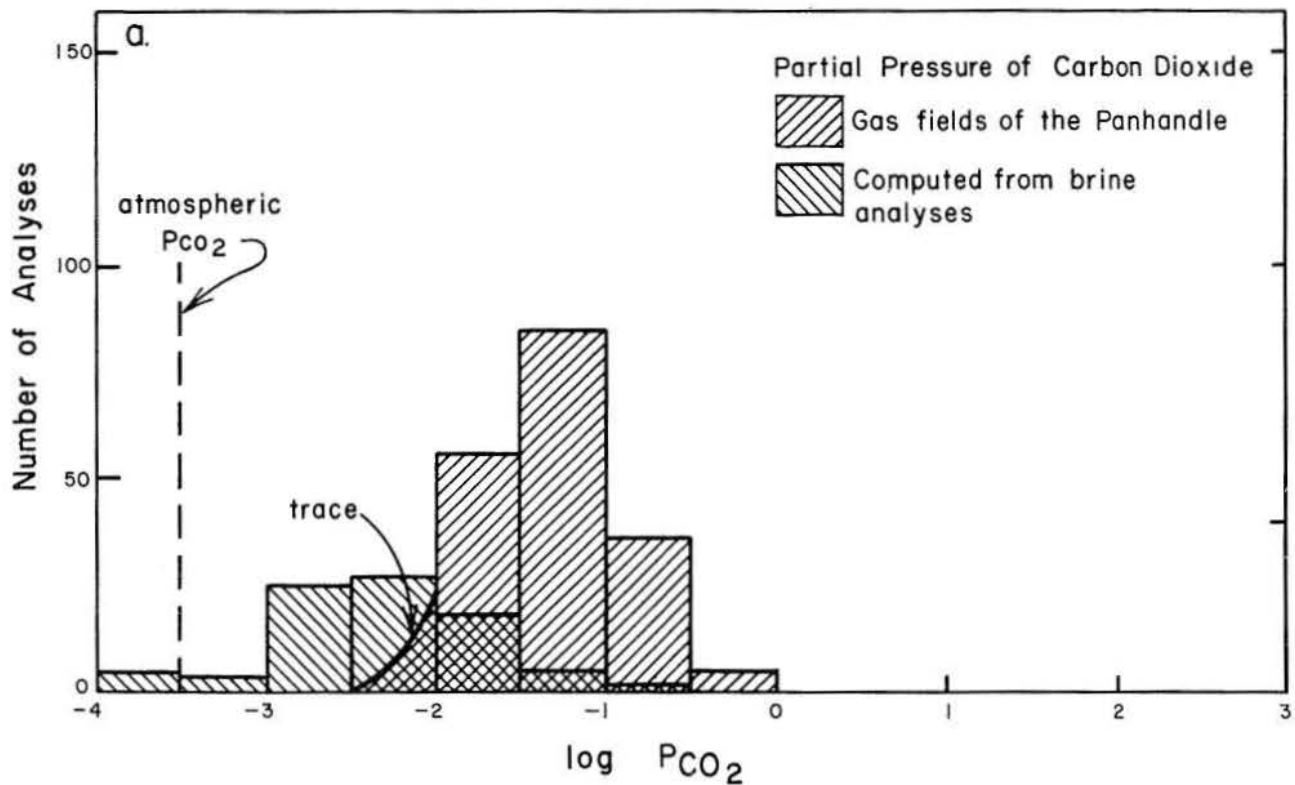
**Figure 20.** *Distribution of $CO_2$ partial pressure in oil and gas fields in the Palo Duro and Dalhart Basins. Also shown is the distribution of log $P_{CO_2}$ computed with (a) the reported pH and (b) the computed pH at the calcite phase boundary.*

*Table 2. Chemical composition (mg/L) and computed equilibrium conditions for brine samples within the Palo Duro and Dalhart Basins. "Initial Conditions" connotes the analytical values obtained from industry, including the reported pH. The columns under "Calcite Equilibrium" contain the computed pH, $P_{CO_2}$, and slope $\dfrac{\partial\ SI}{\partial\ pH}$ for the same brines at the calcite phase boundary owing to the simulated addition of $CO_2$ to the sample. The saturation index (SI) is for calcite.*

| Sample no. | Ca | Initial Conditions | | | | | | | Calcite Equilibrium | | |
| | | Na | Mg | HCO₃ | Cl | SO₄ | pH | SI | pH | $P_{CO_2}$ (atm) | Slope |
|---|---|---|---|---|---|---|---|---|---|---|---|
| Hartley | 1,100 | 60,310 | 1,069 | 302 | 88,154 | 13,090 | 6.8 | 0.20 | 6.59 | 0.09 | 0.96 |
| Potter 1 | 3,660 | 40,900 | 1,350 | 278 | 71,600 | 2,350 | 7.9 | 1.56 | 6.19 | 0.15 | 0.91 |
| Potter 2 | 7,960 | 56,200 | 1,540 | 173 | 104,000 | 1,600 | 6.8 | 0.64 | 6.15 | 0.10 | 0.98 |
| Potter 3 | 6,578 | 47,193 | 841 | 106 | 85,566 | 1,735 | 8.0 | 1.69 | 6.40 | 0.03 | 0.71 |
| Hall 1 | 32,340 | 58,579 | 2,245 | 56 | 153,982 | 517 | 6.24 | -0.09 | 6.30 | 0.15 | 0.96 |
| Floyd 1 | 6,234 | 84,667 | 1,782 | 132 | 146,281 | 1,035 | 6.32 | 0.06 | 6.26 | 0.07 | 0.95 |
| Floyd 2 | 5,560 | 34,600 | 1,848 | 581 | 65,600 | 3,640 | 6.7 | 0.96 | 5.80 | 0.62 | 0.99 |
| Motley 1 | 4,927 | 33,177 | 1,933 | 99 | 63,800 | 2,350 | 6.7 | 0.07 | 6.63 | 0.15 | 0.98 |
| Motley 3 | 3,920 | 46,112 | 1,972 | 296 | 71,050 | 1,450 | 7.5 | 1.21 | 6.20 | 0.15 | 0.96 |
| Lamb | 15,120 | 46,607 | 3,072 | 195 | 106,500 | 1,700 | 6.4 | 0.42 | 6.00 | 0.09 | 0.99 |
| Hockley 1 | 3,823 | 83,135 | 884 | 333 | 137,190 | 588 | 6.9 | 0.96 | 5.80 | 0.56 | 0.95 |
| Hockley 2 | 4,687 | 18,907 | 2,534 | 652 | 42,777 | 2,252 | 6.4 | 0.63 | 5.80 | 0.43 | 0.99 |
| Hockley 3 | 1,840 | 16,347 | 488 | 927 | 27,300 | 3,400 | 7.2 | 1.50 | 5.70 | 1.28 | 0.97 |
| Hockley 4 | 3,286 | 29,581 | 648 | 801 | 51,304 | 2,120 | 6.6 | 1.02 | 5.70 | 0.91 | 0.98 |
| Crosby 1 | 6,880 | 30,143 | 2,246 | 139 | 62,891 | 2,913 | 8.6 | 1.76 | 6.35 | 0.04 | 0.79 |
| Crosby 2 | 8,164 | 80,271 | 992 | 187 | 140,729 | 365 | 7.31 | 1.23 | 6.00 | 0.15 | 0.94 |

suggest that the brines and the carbonate host rocks are in equilibrium, and the $P_{CO_2}$ is constrained to follow the calcite phase boundary, as discussed herein. Results of brine analyses were processed in two stages: (1) analyses of data from the Palo Duro and Dalhart Basins and (2) analyses of data from the entire Panhandle region. The somewhat arbitrary division is intended to distinguish brines not obviously related to hydrocarbon production from the extremely productive Panhandle oil and gas field and adjacent fields.

Of the 121 analyses of brines from Wolfcamp carbonate strata, only 16 samples are from the Palo Duro and Dalhart Basins. These data are tabulated (table 2) for comparison, and a complete list of all analyses is given in appendix C; the saturation indices are shown in figure 21.

Significantly, a plot of calcite saturation index against pH indicates a strong correlation toward a slope of unity in both the Palo Duro Basin and all Wolfcamp carbonate samples (figs. 18 and 21). The stepwise addition of $CO_2$ to the solution with recalculation of pH, speciation, and saturation state moves the computed saturation toward the

calcite phase boundary but retains this slope of 1. Slopes of reaction paths for each brine sample illustrated in figure 21 are given in table 2; all but two conform essentially to the same slope.

The addition of $CO_2$ to the initial brine composition increases total carbon but does not affect alkalinity. Consequently, the net effect is an increase in carbonic acid, a lowering of pH, and a redistribution of the carbonate species as well as any other pH-dependent complexes and ion pairs.

The reaction path depends on temperature, pressure, ionic strength, pH, and total solution composition. The model computes the reaction state of the brine at the in situ temperature, which remains constant. Pressure effects are assumed to be negligible at these depths, and composition of the total solution is constant except for the $CO_2$ increase, which enters the mass balance as increasing total carbon. Ionic strength will alter slightly because of the redistribution of charge among species.

The change in the saturation state with pH is simply the derivative of the activity product minus the equilibrium constant with pH at constant temperature and pressure (T, P):
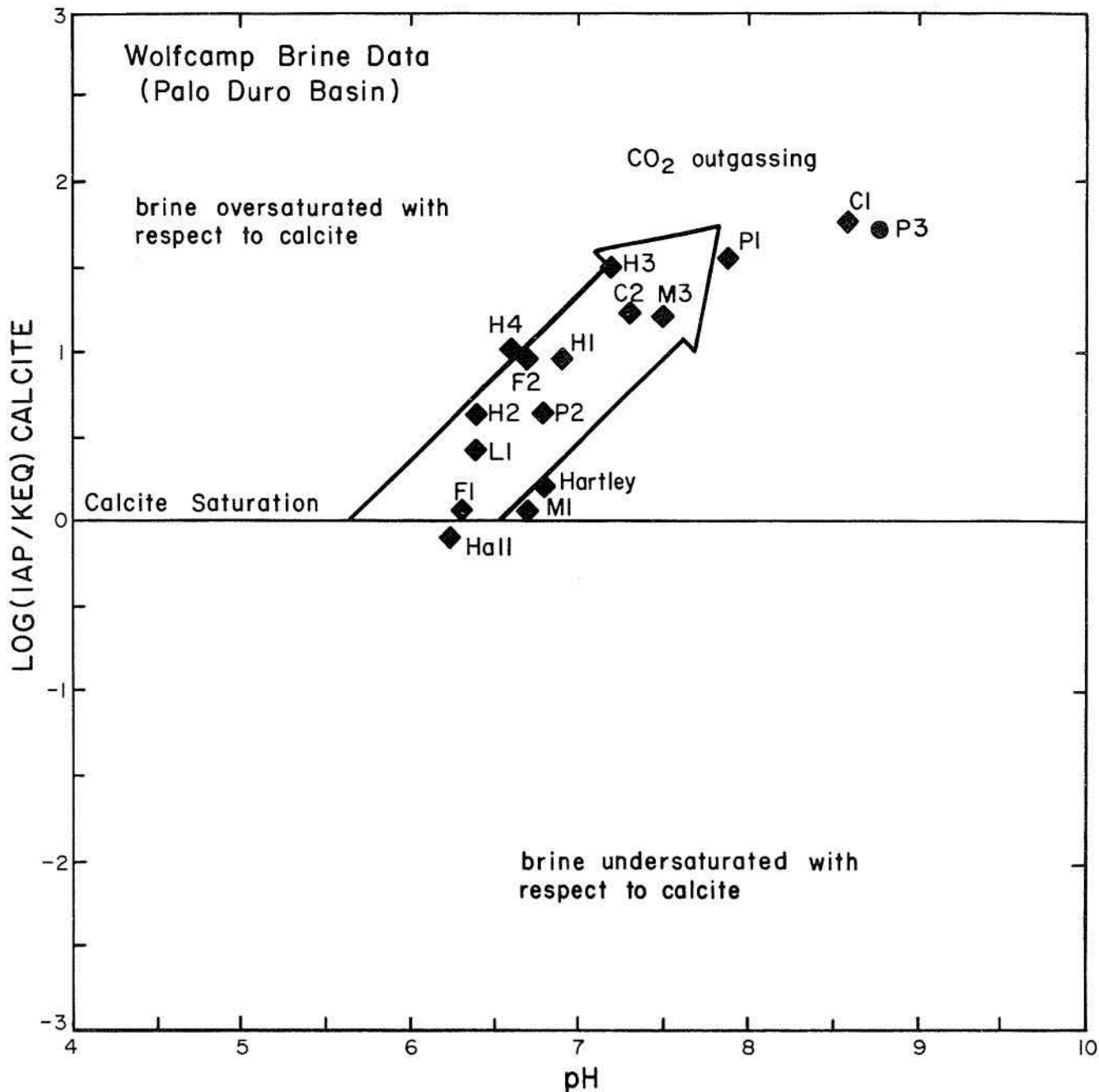
**Figure 21.** *Computed saturation states for brines within the Palo Duro and Dalhart Basins using the reported pH values. For identification of data points, see table 2.*

$$\left(\frac{\partial(\log \text{Iap} - \log \text{Keq})}{\partial \text{pH}}\right)_{T,P} = \left(\frac{\partial \log \text{Iap}}{\partial \text{pH}}\right)_{T,P}$$

Inserting the activity product for calcite,

$$\left(\frac{\partial \log \text{Iap}}{\partial \text{pH}}\right)_{T,P} = \left(\frac{\partial \log (a_{Ca^{2+}} \cdot a_{CO_3^{2-}})}{\partial \text{pH}}\right)_{T,P}$$

$$= \left(\frac{\partial \log (\gamma_{Ca^{2+}} \cdot m_{Ca^{2+}} \cdot \gamma_{CO_3^{2-}} \cdot m_{CO_3^{2-}})}{\partial \text{pH}}\right)_{T,P}$$

Ionic strength changes are negligible, temperature and solution composition remain constant, and the change in ion pairing with pH over the range of interest does not alter the concentration of free calcium significantly. Consequently,

31

*Table 3. Compositions of hypothetical brine in equilibrium with calcite for computations of changes in the saturation state with $CO_2$ outgassing (see fig. 22).*

| | | mg/L | | | | | |
|---|---|---|---|---|---|---|---|
| Brine | T(°C) | Na | Ca | Cl | HCO₃ | pH | $P_{CO_2}$(atm) |
| A | 37.6 | 54,783 | 11,527 | 107,345 | 610 | 5.50 | 1.55 |
| A | 37.6 | 54,576 | 11,527 | 107,345 | 61 | 6.50 | 0.012 |
| A | 37.6 | 54,555 | 11,527 | 107,345 | 6 | 7.55 | 0.0001 |

$$\left(\frac{\partial \log \text{Iap}}{\partial \text{pH}}\right)_{T, P} = \left(\frac{\partial \log m\, CO_3^{2-}}{\partial \text{pH}}\right)_{T, P}$$

$$\left(\frac{\partial \log \text{Iap}}{\partial \text{pH}}\right)_{T, P} \cong 1.0$$

In saline waters, ion pairing of normally more weakly associated species lowers the activity of free ions, and the reduction of free water relative to the bound water of hydration tends to elevate the activity of all species. The net effect is a relatively linear translation of the derivative of the concentration of the species with pH owing to the reduction or increase in concentration. The derivative of carbonate concentration with pH in the range of interest (pH 6.0 to 8.5) is relatively linear with a slope of 1.

Consider the theoretical behavior of simple hypothetical brines with compositions given in table 3. If the brines are initially in equilibrium with calcite, the compositions would plot at points A, A′, and A″ (fig. 22). Upon exposure to atmospheric conditions, the computed saturation index for calcite will follow the solid line as $CO_2$ outgasses and the brine approaches equilibrium with atmospheric $P_{CO_2}$. If precipitation of calcite occurs, then the saturation index will decrease with a slope equivalent to the dashed line as acidity increases with deprotonation of bicarbonate. The pH values reported by industry appear to have been taken before calcite precipitation, resulting in the linear alignment of computed saturation indices with a slope of unity.

All Wolfcamp carbonate brine analyses from the Panhandle were translated to the calcite phase boundary by $CO_2$ addition. The equilibrium $P_{CO_2}$ over these solutions was compared with that of natural gas reservoirs, and the data are shown as histograms (fig. 20). The computed $P_{CO_2}$ for brines compares remarkably well with the reservoirs, and the values from within the basin show no significant variation in $P_{CO_2}$ distribution. This similarity suggests that $CO_2$ is buffered by the carbonate host rock and that the brines are in equilibrium with calcite. The linear distribution of computed saturation states when plotted with pH also indicates that the brines were in equilibrium but that $CO_2$ loss has occurred during sampling.

Data from Sherman County illustrate that other processes may be active during sampling (fig. 23). At least 30 percent of the samples are undersaturated with respect to calcite, yet still align themselves along the slope for $CO_2$ loss. The laboratory personnel analyzing the samples noted that the brines appear "rusty"; and in general, a value for iron concentration is reported. If ferrous iron is present in these samples, whether from the formation brine or corrosion of the drill pipe, it will oxidize on exposure to atmospheric $O_2$, the pH will drop, and "rusty" iron hydroxide will precipitate. This process will also alter pH without affecting alkalinity; consequently, the derivatives of saturation state with pH will remain at unity, but the lowered pH results in the computation of an undersaturated condition.

## CONCLUSIONS

Regional hydraulic gradients in the Palo Duro and Dalhart Basins indicate that the brines are moving eastward. The evaporite section acts as a low-permeability barrier above the transmissive carbonate and granite-wash facies. Owing to the elevated topography, the central part of the basin appears to be underpressured; however, the horizontal head gradients are comparable to the regional topographic slope.

The scarcity of oil and gas production in the basins enhances the attractiveness of these basins as potential nuclear waste repository sites;
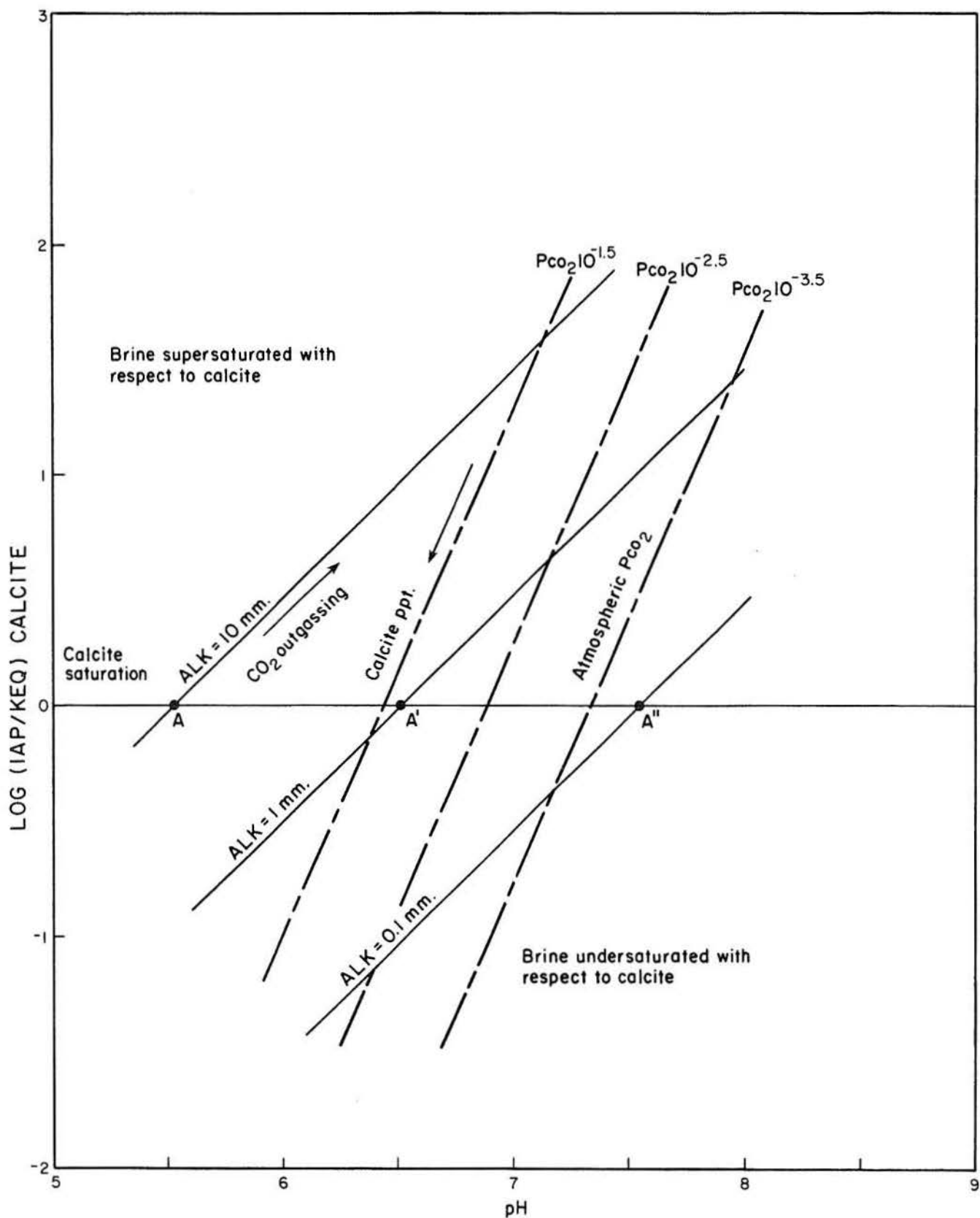
**Figure 22.** *Theoretical behavior of the computed saturation index (SI) with respect to pH accompanying mass transfer of CO₂. Solid lines illustrate path of the SI without calcite precipitation, whereas dashed lines indicate the reaction path commensurate with calcite precipitation after some degree of saturation is attained.*
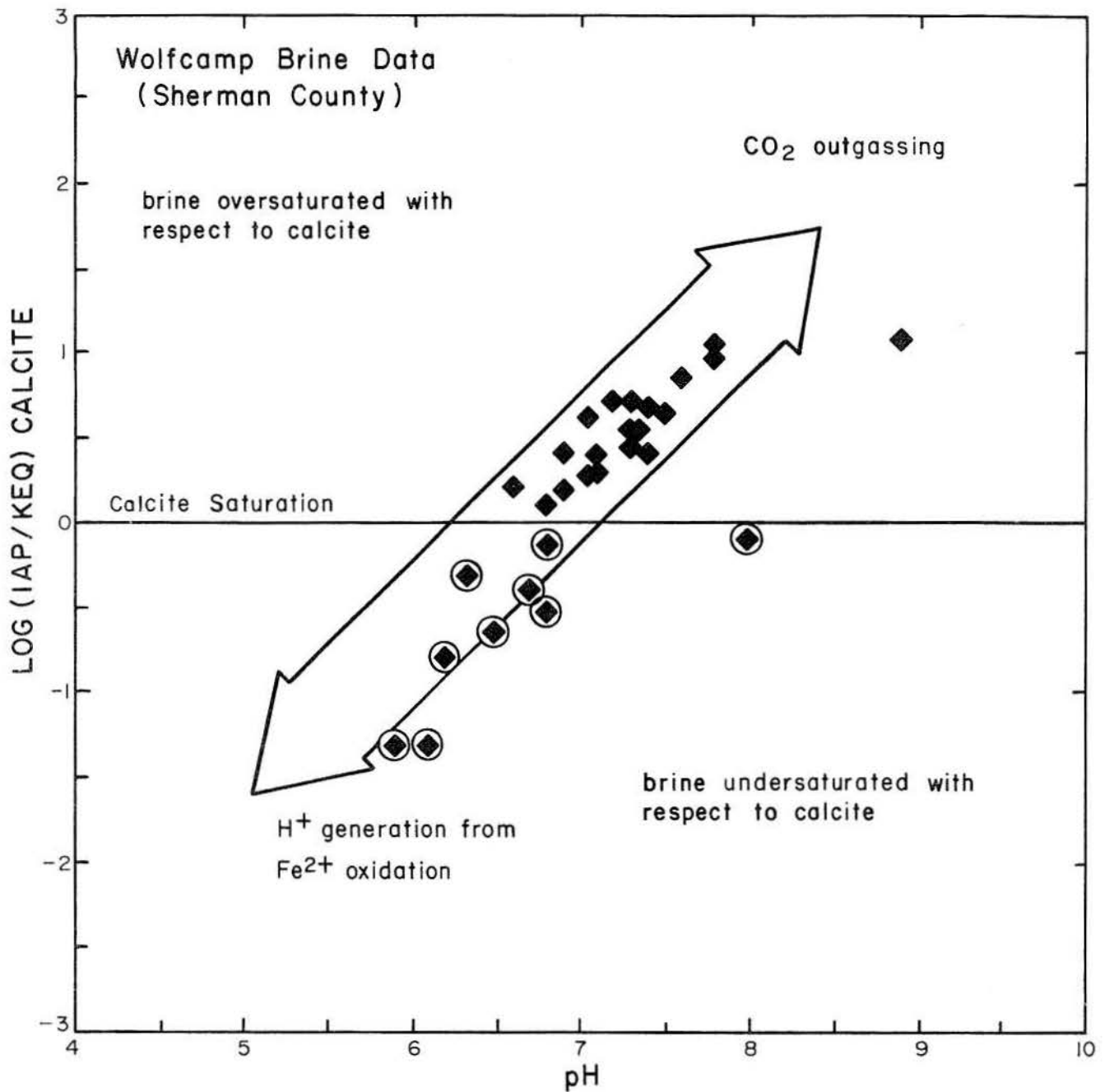
**Figure 23.** *Computed saturation states for Wolfcamp carbonate brines from Sherman County, illustrating the effect of CO₂ loss and iron oxidation.*

however, the lack of hydrocarbon resources results in a lack of data on the chemistry of the deep brines and formation pressures. Available data indicate regional similarity in salinity, which is probably derived from dissolution of evaporites early in the flow path. The basin system is hydraulically contiguous and may have been through-flowing since the early Tertiary; consequently, as many as 50 to 60 pore volumes may have flushed the basins.

Recently developed computer programs were useful in evaluating the brine reaction state. Carbon dioxide loss and iron oxidation during sampling have altered pH values of the brine; however, a reconstruction of in situ $P_{CO_2}$ indicates

that the brines are in equilibrium with the calcite in the carbonate host rocks. Wolfcamp carbonate brines appear to be following the anhydrite phase boundary; however, the granite-wash brines are not in equilibrium with anhydrite because of sulfate reduction.

Future exploratory drilling will be essential for properly collecting and preserving brine samples and obtaining pressure measurements in the most advantageous locations. It is encouraging that drill-stem-test pressure data and brine analyses from wildcat exploration programs are to some extent useful in interpreting the basin characteristics.

## ═══ ACKNOWLEDGMENTS ═══

## ═══ REFERENCES ═══

Allen, B. L., Bolen, E. G., Dregne, H. E., Kitchen, J. W., Mertes, J. D., Reeves, C. C., Jr., Sweazy, R. M., and Wells, D. M., 1971, Environmental impact analysis—salt retention structures upper Brazos River Basin, Texas: Texas Tech University, Water Resources Center, WRC-71-3, 165 p.

Barnes, I., and Clarke, F. E., 1969, Chemical properties of ground water and their corrosion and encrustation effects on wells: U.S. Geological Survey Professional Paper 498-D, 58 p.

Bassett, R. L., and Bentley, M. E., in press, Geochemistry and hydrodynamics of deep-basin brines, Palo Duro and Dalhart Basins, Texas: Journal of Hydrology.

Bassett, R. L., and Griffin, J. A., 1981, AQ/SALT: a mathematical model for computing the reaction potential of brines, *in* Gustavson, T. C., Bassett, R. L., Finley, R. J., Goldstein, A. G., Handford, C. R., McGowen, J. H., Presley, M. W., Baumgardner, R. W., Jr., Bentley, M. E., Dutton, S. P., Hoadley, A. D., Howard, R. C., McGookey, D. A., McGillis, K. A., Palmer, D. P., Ramondetta, P. J., Roedder, E., Simpkins, W. W., and Wiggins, W. D., Geology and geohydrology of the Palo Duro Basin, Texas Panhandle—a report on the progress of nuclear waste isolation feasibility studies (1980): The University of Texas at Austin, Bureau of Economic Geology Geological Circular 81-3, p. 123-125.

Bassett, R. L., and Griffin, J. A., in preparation, AQ/SALT: a model for computing the reaction state of brines: The University of Texas at Austin, Bureau of Economic Geology Geological Circular.

Bassett, R. L., Bentley, M. E., Duncan, E. D., and Griffin, J. A., 1980, Predicting the reaction state of brines in proposed regions of nuclear waste isolation, *in* Scientific basis for nuclear waste management: Materials Research Society Symposium, v. 3, p. 2295-2310.

Bassett, R. L., and Palmer, D. P., 1981, Clay mineralogy of the Palo Duro Basin evaporite sequences, Randall County core, *in* Gustavson, T. C., Bassett, R. L., Finley, R. J., Goldstein, A. G., Handford, C. R., McGowen, J. H., Presley, M. W., Baumgardner, R. W., Jr., Bentley, M. E., Dutton, S. P., Hoadley, A. D., Howard, R. C., McGookey, D. A., McGillis, K. A., Palmer, D. P., Ramondetta, P. J., Roedder, E., Simpkins, W. W., and Wiggins, W. D., Geology and geohydrology of the Palo Duro Basin, Texas Panhandle—a report on the progress of nuclear waste isolation feasibility studies (1980): The University of Texas at Austin, Bureau of Economic Geology Geological Circular 81-3, p. 108-118.

Bentley, M. E., 1981, Regional hydraulics of brine aquifers, Palo Duro and Dalhart Basins, Texas, *in* Gustavson, T. C., Bassett, R. L., Finley, R. J., Goldstein, A. G., Handford, C. R., McGowen, J. H., Presley, M. W., Baumgardner, R. W., Jr., Bentley, M. E., Dutton, S. P., Hoadley, A. D., Howard, R. C., McGookey, D. A., McGillis, K. A., Palmer, D. P., Ramondetta, P. J., Roedder, E., Simpkins, W. W., and Wiggins, W. D., Geology and geohydrology of the Palo Duro Basin, Texas Panhandle—a report on the progress of nuclear waste isolation feasibility studies (1980): The University of Texas at Austin, Bureau of Economic Geology Geological Circular 81-3, p. 93-96.

Berry, F. A. F., 1958, Hydrodynamics and geochemistry of the Jurassic and Cretaceous Systems in the San Juan Basin, northwestern New Mexico and southwestern Colorado: Stanford University, Ph.D. dissertation, 192 p.

Best, J. B., 1961, Pre-Pennsylvanian structure and paleogeology of the Palo Duro Basin in the Texas Panhandle, *in* Geological symposium, western Oklahoma and adjacent Texas: Norman, University of Oklahoma, p. 5-15.

Birsa, D. S., 1977, Subsurface geology of the Palo Duro Basin, Texas Panhandle: The University of Texas at Austin, Ph.D. dissertation, 360 p.

Black, W. M., 1956, A review of drill-stem testing techniques and analysis: Journal of Petroleum Technology, June, p. 21-30.

Bond, D. C., 1972, Hydrodynamics in deep aquifers of the Illinois Basin: Illinois State Geological Survey Circular 470, 51 p.

Carpenter, A. B., 1978, Origin and chemical evolution of brines in sedimentary basins: Oklahoma Geological Survey Circular 79, p. 60-77.

Carpenter, A. B., and Miller, J. C., 1969, Geochemistry of saline subsurface water, Saline County (Missouri): Chemical Geology, v. 4, p. 135-167.

Clayton, R. N., Friedman, I., Graf, D. L., Mayeda, T. K., Meents, W. F., and Shimp, N. F., 1966, The origin of saline formation waters: I. Isotopic composition: Journal of Geophysical Research, v. 71, p. 3869-3882.

Collins, A. G., 1975, Geochemistry of oilfield brines: Amsterdam, Elsevier, 496 p.

Cronin, J. G., 1961, A summary of the occurrence and development of ground water in the Southern High Plains of Texas: Texas Board of Water Engineers Bulletin 6107, 104 p.

Cronin, J. G., and Wells, L. C., 1960, Geology and ground-water resources of Hale County, Texas: Texas Board of Water Engineers Bulletin 6010, 146 p.

Debye, P., and Hückel, E., 1923, Zur Theorie der Electrolyte: Physikalische Zeitschrift, v. 24, p. 185-208.

Dutton, S. P., 1980, Depositional systems and hydrocarbon resource potential of the Pennsylvanian System, Palo Duro and Dalhart Basins, Texas Panhandle: The University of Texas at Austin, Bureau of Economic Geology Geological Circular 80-8, 49 p.

———— 1982, Pennsylvanian fan-delta and carbonate deposition, Mobeetie Field, Texas Panhandle: American Association of Petroleum Geologists Bulletin, v. 66, no. 4, p. 389-407.

Dutton, S. P., Finley, R. J., Galloway, W. E., Gustavson, T. C., Handford, C. R., and Presley, M. W., 1979, Geology and geohydrology of the Palo Duro Basin, Texas Panhandle, a report on the progress of nuclear waste isolation feasibility studies (1978): The University of Texas at Austin, Bureau of Economic Geology Geological Circular 79-1, 99 p.

Earlougher, R. C., Jr., 1977, Advances in well test analysis: Society of Petroleum Engineers/American Institute of Mining Engineers, Henry L. Doherty Series, v. 5, 264 p.

Folk, R. L., and Land, L. S., 1975, Mg/Ca ratio and salinity: two controls over crystallization of dolomite: American Association of Petroleum Geologists Bulletin, v. 59, no. 1, p. 60-68.

Geotechnical Engineers, Inc., 1978, Final report on uncertainties in the detection, measurement, and analysis of selected features pertinent to deep geologic repositories: submitted to University of California, Lawrence Livermore Laboratory, Project 77393, 96 p.

Gustavson, T. C., Bassett, R. L., Finley, R. J., Goldstein, A. G., Handford, C. R., McGowen, J. H., Presley, M. W., Baumgardner, R. W., Jr., Bentley, M. E., Dutton, S. P., Hoadley, A. D., Howard, R. C., McGookey, D. A., McGillis, K. A., Palmer, D. P., Ramondetta, P. J., Roedder, E., Simpkins, W. W., and Wiggins, W. D., 1981, Geology and geohydrology of the Palo Duro Basin, Texas Panhandle—a report on the progress of nuclear waste isolation feasibility studies (1980): The University of Texas at Austin, Bureau of Economic Geology Geological Circular 81-3, 173 p.

Gustavson, T. C., Finley, R. J., and McGillis, K. A., 1980a, Regional dissolution of Permian salt in the Anadarko, Dalhart, and Palo Duro Basins of the Texas Panhandle: The University of Texas at Austin, Bureau of Economic Geology Report of Investigations No. 106, 40 p.

Gustavson, T. C., Presley, M. W., Handford, C. R., Finley, R. J., Dutton, S. P., Baumgardner, R. W., Jr., McGillis, K. A., and Simpkins, W. W., 1980b, Geology and geohydrology of the Palo Duro Basin, Texas Panhandle—a report on the progress of nuclear waste isolation feasibility studies (1979): The University of Texas at Austin, Bureau of Economic Geology Geological Circular 80-7, 99 p.

Gutentag, E. D., and Weeks, J. B., 1980, The water table in the High Plains aquifer in 1978 in parts of Colorado, Kansas, Nebraska, New Mexico, Oklahoma, South Dakota, Texas, and Wyoming: U.S. Geological Survey, Hydrologic Investigations Atlas HA-642.

Handford, C. R., 1980, Lower Permian facies of the Palo Duro Basin, Texas: The University of Texas at Austin, Bureau of Economic Geology Report of Investigations No. 102, 31 p.

Handford, C. R., and Dutton, S. P., 1980, Pennsylvanian - Early Permian depositional systems and shelf-margin evolution, Palo Duro Basin,

Texas: American Association of Petroleum Geologists Bulletin, v. 64, no. 1, p. 88-106.

Handford, C. R., Wiggins, W. D., Palmer, D. P., and Bassett, R. L., in preparation, Sedimentology, petrography, and diagenesis of Permian evaporites, Randall County, Texas: The University of Texas at Austin, Bureau of Economic Geology Report of Investigations.

Hanshaw, B. B., and Bredehoeft, J. D., 1968a, On the maintenance of anomalous fluid pressures: I. Thick sedimentary sequences: Geological Society of America Bulletin, v. 79, p. 1097-1106.

_____ 1968b, On the maintenance of anomalous fluid pressures: II. Source layer at depth: Geological Society of America Bulletin, v. 79, p. 1107-1122.

Hanshaw, B. B., and Hill, G. A., 1969, Geochemistry and hydrodynamics of the Paradox Basin region, Utah, Colorado, and New Mexico: Chemical Geology, v. 4, p. 263-294.

Harvie, C. E., and Weare, J. H., 1980, The prediction of mineral solubilities in natural waters: Geochimica et Cosmochimica Acta, v. 44, p. 981-997.

Harvie, C. E., Weare, J. H., Hardie, L. D., and Eugster, H. P., 1980, Evaporation of sea water: calculated mineral sequences: Science, v. 4, p. 498-500.

Hitchon, Brian, 1963a, Geochemical studies of natural gas: Part I. Hydrocarbons in western Canadian natural gases: Journal of Canadian Petroleum Technology, v. 2, p. 60-73.

_____ 1963b, Geochemical studies of natural gas: Part II. Acid gases in western Canadian natural gases: Journal of Canadian Petroleum Technology, v. 2, p. 100-116.

_____ 1963c, Geochemical studies of natural gas: Part III. Inert gases in western Canadian natural gases: Journal of Canadian Petroleum Technology, v. 2, p. 165-176.

_____ 1969a, Fluid flow in the western Canada sedimentary basin: I. Effect of topography: Water Resources Research, v. 5, p. 186-195.

_____ 1969b, Fluid flow in the western Canada sedimentary basin: II. Effect of geology: Water Resources Research, v. 5, p. 460-469.

Hitchon, B., and Hayes, J., 1971, Hydrodynamics and hydrocarbon occurrences, Surat Basin, Queensland, Australia: Water Resources Research, v. 7, p. 658-676.

Horner, D. R., 1951, Pressure build-up in wells: Proceedings, Third World Petroleum Congress, Leiden, v. 2, p. 503-507.

Hunt, J. M., 1979, Petroleum geochemistry and geology: San Francisco, Freeman, 617 p.

Johnson, K. S., 1976, Evaluation of Permian salt deposits in the Texas Panhandle and western Oklahoma for underground storage of radioactive wastes: Oak Ridge, Tennessee, Report to Union Carbide Corporation, Oak Ridge National Laboratories.

Keys, W. S., and MacCary, L. M., 1971, Application of borehole geophysics to water-resources investigations, in U.S. Geological Survey, Techniques in water resources investigations, Book 2, Chapter E1: 126 p.

Kharaka, Y. K., and Barnes, I., 1973, SOLMNEQ: solution-mineral equilibrium computations: National Technical Information Service Technical Report PB214-899, 82 p.

Larson, T. G., 1971, Hydrodynamic interpretation of the Mid-Continent: American Association of Petroleum Geologists Memoir 15, p. 1043-1046.

Leifeste, D. K., Blakey, J. F., and Hughes, L. S., 1971, Reconnaissance of the chemical quality of surface waters of the Red River Basin, Texas: Texas Water Development Board Report 129, 68 p.

Matthews, C. S., and Russell, D. G., 1967, Pressure buildup and flow tests in wells: Society of Petroleum Engineers/American Institute of Mining Engineers, Henry L. Doherty Series, v. 1, 167 p.

McGowen, J. H., Granata, G. E., and Seni, S. J., 1979, Depositional framework of the Lower Dockum Group (Triassic): The University of Texas at Austin, Bureau of Economic Geology Report of Investigations No. 97, 60 p.

McNeal, R. P., 1965, Hydrodynamics of the Permian Basin, in Young, A., and Galley, J. E., eds., Fluids in subsurface environments: American Association of Petroleum Geologists Memoir 4, p. 308-326.

Moore, B. J., 1976, Analyses of natural gases, 1917-74: Bureau of Mines Computer Printout 1-76, NTIS PB-251 202, 889 p.

Myers, B. N., 1969, Compilation of results of aquifer tests in Texas: Texas Water Development Board Report 98, 532 p.

National Research Council, 1928, International critical tables: New York, McGraw-Hill, v. 4, 235 p.

Nicholson, J. H., 1960, Geology of the Texas Panhandle, in Aspects of the geology of Texas, a symposium: University of Texas, Austin, Bureau of Economic Geology Publication No. 6017, p. 51-64.

Panhandle Geological Society, 1961, Oil and gas fields of the Texas and Oklahoma Panhandles: Panhandle Geological Society, 264 p.

Petroleum Information Corporation, 1980, Oil and gas map of Texas: Denver, scale 1:862,000, 1 sheet.

Pitzer, K. S., 1979, Electrolyte theory—improvements since Debye and Hückel: Accounts of Chemical Research, v. 19, p. 371-377.

Rittenhouse, G., 1967, Bromine in oil-field waters and its use in determining possibilities or origin of these waters: American Association of Petroleum Geologists Bulletin, v. 51, p. 2340-2440.

Rogatz, H., 1939, Geology of the Panhandle oil and gas field: American Association of Petroleum Geologists Bulletin, v. 23, p. 983-1053.

Scatchard, G., 1968, The excess free energy and related properties of solutions containing electrolytes: Journal of American Chemical Society, v. 30, p. 3124-3127.

Schlumberger, 1972, Log interpretation: I. Principles: New York, Schlumberger Limited, 113 p.

Seni, S. J., 1980, Sand-body geometry and depositional systems, Ogallala Formation, Texas: The University of Texas at Austin, Bureau of Economic Geology Report of Investigations No. 105, 35 p.

Texas Department of Water Resources, in press, Approximate altitude of water levels in the High Plains aquifer in Texas, 1980.

Tóth, J., 1978, Gravity-induced cross-formational flow of formation fluids, Red Earth region, Alberta, Canada: analysis, patterns, and evolution: Water Resources Research, v. 14, p. 805-843.

Weeks, J. B., and Gutentag, E. D., 1981, Bedrock geology, altitude of base, and saturated thickness of the High Plains aquifer in parts of Colorado, Kansas, Nebraska, New Mexico, Oklahoma, South Dakota, Texas, and Wyoming: U.S. Geological Survey, Hydrologic Investigations Atlas HA-648.

White, D. E., 1965, Saline waters of sedimentary rocks, in Young, A., and Galley, J. E., eds., Fluids in subsurface environments: American Association of Petroleum Geologists Memoir 4, p. 342-366.

## APPENDIX A: Horner Plots for Wolfcamp Carbonates

The drill-stem-test charts received from operators in the Palo Duro Basin have been analyzed according to the Horner method (Horner, 1951). The equation described by Horner (equation 1) is an approximation of an exact solution for pressure changes in a single well in an infinite reservoir:

$$Pw = Po - \frac{q\,\mu}{4\pi\,kh} \ln \frac{(to + Dt)}{Dt} \quad (1)$$

where
- $h$ = thickness of the tested interval (ft)
- $k$ = average permeability (md)
- $Po$ = undisturbed formation pressure (psi)
- $Pw$ = pressure at the well bore (psi)
- $q$ = rate of production

- $qa$ = average rate of production in the previous flowing period (bbl/d)
- $to$ = length of production time (hr)
- $Dt$ = elapsed time since pressure build-up began after final production period (hr)
- $\mu$ = viscosity of the fluid (cp)

On conversion of equation 1 to standard units employed by the petroleum industry the expression becomes

$$Pw = Po - \frac{162.6\,qa\,\mu}{kh} \log \frac{to + Dt}{Dt} \quad (2)$$

A semilog plot of the pressure data (Pw) against $\log[(to + Dt)/Dt]$ should approach a straight line after the early production effects have diminished. The slope (m) of the straight-line part of this plot is computed as

$$m = \frac{\Delta\,Pw}{\text{cycle of log } (to + Dt)/Dt} \quad (3)$$

which reduces equation 2 to

$$k = \frac{162.6\,qa\,\mu}{mh} \quad (4)$$

Extrapolation of the straight line according to equation 5

$$\log \frac{to + Dt}{Dt} = 0 \quad (5)$$

will yield the estimated undisturbed formation pressure where Pw equals Po.

The Horner plots shown in figures A1 through A19 summarize the available data for drill-stem tests in the Wolfcamp carbonates. Slope (m), correlation coefficient (r), number of points used for the extrapolation (n), and the extrapolated formation pressures (Pi and Pf) are tabulated for the initial shut-in pressure (ISIP) and final shut-in pressure test (FSIP), respectively. Equivalent fresh-water heads ($H_{ISIP}$, $H_{FSIP}$) have been computed for each extrapolated undisturbed formation pressure (Po) by dividing by 0.433 psi/ft and correcting for elevation. Permeability was determined from equation 4 using the data from the Horner plot and information provided with the drill-stem-test chart obtained from the service company. These data are summarized in table A-1.
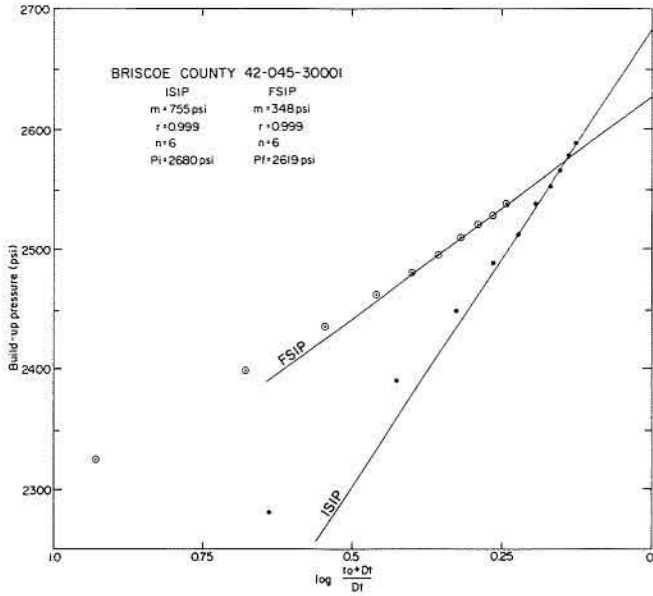
*Figure A-1.*
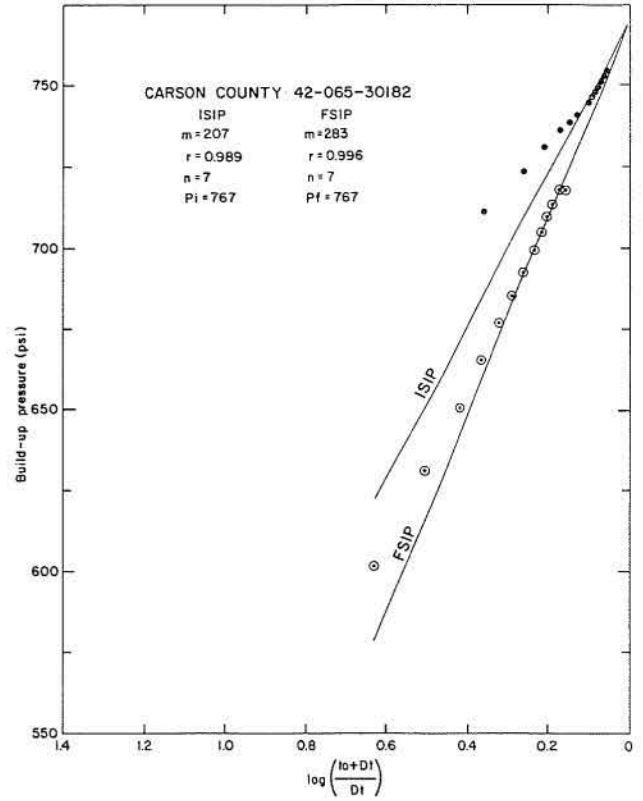


*Figure A-2.*
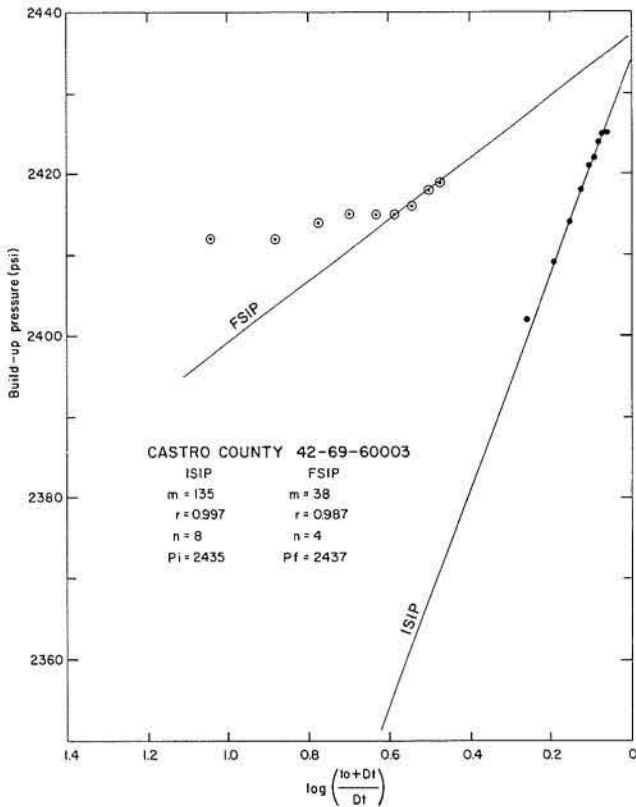


*Figure A-3.*
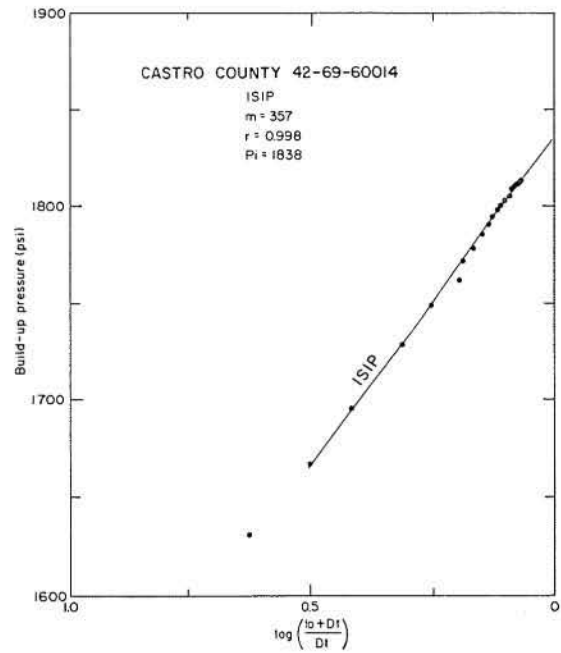


*Figure A-4.*
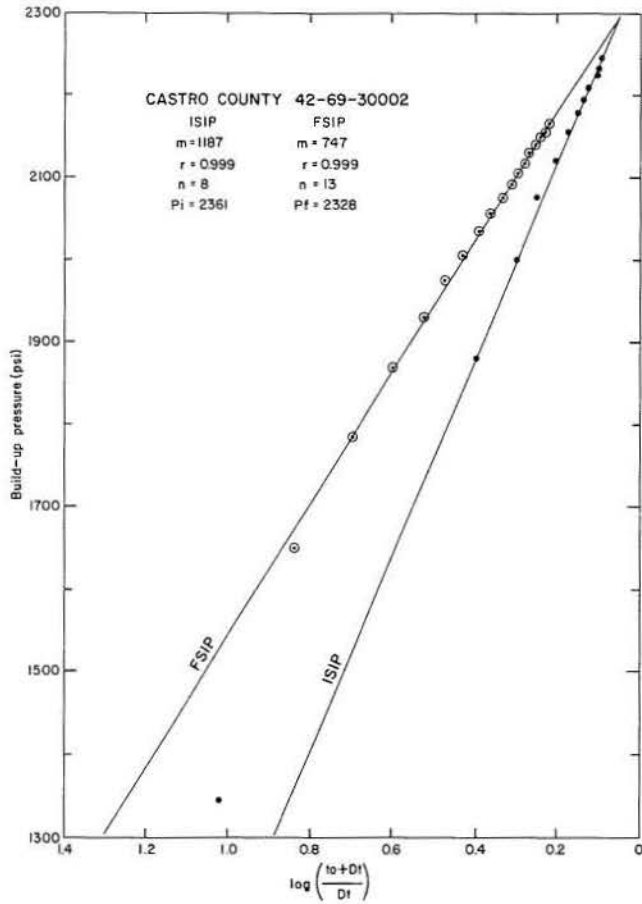
Figure A-5.
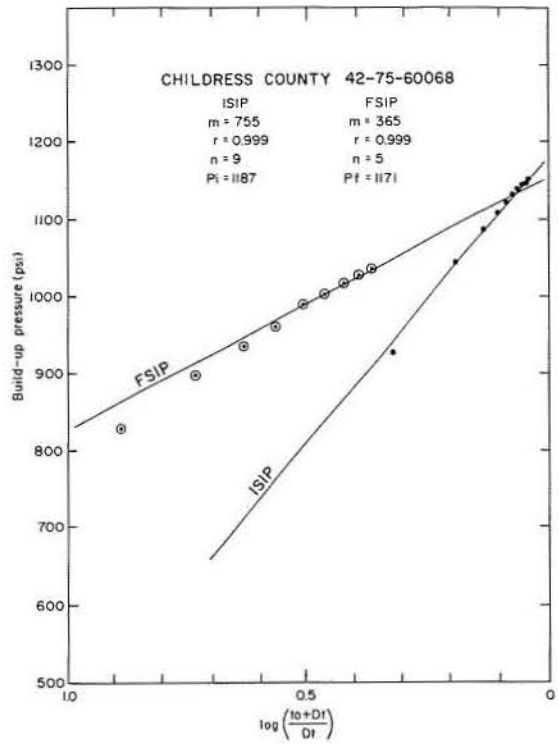


Figure A-6.
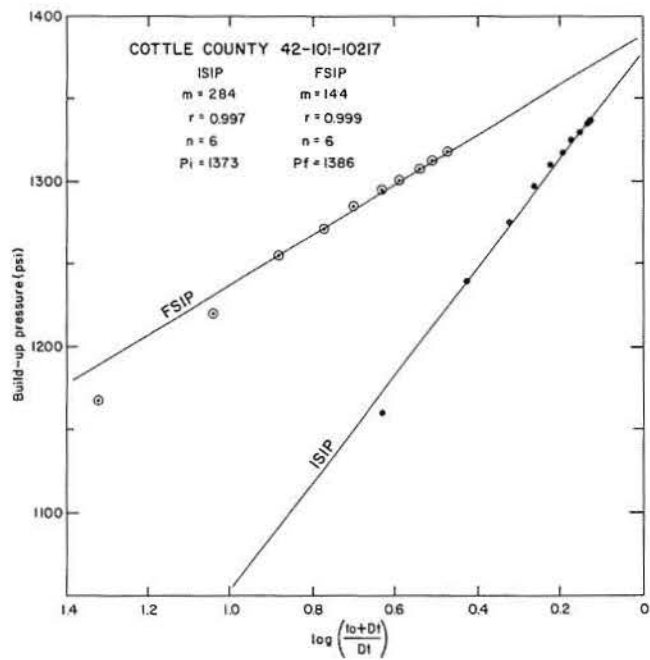


Figure A-7.



Figure A-8.

40
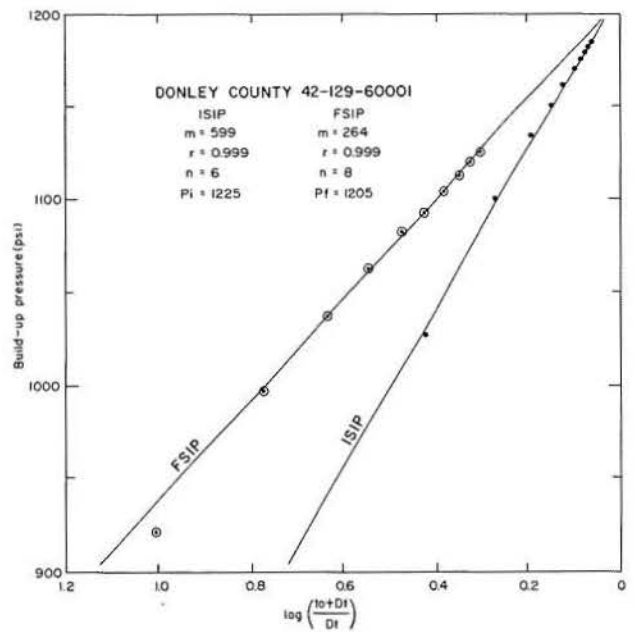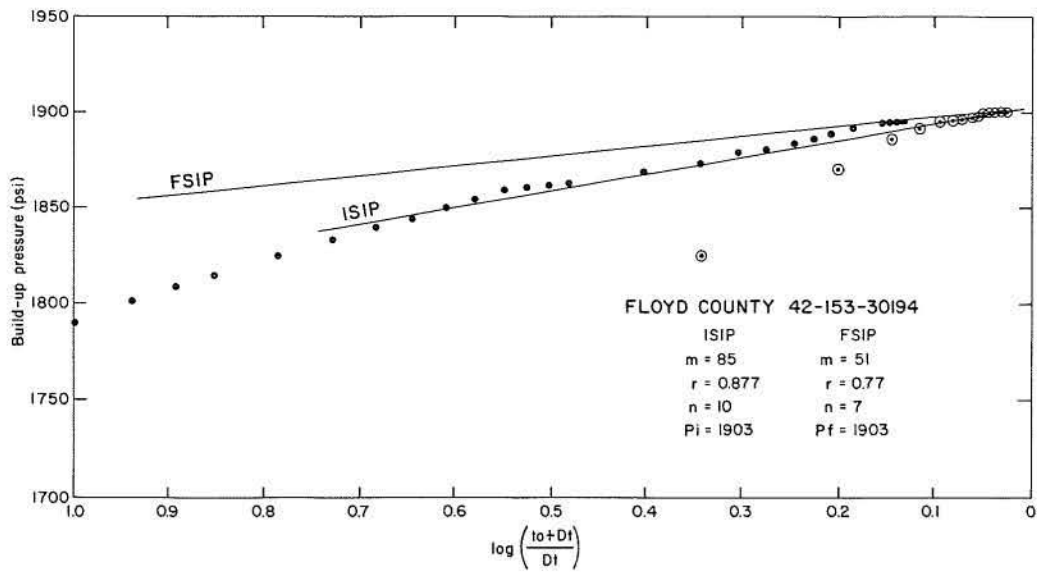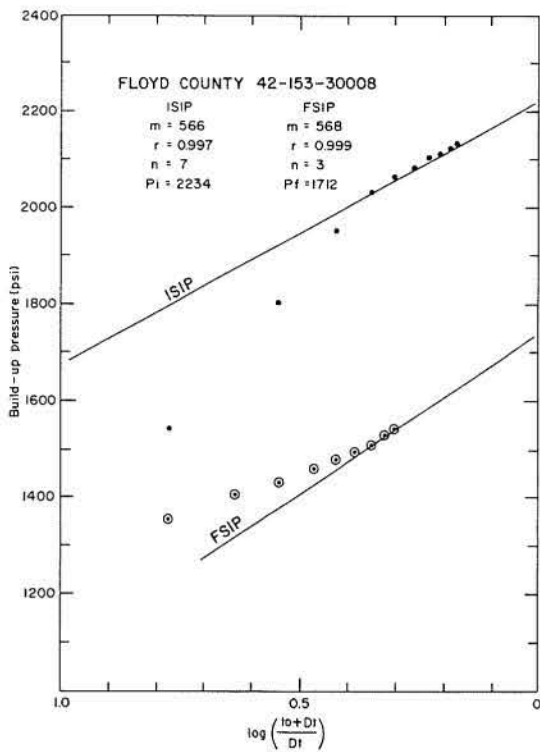
Figure A-9.



Figure A-10.
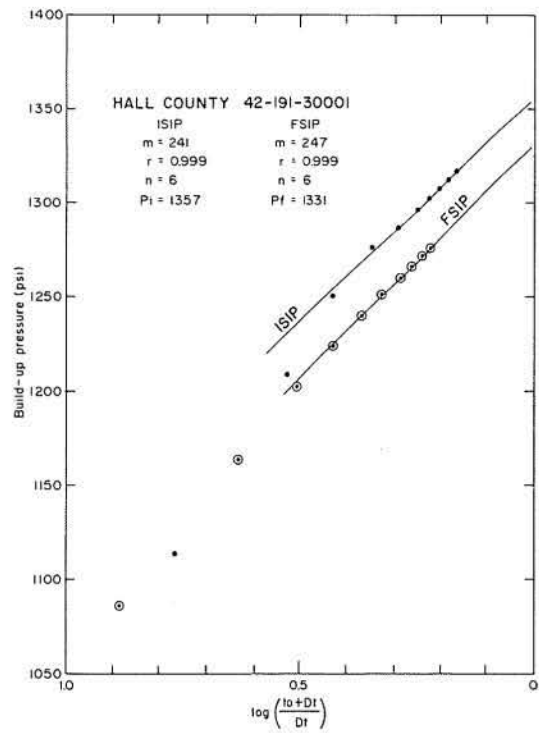


Figure A-11.

41
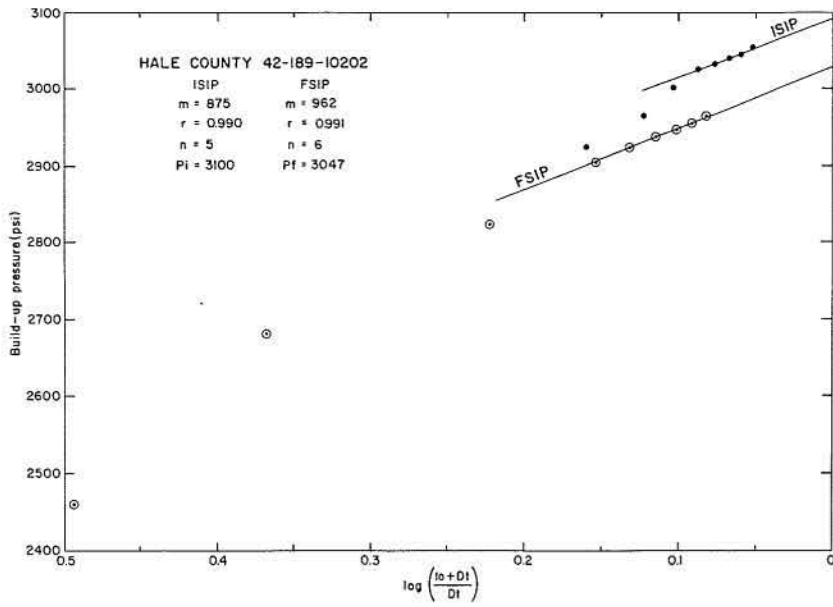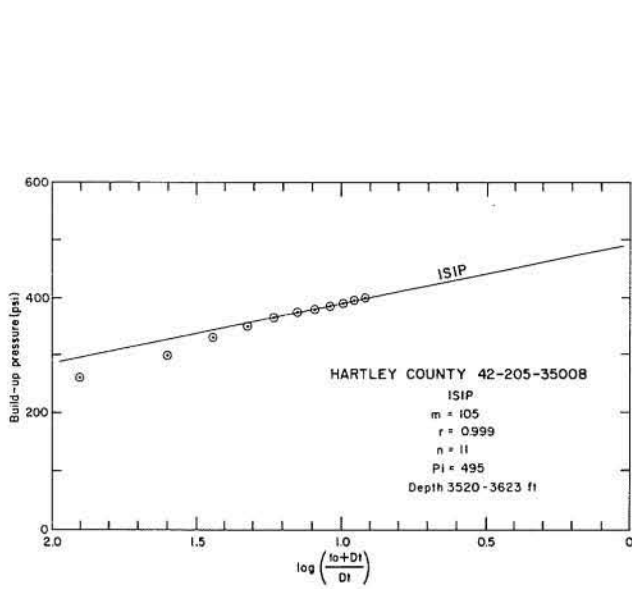
**Figure A-12.**



**Figure A-13.**



**Figure A-14.**

42
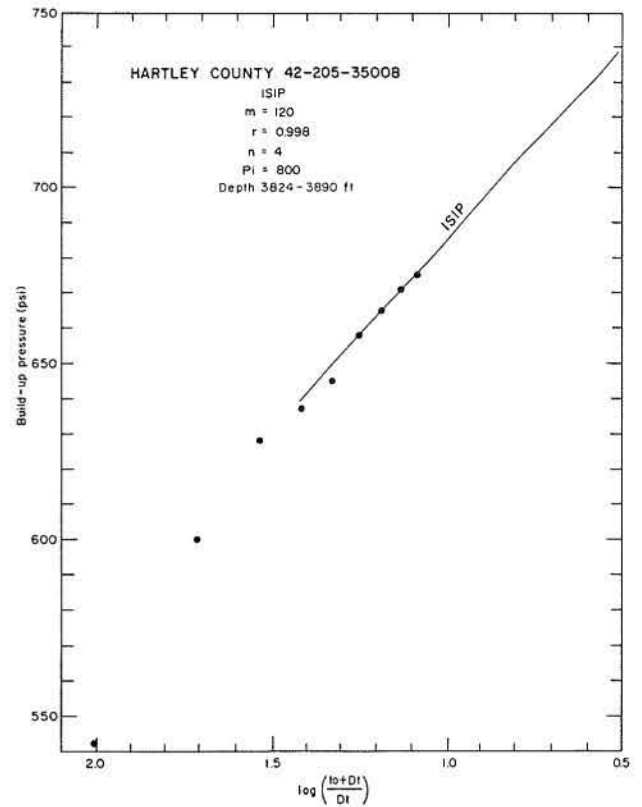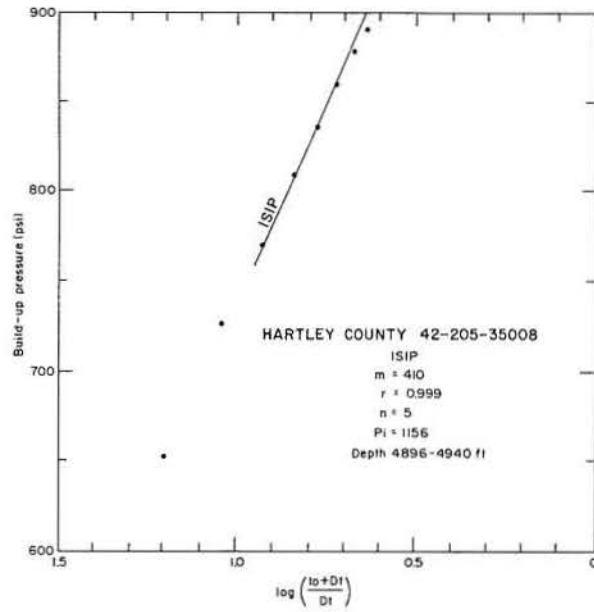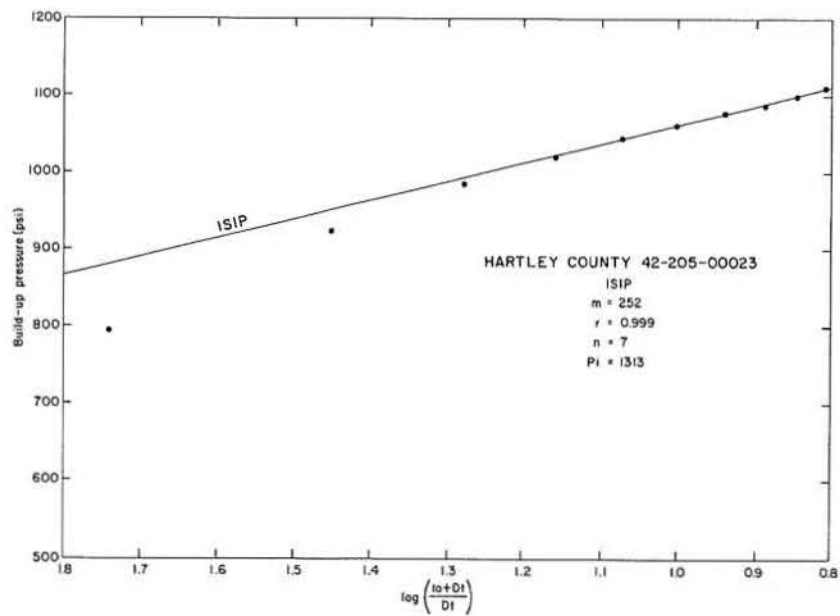
Figure A-15.



Figure A-16.
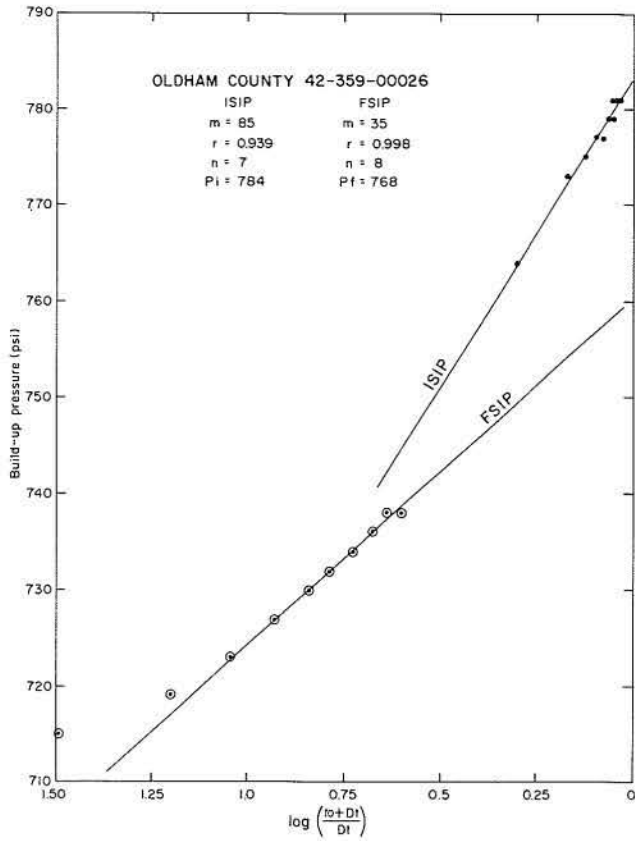
Figure A-17.
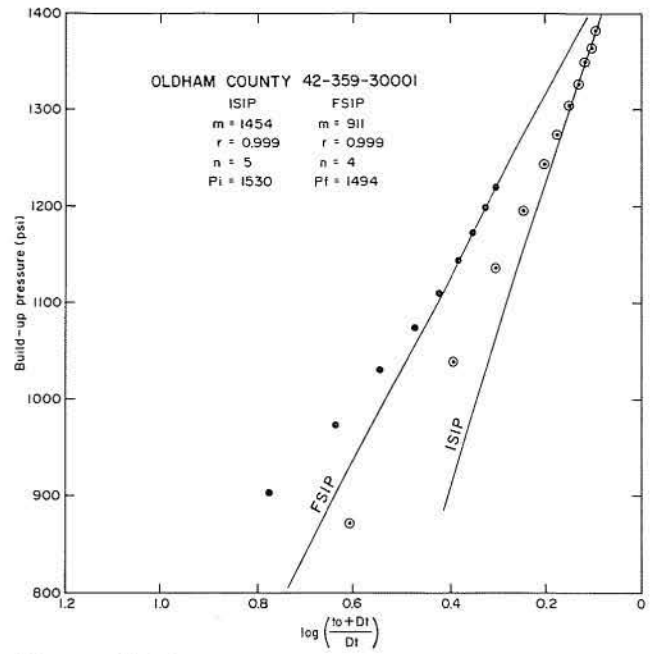


Figure A-18.



Figure A-19.

44
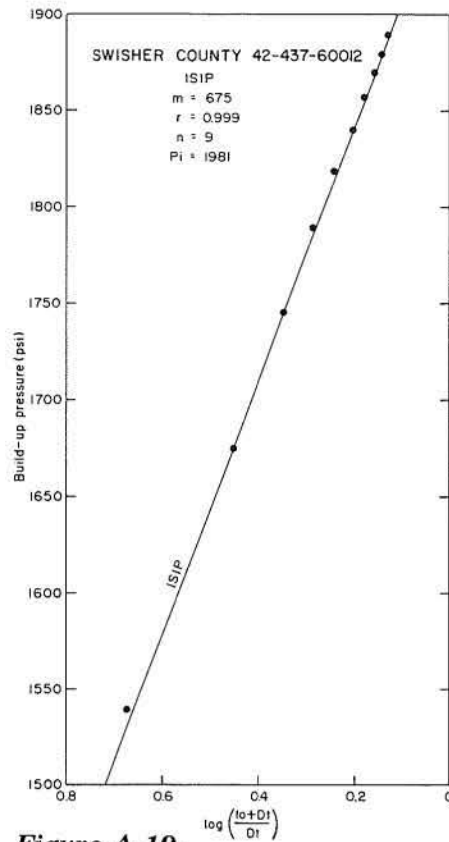
Table A-1. Hydraulic parameters derived from an analysis of drill-stem-test charts using the Horner method (1951). The selected permeability and hydraulic values are underscored in the table.

| County | BEG well no. | Company | API no. | Depth tested (ft) | Thickness (ft) | K_ISIP (md) | K_FSIP (md) | H_ISIP (ft) | H_FSIP (ft) | Comments††† |
|---|---|---|---|---|---|---|---|---|---|---|
| Briscoe | 21 | Cockrell | 42-045-30001 | 6,344-6,411 | 67 | 8.5 | 1.31 | 3,105† | 2,964† | L. Wfc. shelf** |
| Carson | 38 | Shenandoah | 42-065-30182 | 3,601-3,615 | 14 | 1.1 | 0.24 | 1,551 | 1,551 | M. Wfc. back shelf** |
| Castro | 1 | Amarillo | 42-069-60003 | 6,909-7,059 | 150 | 64.0 | 26.0 | 2,500 | 2,505 | M. Wfc. por. dol. |
| Castro | 7 | Union | 42-069-60014 | 5,183-5,228 | 45 | 6.0 | — | 2,750 | — | T. Wfc. sl. por. (sabk.) |
| Castro | 7 | Union | 42-069-60014 | 5,838-5,932 | 94 | *** | *** | 2,206 | 2,206 | M. Wfc. chalky ls. |
| Castro | 10 | Phillips | 42-069-30002 | 6,762-6,782 | 20 | 0.36 | 0.27 | 2,560 | 2,483 | U. Wfc. sl. por. dol. ls. (sabk.) |
| Childress | 76 | Westex | 42-075-60068 | 2,633-2,663 | 30 | 0.95 | 0.03 | 1,818 | 1,781 | U. Wfc. dol. and ls.** |
| Cottle | 10 | Murphy | 42-101-10217 | 3,169-3,178 | 9 | 15.5 | 8.8 | 1,867 | 1,897 | U. Wfc. sl. calc. dol. (sabk.) |
| Donley | 31 | Shell | 42-129-60001 | 3,350-3,399 | 49 | 0.51 | 0.79 | 1,797 | 1,754 | U. Wfc. por. ls. (sabk.) |
| Floyd | * | Amoco | 42-153-30194 | 5,500-5,581 | 81 | 8.9 | 8.3 | 2,081 | 2,081 | * |
| Floyd | * | Ken Pet. | 42-153-30008 | 4,660-4,750 | 90 | 0.68 | 0.59 | 3,597†† | 2,392†† | * |
| Hale | 6 | Mobil | 42-189-10202 | 7,864-8,036 | 172 | 1.04 | 0.1 | 2,583 | 2,461 | L. Wfc. sl. por. ls. (?) may be U. Penn. |
| Hall | * | Americas | 42-191-30001 | 3,365-3,390 | 25 | 0.62 | 0.44 | 1,890 | 1,830 | * |
| Hartley | 13 | Standard | 42-205-35008 | 3,520-3,623 | 66 | 0.77 | — | 1,381 | — | T. Wfc. an. dol. (sabk.) |
| Hartley | 13 | Standard | 42-205-35008 | 3,824-3,890 | 66 | 1.0 | — | 1,796 | — | U. Wfc. dol. ls. (sabk.) |
| Hartley | 13 | Standard | 42-205-35008 | 4,896-4,940 | 44 | 0.24 | — | 1,574 | — | L. Wfc. calc. ss. |
| Hartley | 16 | Standard | 42-205-00023 | 3,916-3,957 | 41 | 1.75 | — | 3,007 | — | U. Wfc. dol. ls. (sabk.) |
| ***Lamb | * | Gulf | 42-279-30045 | 7,352-7,404 | 52 |  | *** | 2,522 | 2,510 | * |
| ***Motley | 13 | Mobil | 42-345-00015 | 4,674-4,715 | 41 |  | *** | 1,950 | 1,947 | U. Wfc. dol. (sabk.) |
| Oldham | 4 | Shell | 42-359-00026 | 3,446-3,471 | 25 | 27.0 | 44.0 | 1,945 | 1,908 | U. Wfc. ** |
| Oldham | 48 | Shell | 42-359-30001 | 5,340-5,367 | 27 | 1.0 | 0.6 | 1,824 | 1,741 | M. Wfc. ls. |
| ***Potter | 26 | Rice | 42-375-35013 | 3,907-4,050 | 143 |  | *** | 1,486 | — | T. Wfc. por. dol. |
| Swisher | 8 | Burdell | 42-437-60012 | 5,765-5,796 | 31 | 0.1 | — | 2,360 | — | U. Wfc. por. ls. |

† The head values appear to be anomalously high compared with surrounding values; however, the test appears acceptable mechanically.

†† A 1,000-psi difference between ISIP and FSIP is not explainable at this time; the higher value is selected.

††† L. = lower, M. = mid, U. = upper, ls. = limestone, dol. = dolomite, por. = porous, sl. = slightly, T. = top, Wfc. = Wolfcamp, calc. = calcareous, sabk. = sabkha may have influenced dolomitization, Penn. = Pennsylvanian, an. = anhydritic.

* no log information   **no sample log   ***build-up test reached formation pressure; permeability cannot be computed; consequently an illustration of the data is not provided on the following pages.

— only one shut-in period.

# APPENDIX B:
## Chemical Composition
### of Formation Brines

The chemical compositions of brines listed in the following tables were obtained from either the Petroleum Data System Brine file at the University of Oklahoma or from petroleum companies that forwarded these analyses to us along with additional information on drill-stem tests conducted in the Palo Duro Basin. None of the brines were collected or analyzed by the BEG; consequently, only standard industry procedures were employed during their collection.

Substantial outgassing of $CO_2$ has undoubtedly occurred during sampling (see text); thus, the reported pH is, in general, too high. As a result, the brines all compute to be supersaturated with respect to calcite. A computer simulation program was used to compute a new pH for Wolfcamp brines, which represents the most likely in situ partial pressure of $CO_2$ at the calcite phase boundary. We suggest that this computed value is representative of the brine pH in the formation, and consequently we list this value with the analyses in the following tables as "$pH_c$." The constraints on the brine chemistry of granite-wash aquifers are less clear. Therefore, the computed values for pH are not listed, pending further investigation. Hydrologic test wells currently being drilled will provide the first brine samples collected by the BEG from the Permian and Pennsylvanian granite-wash aquifers.

The wells from which these samples were collected can be located by comparing the underlined TDS values on figures 10 and 11 with those listed in table B-1. Temperatures are computed using the average geothermal gradient for the region (0.611°C/100 ft).

*Table B-1. Chemical composition of brines collected from wells penetrating the Wolfcamp deep-basin aquifer.*

| | | | | | | | | | | | |
|---|---|---|---|---|---|---|---|---|---|---|---|
| **WOLFCAMP CARBONATES** | | | | | | | | | | | |
| County | Depth (ft) | TDS (mg/L) | Temp (°C) | Reported pH | Ca (mg/L) | Na (mg/L) | Mg (mg/L) | HCO$_3$ (mg/L) | Cl (mg/L) | SO$_4$ (mg/L) | pH$_c$ |
| Hartley | 4,469-4,520 | 164,026 | 45.6 | 6.8 | 1,100 | 60,310 | 1,069 | 302 | 88,154 | 13,090 | 6.59 |
| Potter | 4,573-5,395 | 120,000 | 46.2 | 7.9 | 3,660 | 40,900 | 1,350 | 278 | 71,600 | 2,350 | 6.19 |
| Potter | 4,824-4,875 | 172,000 | 47.8 | 6.8 | 7,960 | 56,200 | 1,540 | 173 | 104,000 | 1,600 | 6.15 |
| Potter | 4,790 | 142,121 | 47.3 | 8.8 | 6,578 | 47,193 | 841 | 106 | 85,566 | 1,735 | 6.40 |
| Moore | 3,300-3,310 | 116,228 | 38.5 | 7.0 | 1,344 | 42,692 | 510 | 82 | 64,271 | 7,326 | 7.00 |
| Moore | 3,310-3,315 | 133,399 | 38.5 | 7.0 | 1,165 | 49,185 | 697 | 401 | 73,579 | 8,365 | 6.50 |
| Moore | 3,224 | 132,376 | 38.0 | 7.0 | 1,358 | 49,810 | 725 | 172 | 76,090 | 5,119 | 6.81 |
| Moore | 3,818 | 139,493 | 41.6 | 7.0 | 5,657 | 45,060 | 2,224 | 49 | 84,610 | 1,892 | 6.87 |
| Moore | 3,224 | 120,953 | 38.0 | 7.0 | 3,800 | 41,564 | 1,018 | 0 | 71,300 | 2,992 | — |
| Moore | 3,224 | 160,822 | 38.0 | 7.0 | 5,380 | 54,905 | 1,493 | 131 | 97,181 | 1,729 | 6.44 |
| Moore | 3,224 | 180,247 | 38.0 | 7.0 | 3,929 | 64,283 | 1,284 | 171 | 107,437 | 3,141 | 6.41 |
| Moore | 3,073-3,274 | 177,402 | 37.1 | 6.9 | 3,563 | 64,177 | 898 | 73 | 105,431 | 3,259 | 6.82 |
| Moore | 3,200 | 127,058 | 37.9 | 7.0 | 2,347 | 45,541 | 865 | 210 | 73,184 | 4,908 | 6.52 |
| Moore | 3,173 | 150,834 | 37.7 | 7.0 | 2,001 | 55,171 | 865 | 269 | 86,718 | 5,808 | 6.47 |
| Moore | 3,242 | 136,984 | 38.1 | 7.0 | 3,205 | 47,742 | 1,452 | 93 | 80,700 | 3,789 | 6.78 |
| Wheeler | 1,969-2,018 | 166,835 | 30.3 | 6.2 | 10,024 | 49,168 | 3,393 | 479 | 101,920 | 1,850 | 6.20 |
| Hutchinson | 2,600 | 154,115 | 34.2 | 7.0 | 3,183 | 54,512 | 1,425 | 237 | 90,877 | 3,881 | 6.40 |
| Hutchinson | 3,005 | 158,938 | 36.7 | 7.0 | 3,942 | 55,658 | 1,434 | 234 | 94,651 | 3,017 | 6.30 |
| Hutchinson | 3,040 | 156,592 | 36.9 | 7.0 | 2,811 | 56,243 | 1,167 | 273 | 91,839 | 4,256 | 6.35 |
| Hutchinson | 3,200 | 152,562 | 38.0 | 7.0 | 8,586 | 47,372 | 2,008 | 134 | 92,561 | 1,898 | 6.31 |
| Hutchinson | 3,200 | 174,353 | 37.9 | 7.3 | 10,870 | 52,144 | 2,874 | 121 | 106,614 | 1,728 | 6.30 |
| Hutchinson | 3,160 | 169,457 | 37.6 | 7.2 | 10,961 | 49,973 | 3,003 | 188 | 104,228 | 1,101 | 6.11 |
| Hutchinson | 3,200 | 175,373 | 38.0 | 7.0 | 9,767 | 54,990 | 2,069 | 162 | 106,729 | 1,654 | 6.19 |
| Hutchinson | 3,200 | 168,375 | 38.0 | 7.4 | 21,038 | 38,674 | 2,978 | 135 | 104,510 | 1,092 | 6.11 |
| Hutchinson | 3,224 | 165,968 | 38.0 | 7.5 | 9,964 | 50,280 | 2,569 | 121 | 101,093 | 1,939 | 6.33 |
| Hutchinson | 3,224 | 168,625 | 38.0 | 7.7 | 10,537 | 50,277 | 2,841 | 108 | 102,845 | 2,014 | 6.36 |
| Hutchinson | 3,224 | 167,658 | 38.0 | 5.9 | 9,155 | 52,749 | 1,982 | 54 | 101,851 | 1,864 | 6.37 |
| Hutchinson | 3,226 | 164,801 | 38.0 | 6.7 | 9,496 | 50,387 | 2,525 | 204 | 100,268 | 1,918 | 6.11 |
| Hutchinson | 3,224 | 173,664 | 38.0 | 7.5 | 10,547 | 51,871 | 3,145 | 135 | 106,867 | 1,098 | 6.27 |

| County | Depth (ft) | TDS (mg/L) | Temp (°C) | Reported pH | Ca (mg/L) | Na (mg/L) | Mg (mg/L) | HCO₃ (mg/L) | Cl (mg/L) | SO₄ (mg/L) | pHc |
|--------|-----------|-----------|-----------|-------------|-----------|-----------|-----------|-------------|-----------|-----------|-----|
| Hutchinson | 3,160 | 174,055 | 37.6 | 7.4 | 11,527 | 52,654 | 2,033 | 188 | 106,481 | 1,169 | 6.09 |
| Hutchinson | 2,960 | 162,794 | 36.4 | 7.5 | 9,701 | 50,242 | 1,980 | 161 | 98,991 | 1,717 | 6.20 |
| Hutchinson | 3,224 | 166,372 | 38.0 | 7.2 | 9,095 | 51,183 | 2,707 | 157 | 101,433 | 1,795 | 6.24 |
| Hutchinson | 3,224 | 177,774 | 38.0 | 8.3 | 8,112 | 56,818 | 2,653 | 135 | 108,041 | 1,946 | 6.33 |
| Hutchinson | 3,224 | 178,885 | 38.0 | 8.5 | 5,550 | 61,007 | 1,960 | 176 | 106,027 | 2,947 | 6.31 |
| Hutchinson | 3,224 | 144,000 | 38.0 | 7.5 | 3,240 | 50,200 | 1,540 | 378 | 85,100 | 3,100 | 7.50(?) |
| Hutchinson | 3,279 | 146,000 | 38.3 | 7.5 | 4,000 | 50,500 | 1,520 | 122 | 87,600 | 2,050 | 6.58 |
| Hutchinson | 2,978 | 158,459 | 36.5 | 7.0 | 4,552 | 54,444 | 1,661 | 390 | 94,501 | 2,911 | 6.04 |
| Hutchinson | 3,255 | 149,500 | 38.2 | 7.2 | 6,000 | 45,400 | 2,300 | 261 | 85,400 | 1,800 | 6.25 |
| Hutchinson | 3,224 | 138,000 | 38.0 | 8.2 | 2,500 | 48,600 | 1,100 | 67 | 81,400 | 4,100 | — (?) |
| Hutchinson | 3,262 | 130,100 | 38.2 | 8.7 | 2,700 | 43,700 | 1,100 | 55 | 74,300 | 3,500 | — |
| Hutchinson | 3,250 | 144,460 | 38.2 | 8.8 | 2,500 | 47,800 | 1,000 | 92 | 80,100 | 3,900 | 6.85 |
| Hutchinson | 3,979 | 144,000 | 42.6 | 8.0 | 2,480 | 52,000 | 976 | 156 | 84,400 | 4,000 | — |
| Hutchinson | 3,224 | 149,000 | 38.0 | 7.7 | 3,600 | 52,400 | 1,370 | 293 | 89,000 | 2,780 | 6.35 |
| Hutchinson | 3,237 | 143,000 | 38.1 | 7.6 | 5,880 | 46,300 | 2,100 | 210 | 86,500 | 1,850 | 6.31 |
| Hutchinson | 3,220 | 141,000 | 38.0 | 7.1 | 6,160 | 45,100 | 2,210 | 278 | 85,500 | 1,800 | 6.38 |
| Hutchinson | 3,061 | 180,473 | 37.0 | 7.7 | 8,757 | 57,563 | 2,279 | 100 | 109,707 | 1,787 | 6.44 |
| Hutchinson | 3,224 | 146,846 | 38.0 | 7.0 | 7,453 | 45,984 | 2,112 | 310 | 89,171 | 1,781 | 7.00 |
| Hutchinson | 3,061 | 139,767 | 37.0 | 7.0 | 6,137 | 45,309 | 1,764 | 321 | 84,335 | 1,900 | 6.04 |
| Hutchinson | 3,078 | 159,397 | 37.1 | 7.0 | 6,504 | 52,459 | 1,815 | 297 | 96,241 | 2,023 | 6.04 |
| Hutchinson | 3,085 | 155,587 | 37.1 | 7.0 | 7,694 | 49,539 | 1,983 | 168 | 94,464 | 1,736 | 6.24 |
| Hutchinson | 3,224 | 166,090 | 38.0 | 7.0 | 4,213 | 58,037 | 1,524 | 238 | 98,954 | 3,122 | 6.26 |
| Hutchinson | 3,001 | 163,370 | 36.6 | 7.0 | 5,798 | 55,275 | 1,954 | 0 | 98,303 | 2,146 | — |
| Hutchinson | 2,990 | 160,349 | 36.5 | 7.0 | 5,834 | 55,337 | 1,556 | 276 | 98,517 | 2,121 | 6.11 |
| Hutchinson | 2,888 | 162,272 | 36.0 | 7.0 | 3,967 | 56,885 | 1,419 | 657 | 96,284 | 3,057 | 7.00 |
| Hutchinson | 3,187 | 154,448 | 37.8 | 7.0 | 7,047 | 49,395 | 2,246 | 51 | 93,803 | 1,903 | 6.80 |
| Hutchinson | 3,213 | 160,349 | 37.9 | 7.0 | 6,192 | 52,308 | 2,139 | 171 | 97,423 | 2,114 | 6.30 |
| Hutchinson | 8,078 | 144,225 | 67.7 | 7.0 | 5,885 | 47,466 | 1,643 | 269 | 87,081 | 1,831 | 7.00 |
| Hutchinson | 2,398 | 143,000 | 32.9 | 7.8 | 1,860 | 52,400 | 820 | 396 | 82,300 | 5,400 | 6.47 |
| Hutchinson | 3,224 | 142,000 | 38.0 | 8.1 | 1,860 | 52,100 | 783 | 299 | 81,900 | 5,300 | 6.50 |
| Hutchinson | 3,297 | 144,000 | 38.4 | 8.3 | 1,920 | 52,600 | 820 | 293 | 83,000 | 5,150 | 6.56 |
| Hutchinson | 3,278 | 144,000 | 38.3 | 8.1 | 1,920 | 52,500 | 820 | 366 | 82,600 | 5,300 | 6.48 |
| Ochiltree | 3,746 | 188,523 | 41.2 | 7.2 | 6,358 | 63,785 | 2,068 | 171 | 114,166 | 1,975 | 6.26 |
| Carson | 3,060 | 178,000 | 37.0 | 7.1 | 7,850 | 76,752 | 2,350 | 58 | 89,700 | 1,290 | 6.73 |
| Floyd | 6,598 | 240,575 | 58.6 | 6.3 | 6,234 | 84,667 | 1,782 | 132 | 146,281 | 1,053 | 6.26 |
| Floyd | 5,800-5,900 | 111,829 | 53.7 | 6.7 | 5,560 | 34,600 | 1,848 | 581 | 65,600 | 3,640 | 6.70 |
| Hall | 3,831 | 248,006 | 41.7 | 6.2 | 32,340 | 58,579 | 2,245 | 56 | 153,982 | 517 | 6.33 |
| Hansford | 3,157 | 158,971 | 37.6 | 7.6 | 2,304 | 58,428 | 860 | 337 | 96,251 | 572 | 6.30 |
| Hansford | 3,240 | 173,421 | 38.1 | 7.3 | 5,159 | 60,396 | 1,188 | 190 | 104,484 | 1,789 | 6.28 |
| Hansford | 3,077 | 102,260 | 37.1 | 7.4 | 1,114 | 37,153 | 573 | 745 | 55,685 | 6,776 | 6.27 |
| Hansford | 3,060 | 144,322 | 37.0 | 7.3 | 1,794 | 52,627 | 729 | 363 | 78,721 | 10,085 | 6.40 |
| Hemphill | 4,365 | 268,178 | 45.0 | 6.7 | 4,058 | 99,139 | 1,177 | 106 | 162,710 | 968 | 6.53 |
| Roberts | 3,550 | 184,280 | 40.0 | 6.5 | 25,792 | 22,530 | 14,160 | 110 | 121,360 | 329 | 6.25 |
| Roberts | 3,552 | 174,600 | 40.0 | 6.9 | 11,014 | 51,287 | 3,406 | 230 | 107,666 | 975 | 6.02 |
| Roberts | 3,538 | 223,281 | 39.9 | 7.8 | 6,906 | 76,807 | 2,098 | 92 | 135,338 | 1,953 | 6.50 |
| Motley | 3,131-3,156 | 106,286 | 37.4 | 6.7 | 4,927 | 33,177 | 1,933 | 99 | 63,800 | 2,350 | 6.63 |
| Motley | 4,200 | 124,316 | 44.0 | 6.6 | 19,948 | 22,396 | 2,940 | 342 | 76,735 | 1,951 | 6.60 |
| Motley | 4,157 | 129,955 | 43.7 | 6.7 | 22,592 | 20,561 | 3,699 | 264 | 80,721 | 2,115 | 6.70 |
| Sherman | 3,007 | 106,739 | 36.7 | 7.1 | 3,603 | 35,970 | 1,124 | 90 | 62,426 | 3,523 | 6.76 |
| Sherman | 3,040 | 111,715 | 36.9 | 6.9 | 4,209 | 36,502 | 1,527 | 157 | 65,796 | 3,428 | 6.47 |
| Sherman | 3,040 | 93,867 | 36.9 | 7.0 | 3,403 | 30,849 | 1,176 | 77 | 52,948 | 5,411 | 6.85 |
| Sherman | 3,032 | 178,281 | 36.8 | 7.4 | 1,368 | 66,430 | 469 | 127 | 95,338 | 14,546 | 6.95 |
| Sherman | 3,032 | 180,200 | 36.8 | 7.8 | 1,224 | 66,853 | 769 | 254 | 96,520 | 14,576 | 6.70 |
| Sherman | 3,032 | 190,868 | 36.8 | 7.3 | 1,164 | 71,240 | 728 | 231 | 103,435 | 14,068 | 6.76 |
| Sherman | 3,032 | 174,224 | 36.8 | 7.5 | 1,462 | 42,360 | 668 | 184 | 38,197 | 13,931 | 6.80 |
| Sherman | 2,997 | 107,317 | 36.6 | 6.7 | 3,394 | 35,907 | 1,457 | 45 | 62,862 | 3,650 | 6.70 |

| County | Depth (ft) | TDS (mg/L) | Temp (°C) | Reported pH | Ca (mg/L) | Na (mg/L) | Mg (mg/L) | HCO$_3$ (mg/L) | Cl (mg/L) | SO$_4$ (mg/L) | pH$_c$ |
|---|---|---|---|---|---|---|---|---|---|---|---|
| Sherman | 3,139 | 339,529 | 37.5 | 6.6 | 14,686 | 112,163 | 3,474 | 72 | 208,221 | 910 | 6.38 |
| Sherman | 2,842 | 185,592 | 35.7 | 8.0 | 4,787 | 64,972 | 1,644 | 6 | 111,096 | 3,085 | — (?) |
| Sherman | 2,842 | 184,650 | 35.7 | 5.9 | 4,683 | 64,600 | 1,714 | 26 | 110,507 | 3,117 | 5.90 |
| Sherman | 3,139 | 194,385 | 37.5 | 7.8 | 2,800 | 70,116 | 1,789 | 149 | 114,175 | 5,352 | 6.62 |
| Sherman | 3,046 | 201,359 | 36.9 | 7.0 | 3,303 | 73,307 | 1,232 | 109 | 119,305 | 4,100 | 6.68 |
| Sherman | 3,046 | 199,027 | 36.9 | 6.8 | 3,965 | 71,668 | 1,248 | 54 | 118,140 | 3,949 | 6.94 |
| Sherman | 3,046 | 208,477 | 36.9 | 7.6 | 3,404 | 75,747 | 1,392 | 112 | 123,660 | 4,153 | 6.66 |
| Sherman | 3,046 | 202,323 | 36.9 | 7.3 | 3,590 | 73,130 | 1,386 | 98 | 119,939 | 4,177 | 6.70 |
| Sherman | 3,046 | 223,712 | 36.9 | 7.3 | 7,818 | 75,913 | 2,220 | 82 | 135,956 | 1,721 | 6.54 |
| Sherman | 3,305 | 210,249 | 38.5 | 7.1 | 7,665 | 70,951 | 2,106 | 47 | 127,656 | 1,818 | 6.78 |
| Sherman | 3,305 | 214,484 | 38.5 | 6.5 | 7,558 | 72,945 | 1,972 | 20 | 130,164 | 1,822 | 6.50 |
| Sherman | 3,305 | 227,980 | 38.5 | 7.2 | 8,038 | 77,549 | 2,086 | 96 | 138,419 | 1,789 | 6.44 |
| Sherman | 3,361 | 235,831 | 38.8 | 7.1 | 9,571 | 78,096 | 2,671 | 96 | 143,898 | 1,495 | 6.40 |
| Sherman | 3,361 | 232,688 | 38.8 | 7.0 | 9,439 | 76,761 | 2,887 | 152 | 142,044 | 1,493 | 6.21 |
| Sherman | 3,361 | 230,970 | 38.8 | 6.1 | 10,262 | 75,007 | 2,955 | 9 | 141,237 | 1,502 | 6.10 |
| Sherman | 3,361 | 340,432 | 38.8 | 6.8 | 1,452 | 129,734 | 1,651 | 46 | 206,593 | 935 | 6.80 |
| Sherman | 2,973 | 134,646 | 36.5 | 6.8 | 3,323 | 45,176 | 2,356 | 124 | 78,414 | 5,250 | 6.68 |
| Sherman | 3,084 | 230,776 | 37.1 | 7.1 | 9,114 | 76,707 | 2,609 | 55 | 140,782 | 1,507 | 6.67 |
| Sherman | 3,084 | 231,294 | 37.1 | 6.9 | 9,284 | 76,615 | 2,678 | 51 | 141,113 | 1,550 | 6.70 |
| Sherman | 3,084 | 231,238 | 37.1 | 8.9 | 6,946 | 76,352 | 2,910 | 41 | 141,544 | 1,174 | 6.89 |
| Sherman | 3,469 | 247,757 | 39.5 | 6.2 | 9,751 | 77,408 | 6,016 | 27 | 152,662 | 1,889 | 6.20 |
| Sherman | 3,330 | 193,111 | 38.6 | 7.8 | 2,820 | 70,178 | 1,416 | 142 | 113,280 | 5,272 | 6.62 |
| Sherman | 3,330 | 198,820 | 38.6 | 7.3 | 2,687 | 72,117 | 1,688 | 95 | 116,665 | 1,206 | 6.81 |
| Sherman | 3,330 | 198,488 | 38.6 | 6.3 | 2,993 | 70,837 | 2,238 | 130 | 116,966 | 5,323 | 6.66 |
| Sherman | 3,330 | 195,470 | 38.6 | 7.4 | 2,688 | 73,253 | 1,552 | 136 | 114,571 | 5,502 | 6.66 |
| Sherman | 2,839 | 198,208 | 35.6 | 7.0 | 14,543 | 47,828 | 9,209 | 38 | 125,595 | 995 | 6.83 |
| Sherman | 3,214 | 167,404 | 37.9 | 7.0 | 1,290 | 62,286 | 681 | 125 | 92,701 | 10,321 | 6.98 |
| Sherman | 3,250 | 145,495 | 38.2 | 7.0 | 1,776 | 53,592 | 663 | 21 | 82,639 | 6,804 | 7.00 |
| Sherman | 3,189 | 167,404 | 37.8 | 7.0 | 1,288 | 62,293 | 685 | 116 | 92,710 | 10,312 | 7.00 |
| Sherman | 3,084 | 232,078 | 37.1 | 7.0 | 9,017 | 77,633 | 2,404 | 55 | 141,386 | 1,581 | 6.67 |
| Lamb | 7,352-7,404 | 173,200 | 63.1 | 6.4 | 15,120 | 46,607 | 3,072 | 195 | 106,500 | 1,700 | 6.40 |
| Crosby | 4,363-4,439 | 105,214 | 44.9 | 8.6 | 6,880 | 30,143 | 2,246 | 139 | 62,891 | 2,913 | 6.35 |
| Crosby | 7,650-7,683 | 230,710 | 64.8 | 7.3 | 8,164 | 80,271 | 992 | 187 | 140,729 | 365 | 7.31 |
| Hockley | 8,904-8,990 | 226,254 | 73.0 | 6.9 | 3,823 | 83,135 | 884 | 333 | 137,190 | 588 | 6.90 |
| Hockley | 8,634-8,676 | 71,811 | 71.2 | 6.4 | 4,687 | 18,907 | 2,534 | 652 | 42,777 | 2,252 | 6.40 |
| Hockley | 8,546-8,626 | 50,595 | 70.8 | 7.2 | 1,840 | 16,347 | 488 | 927 | 27,300 | 3,400 | 7.20 |
| Hockley | 9,642-9,648 | 87,741 | 77.2 | 6.6 | 3,286 | 29,581 | 648 | 801 | 51,304 | 2,120 | 6.60 |
| Motley | 2,970-3,022 | 124,800 | 36.6 | 7.5 | 3,920 | 46,112 | 1,972 | 296 | 71,050 | 1,450 | — |

## GRANITE WASH

| County | Depth (ft) | TDS (mg/L) | Temp (°C) | Reported pH | Ca (mg/L) | Na (mg/L) | Mg (mg/L) | HCO$_3$ (mg/L) | Cl (mg/L) | SO$_4$ (mg/L) |
|---|---|---|---|---|---|---|---|---|---|---|
| Hartley | 6,140-6,158 | 189,119 | 55.8 | 5.7 | 9,721 | 61,511 | 1,422 | 41 | 115,360 | 1,142 |
| Oldham | 7,122-7,143 | 219,091 | 61.8 | 5.5 | 9,600 | 73,490 | 1,380 | 61 | 133,660 | 960 |
| Moore | 3,465 | 141,291 | 39.5 | 6.6 | 10,143 | 41,917 | 1,487 | 72 | 85,259 | 2,304 |
| Moore | 3,461 | 143,568 | 39.5 | 6.3 | 10,152 | 42,725 | 1,595 | 13 | 87,277 | 1,724 |
| Moore | 3,466-3,472 | 141,737 | 40.0 | 7.9 | 7,710 | 36,347 | 1,105 | 53 | 72,000 | 1,280 |

*Table B-1 (cont.)*

| County | Depth (ft) | TDS (mg/L) | Temp (°C) | Reported pH | Ca (mg/L) | Na (mg/L) | Mg (mg/L) | HCO₃ (mg/L) | Cl (mg/L) | SO₄ (mg/L) |
|---|---|---|---|---|---|---|---|---|---|---|
| Moore | 3,490 | 145,330 | 39.6 | 7.0 | 9,067 | 44,756 | 1,575 | 130 | 89,163 | 637 |
| Moore | 3,851-3,871 | 138,365 | 41.8 | 6.8 | 10,502 | 40,876 | 1,275 | 66 | 84,561 | 1,034 |
| Hutchinson | 3,105-3,117 | 183,045 | 37.3 | 7.0 | 7,847 | 59,778 | 2,250 | 83 | 112,528 | 67 |
| Wheeler | 6,554-6,569 | 251,103 | 58.3 | 6.4 | 35,017 | 56,938 | 2,138 | 42 | 156,025 | 492 |
| Wheeler | 9,148-9,375 | 208,575 | 75.2 | 5.8 | 15,300 | 60,253 | 2,500 | 116 | 129,000 | 176 |
| Wheeler | 8,279-8,283 | 222,672 | 68.9 | 5.5 | 15,000 | 65,759 | 2,940 | 18 | 138,000 | 5 |
| Wheeler | 8,038-8,044 | 232,772 | 67.4 | 5.5 | 19,000 | 65,840 | 2,240 | 12 | 144,000 | 130 |
| Wheeler | 8,308-8,366 | 254,978 | 69.1 | 5.1 | 16,678 | 77,789 | 2,845 | 8 | 157,657 | 0 |
| Wheeler | 8,491-8,530 | 255,653 | 70.2 | 4.5 | 17,355 | 76,431 | 3,415 | 0 | 158,393 | 46 |
| Wheeler | 7,978-8,018 | 254,600 | 67.0 | 6.4 | 20,143 | 73,894 | 2,818 | 72 | 157,657 | 13 |
| Wheeler | 10,985-11,057 | — | 85.6 | 5.2 | 21,400 | 60,266 | 2,640 | 49 | 143,000 | 7 |
| Wheeler | 7,300 | 249,657 | 62.9 | 5.4 | 16,678 | 74,801 | 3,393 | 4 | 154,770 | 10 |
| Wheeler | 7,473 | 223,986 | 63.9 | 5.2 | 16,718 | 66,129 | 2,401 | 17 | 138,182 | 536 |
| Wheeler | 8,300 | 152,922 | 69.0 | 5.9 | 11,725 | 44,603 | 1,779 | 74 | 94,551 | 187 |
| Wheeler | 7,500 | 243,131 | 64.1 | 5.4 | 15,160 | 73,134 | 3,878 | 11 | 150,912 | 34 |
| Wheeler | 7,260-7,385 | 191,056 | 63.0 | 6.2 | 14,100 | 55,884 | 2,490 | 137 | 118,000 | 445 |
| Wheeler | 7,904-7,940 | 211,466 | 66.7 | 5.8 | 14,600 | 62,038 | 2,850 | 110 | 131,000 | 48 |
| Wheeler | 7,444 | 251,379 | 63.8 | 5.4 | 16,692 | 74,647 | 3,953 | 13 | 156,060 | 11 |
| Wheeler | 7,482 | 226,228 | 64.0 | 5.3 | 18,000 | 65,246 | 2,661 | 11 | 140,056 | 252 |
| Wheeler | 7,708-7,767 | 245,021 | 65.6 | 5.2 | 15,883 | 73,658 | 3,510 | 25 | 151,932 | 11 |
| Wheeler | 7,708-7,767 | 246,904 | 65.6 | 5.1 | 15,998 | 74,310 | 3,487 | 17 | 153,083 | 6 |
| Wheeler | 7,475 | 261,453 | 64.0 | 5.3 | 20,952 | 75,566 | 2,868 | 13 | 161,796 | 256 |
| Wheeler | 7,453 | 210,999 | 63.8 | 5.1 | 16,964 | 60,921 | 2,302 | 49 | 130,410 | 351 |
| Gray | 5,545 | 232,049 | 52.2 | 7.0 | 4,960 | 83,454 | 1,555 | 183 | 141,828 | 69 |
| Gray | 5,162-5,178 | 203,082 | 49.8 | 7.3 | 6,080 | 71,120 | 1,361 | 171 | 124,100 | 250 |
| Gray | 9,558-9,569 | 211,932 | 76.7 | 7.0 | 14,945 | 63,856 | 2,134 | 34 | 130,927 | 474 |
| Gray | 8,808-8,031 | 214,633 | 72.1 | 5.8 | 13,121 | 66,093 | 2,729 | 49 | 132,574 | 65 |
| Gray | 2,808-2,987 | 235,510 | 35.5 | 5.3 | 21,104 | 64,781 | 3,122 | 0 | 146,408 | 0 |
| Gray | 2,908 | 224,286 | 36.1 | 5.3 | 17,358 | 64,097 | 3,330 | 13 | 139,365 | 0 |
| Gray | 2,950 | 199,804 | 36.2 | 4.9 | 13,171 | 59,885 | 2,826 | 0 | 123,920 | 0 |
| Gray | 3,000 | 210,221 | 36.6 | 4.4 | 13,699 | 70,529 | 2,407 | 0 | 122,819 | 0 |
| Gray | 2,950 | 201,628 | 36.3 | 4.4 | 12,598 | 61,952 | 2,355 | 0 | 124,722 | 0 |
| Gray | 3,085 | 244,775 | 37.2 | 7.4 | 2,195 | 68,149 | 2,685 | 27 | 151,816 | 180 |
| Gray | 7,720 | 108,904 | 65.5 | 6.6 | 6,158 | 34,228 | 1,339 | 64 | 67,562 | 38 |
| Gray | >7,720 | 214,044 | 65.5 | 5.0 | 11,920 | 66,943 | 2,711 | 34 | 132,283 | 28 |
| Gray | 3,215 | 209,853 | 37.9 | 6.1 | 19,364 | 55,025 | 3,015 | 12 | 132,434 | 91 |
| Gray | 3,014 | 223,802 | 36.7 | 4.3 | 19,613 | 62,027 | 2,992 | 0 | 138,914 | 255 |
| Gray | 3,142 | 210,995 | 37.5 | 5.6 | 19,436 | 56,817 | 3,197 | 6 | 130,816 | 720 |
| Gray | 3,110 | 213,507 | 37.3 | 4.0 | 19,365 | 57,895 | 3,197 | 0 | 132,436 | 612 |
| Gray | 3,110 | 192,374 | 37.3 | 4.3 | 18,521 | 50,588 | 3,141 | 0 | 119,517 | 605 |
| Gray | 3,100 | 200,182 | 37.2 | 6.2 | 13,761 | 58,978 | 3,094 | 12 | 124,335 | 0 |
| Gray | 3,080 | 201,030 | 37.1 | 6.6 | 13,299 | 60,015 | 2,963 | 12 | 124,738 | 0 |
| Gray | 3,016 | 199,589 | 36.7 | 4.5 | 13,654 | 58,997 | 3,007 | 0 | 123,930 | 0 |
| Gray | 3,250 | 198,769 | 38.2 | 5.3 | 11,561 | 61,323 | 2,767 | 0 | 123,116 | 0 |
| Gray | 3,077 | 199,159 | 37.1 | 5.2 | 10,994 | 62,610 | 2,432 | 0 | 123,122 | 0 |
| Gray | 3,076 | 193,858 | 37.1 | 5.3 | 12,804 | 58,055 | 2,757 | 0 | 120,241 | 0 |
| Gray | 2,950 | 176,163 | 36.3 | 4.9 | 11,613 | 52,800 | 2,492 | 0 | 109,258 | 0 |
| Gray | 2,950 | 177,537 | 36.3 | 4.4 | 11,093 | 54,550 | 2,074 | 0 | 109,820 | 0 |
| Gray | 2,950 | 170,508 | 36.3 | 4.2 | 16,694 | 44,735 | 2,676 | 0 | 106,200 | 203 |
| Gray | 3,300 | 232,174 | 38.5 | 5.6 | 15,206 | 72,620 | 1,099 | 12 | 141,485 | 1,437 |

# APPENDIX C:
## Determination of Resistivity (Salinity) from Spontaneous Potential Logs

The procedure employed to compute salinity is essentially the same as outlined by Schlumberger (1972). The general formula is

$$SSP = -K \log \frac{Rmf}{Rw}$$

where  SSP = static spontaneous potential, read directly from logs
K = coefficient proportional to the absolute temperature
Rmf = resistivity of the mud filtrate
Rw = resistivity of the formation water

A static spontaneous potential (SSP) was determined for every spontaneous potential (SP) log available in the Wolfcamp carbonate and the Permian-Pennsylvanian granite-wash sections (tables C-1 and C-2). The resistivity of the mud, bottom-hole temperature, and measurement temperature are all given as header information on each log chart. Resistivity is converted to the appropriate temperature using the procedure described by Schlumberger (1972) and used in the above equation to compute the resistivity of the formation brine. Finally an equivalent NaCl concentration is determined from the computed resistivity of the formation water.

Such a technique is at best an approximation employed in the absence of actual chemical analyses. Errors may occur in field measurements,

in log interpretation, and in the assumptions inherent in the charts employed. We suspect that the most significant error in these computations results from our assumption that the mud and formation brines are unaffected by the presence of divalent cations, such as calcium and magnesium. Correction factors are available; however, owing to the lack of information concerning the composition of brines and the mud filtrate, it was decided that such corrections were unjustified. The computed values for salinity are all significantly below saturation with respect to halite, and the correction factors have the effect of lowering the estimated salinity values. One concern in the radioactive waste disposal program is whether the brines have the potential to dissolve halite in the overlying evaporite section. Consequently, we have chosen to err on the side of conservatism by converting formation water resistivities to equivalent NaCl solutions. These estimates indicate that the brine is indeed undersaturated, even using this conservative assumption, and would be even more under-saturated if corrections for divalent cations were applied. A tabulation of halite solubility with temperature is given below for comparison (National Research Council, 1928).

| | Halite | |
|---|---|---|
| Temperature | | Solubility |
| °C | °F | ppm |
| 0 | 32 | 262,609 |
| 25 | 77 | 264,235 |
| 50 | 122 | 267,856 |
| 75 | 167 | 273,760 |
| 100 | 212 | 281,386 |

Table C-1. Estimates of TDS (salinity) in the Wolfcamp deep-basin aquifer obtained from analysis of spontaneous potential logs.

| County, log no. | Interval considered (ft) | SP (mV) | T (°F) | Rmf (ohm-m) | Rw (ohm-m) | Estimated TDS (ppm) as NaCl |
|---|---|---|---|---|---|---|
| Armstrong 1 | 3,500-5,100 | 90 | 117 | 0.5 | 0.051 | 100,000 |
| Armstrong 4 | 3,900-5,100 | 80 | 114 | 0.31 | 0.046 | 120,000 |
| Armstrong 16 | 3,700-4,800 | 85 | 104 | 0.42 | 0.051 | 120,000 |
| Briscoe 1 | 4,600-6,000 | 115 | 126 | 0.45 | 0.033 | 160,000 |
| Briscoe 3 | 4,650-6,000 | 110 | 121 | 0.4 | 0.034 | 160,000 |
| Briscoe 6 | 3,700-4,800 | 80 | 104 | 0.38 | 0.051 | 120,000 |
| Briscoe 7 | 3,400-4,600 | 80 | 102 | 0.4 | 0.055 | 110,000 |
| Briscoe 13 | 4,800-6,100 | 85 | 121 | 0.27 | 0.039 | 140,000 |
| Briscoe 16 | 3,670-4,775 | 80 | 112 | 0.43 | 0.058 | 85,000 |

*Table C-1 (cont.)*

| County, log no. | Interval considered (ft) | SP (mV) | T (°F) | Rmf (ohm-m) | Rw (ohm-m) | Estimated TDS (ppm) as NaCl |
|---|---|---|---|---|---|---|
| Briscoe 18 | 4,050-5,270 | 80 | 115 | 0.3 | 0.045 | 120,000 |
| Carson 6 | 2,800-3,200 | 90 | 101 | 0.6 | 0.06 | 90,000 |
| Castro 2 | 5,900-7,300 | 115 | 137 | 0.48 | 0.034 | 140,000 |
| Castro 3 | 5,600-7,100 | 100 | 124 | 0.34 | 0.035 | 150,000 |
| Castro 6 | 5,400-6,850 | 120 | 133 | 0.4 | 0.03 | 170,000 |
| Castro 16 | 5,900-7,500 | 95 | 128 | 0.45 | 0.045 | 100,000 |
| Childress 5 | 2,800-4,400 | 55 | 110 | 0.2 | 0.056 | 90,000 |
| Childress 6 | 2,800-4,400 | 95 | 103 | 0.45 | 0.045 | 140,000 |
| Childress 12 | 2,700-4,100 | 70 | 105 | 0.16 | 0.04 | 150,000 |
| Childress 16 | 2,300-3,900 | 60 | 105 | 0.18 | 0.05 | 120,000 |
| Childress 30 | 2,500-4,200 | 90 | 105 | 0.41 | 0.045 | 130,000 |
| Childress 32 | 2,600-4,100 | 70 | 100 | 0.21 | 0.045 | 140,000 |
| Childress 39 | 2,600-4,100 | 80 | 97 | 0.31 | 0.05 | 130,000 |
| Childress 41 | 2,600-4,100 | 80 | 96 | 0.53 | 0.063 | 95,000 |
| Childress 47 | 2,700-4,100 | 70 | 96 | 0.32 | 0.055 | 120,000 |
| Childress 59 | 2,600-4,200 | 80 | 106 | 0.33 | 0.048 | 125,000 |
| Childress 61 | 2,600-4,200 | 70 | 106 | 0.28 | 0.052 | 110,000 |
| Childress 63 | 2,600-4,200 | 80 | 105 | 0.46 | 0.058 | 90,000 |
| Childress 66 | 2,600-4,200 | 55 | 103 | 0.15 | 0.05 | 120,000 |
| Childress 68 | 2,600-4,100 | 60 | 106 | 0.21 | 0.05 | 120,000 |
| Childress 70 | 2,600-4,100 | 60 | 99 | 0.22 | 0.056 | 110,000 |
| Cochran 243 | 2,800-3,600 | 70 | 95 | 0.52 | 0.078 | 75,000 |
| Collingsworth 22 | 2,300-3,600 | 90 | 96 | 0.53 | 0.051 | 130,000 |
| Collingsworth 25 | 2,600-4,000 | 90 | 96 | 0.42 | 0.047 | 140,000 |
| Cottle 9 | 2,800-4,500 | 90 | 103 | 0.4 | 0.045 | 140,000 |
| Cottle 10 | 2,900-4,750 | 50 | 101 | 0.18 | 0.057 | 100,000 |
| Cottle 20 | 2,800-4,750 | 60 | 100 | 0.24 | 0.057 | 100,000 |
| Cottle 25 | 2,800-4,500 | 90 | 97 | 0.3 | 0.04 | 170,000 |
| Cottle 29 | 3,000-4,800 | 80 | 106 | 0.27 | 0.042 | 140,000 |
| Cottle 30 | 2,600-3,800 | 80 | 106 | 0.35 | 0.051 | 110,000 |
| Cottle 31 | 2,600-3,800 | 70 | 106 | 0.33 | 0.057 | 95,000 |
| Cottle 34 | 2,600-3,850 | 90 | 106 | 0.35 | 0.042 | 150,000 |
| Cottle 36 | 2,500-4,300 | 90 | 110 | 0.34 | 0.042 | 140,000 |
| Cottle 44 | 2,300-3,800 | 70 | 102 | 0.2 | 0.045 | 140,000 |
| Cottle 45 | 2,000-3,500 | 70 | 98 | 0.18 | 0.04 | 170,000 |
| Cottle 46 | 2,000-3,500 | 80 | 97 | 0.45 | 0.057 | 100,000 |
| Cottle 47 | 2,100-3,600 | 110 | 102 | 0.45 | 0.037 | 180,000 |
| Cottle 70 | 2,000-3,700 | 60 | 94 | 0.23 | 0.058 | 110,000 |
| Cottle 108 | 2,300-4,100 | 60 | 102 | 0.25 | 0.058 | 95,000 |
| Cottle 111 | 2,300-4,100 | 70 | 88 | 0.34 | 0.06 | 120,000 |
| Cottle 115 | 2,200-4,000 | 70 | 99 | 0.3 | 0.055 | 110,000 |
| Cottle 116 | 2,100-3,600 | 90 | 102 | 0.5 | 0.051 | 120,000 |
| Cottle 117 | 2,000-3,800 | 80 | 100 | 0.4 | 0.053 | 115,000 |
| Cottle 118 | 2,200-3,900 | 80 | 90 | 0.45 | 0.06 | 110,000 |
| Cottle 119 | 2,000-3,500 | 90 | 99 | 0.24 | 0.037 | 180,000 |
| Cottle 121 | 2,700-4,400 | 70 | 105 | 0.28 | 0.053 | 100,000 |
| Cottle 129 | 2,200-3,700 | 70 | 99 | 0.23 | 0.045 | 145,000 |
| Cottle 131 | 2,200-4,000 | 70 | 106 | 0.27 | 0.05 | 120,000 |
| Crosby 8 | 5,600-7,400 | 60 | 121 | 0.21 | 0.051 | 90,000 |
| Crosby 9 | 5,700-7,500 | 105 | 98 | 0.6 | 0.046 | 140,000 |
| Crosby 17 | 5,700-7,500 | 80 | 126 | 0.19 | 0.035 | 150,000 |
| Dallam 2 | 3,300-3,900 | 80 | 94 | 0.75 | 0.084 | 70,000 |
| Dallam 15 | 3,000-3,600 | 70 | 82 | 0.78 | 0.11 | 60,000 |
| Dallam 16 | 3,000-3,600 | 70 | 82 | 0.78 | 0.11 | 60,000 |
| Dallam 17 | 3,000-3,600 | 70 | 84 | 0.62 | 0.09 | 70,000 |

51

*Table C-1 (cont.)*

| County, log no. | Interval considered (ft) | SP (mV) | T (°F) | Rmf (ohm-m) | Rw (ohm-m) | Estimated TDS (ppm) as NaCl |
|---|---|---|---|---|---|---|
| Dallam 18 | 3,000-3,600 | 100 | 95 | 0.71 | 0.053 | 120,000 |
| Dallam 28 | 3,000-3,800 | 90 | 97 | 0.76 | 0.065 | 90,000 |
| Dallam 36 | 3,150-4,950 | 80 | 96 | 0.72 | 0.081 | 70,000 |
| Dallam 39 | 3,200-4,900 | 80 | 110 | 0.38 | 0.05 | 105,000 |
| Dallam 40 | 3,700-4,950 | 90 | 109 | 0.52 | 0.052 | 100,000 |
| Dallam 41 | 3,800-5,300 | 90 | 104 | 0.4 | 0.45 | 140,000 |
| Dallam 44 | 3,600-4,700 | 60 | 90 | 0.52 | 0.1 | 60,000 |
| Dallam 46 | 3,400-5,100 | 100 | 117 | 0.5 | 0.045 | 120,000 |
| Deaf Smith 5 | 5,100-6,500 | 120 | 121 | 0.58 | 0.035 | 160,000 |
| Deaf Smith 6 | 5,300-6,700 | 100 | 123 | 0.43 | 0.04 | 130,000 |
| Deaf Smith 13 | 5,700-7,300 | 110 | 137 | 0.42 | 0.037 | 130,000 |
| Deaf Smith 14 | 6,000-7,200 | 120 | 139 | 0.35 | 0.028 | 170,000 |
| Deaf Smith 15 | 5,700-7,000 | 100 | 127 | 0.48 | 0.041 | 120,000 |
| Dickens 4 | 4,300-6,100 | 50 | 118 | 0.12 | 0.045 | 120,000 |
| Dickens 8 | 3,400-5,100 | 90 | 105 | 0.44 | 0.045 | 135,000 |
| Dickens 14 | 4,400-5,700 | 110 | 116 | 0.53 | 0.038 | 150,000 |
| Dickens 18 | 3,800-4,900 | 70 | 104 | 0.34 | 0.058 | 95,000 |
| Dickens 21 | 2,800-4,500 | 45 | 105 | 0.19 | 0.063 | 85,000 |
| Dickens 36 | 3,600-5,600 | 70 | 106 | 0.18 | 0.041 | 150,000 |
| Dickens 43 | 3,700-5,200 | 100 | 110 | 0.29 | 0.035 | 170,000 |
| Donley 17 | 2,900-3,400 | 110 | 101 | 0.4 | 0.035 | 190,000 |
| Donley 21 | 3,000-3,300 | 110 | 101 | 0.5 | 0.038 | 180,000 |
| Donley 25 | 3,000-4,300 | 105 | 105 | 0.4 | 0.036 | 180,000 |
| Donley 27 | 2,900-3,600 | 80 | 95 | 0.31 | 0.045 | 150,000 |
| Floyd 2 | 4,500-6,700 | 90 | 113 | 0.39 | 0.045 | 120,000 |
| Floyd 9 | 5,500-7,500 | 50 | 122 | 0.17 | 0.057 | 80,000 |
| Floyd 13 | 5,200-7,200 | 65 | 121 | 0.18 | 0.044 | 110,000 |
| Floyd 29 | 5,000-7,000 | 80 | 116 | 0.38 | 0.052 | 95,000 |
| Gray 3 | 3,450-4,600 | 40 | 113 | 0.026 | 0.029 | 200,000 |
| Gray 7 | 3,900-4,600 | 100 | 116 | 0.46 | 0.059 | 130,000 |
| Gray 12 | 3,850-4,400 | 105 | 120 | 0.45 | 0.037 | 150,000 |
| Gray 14 | 4,000-4,500 | 100 | 116 | 0.33 | 0.035 | 160,000 |
| Gray 18 | 4,400-5,600 | 110 | 127 | 0.4 | 0.034 | 150,000 |
| Gray 25 | 5,100-6,300 | 40 | 109 | 0.12 | 0.053 | 100,000 |
| Gray 28 | 4,400-5,600 | 115 | 128 | 0.29 | 0.028 | 190,000 |
| Gray 31 | 4,200-5,500 | 100 | 125 | 0.42 | 0.04 | 130,000 |
| Gray 32 | 4,100-5,800 | 100 | 112 | 0.3 | 0.035 | 170,000 |
| Gray 33 | 4,100-5,800 | 115 | 112 | 0.64 | 0.039 | 150,000 |
| Gray 41 | 3,850-5,300 | 110 | 116 | 0.5 | 0.037 | 150,000 |
| Gray 43 | 3,700-5,300 | 110 | 115 | 0.45 | 0.035 | 160,000 |
| Gray 44 | 3,700-5,200 | 90 | 122 | 0.32 | 0.04 | 130,000 |
| Gray 47 | 3,800-5,700 | 80 | 115 | 0.35 | 0.05 | 100,000 |
| Gray 48 | 3,800-5,700 | 80 | 113 | 0.42 | 0.055 | 90,000 |
| Hale 33 | 6,400-7,900 | 60 | 138 | 0.14 | 0.04 | 110,000 |
| Hale 42 | 7,300-9,150 | 110 | 134 | 0.35 | 0.03 | 160,000 |
| Hale 56 | 5,500-7,900 | 120 | 137 | 0.38 | 0.028 | 180,000 |
| Hall 1 | 3,100-5,000 | 90 | 95 | 0.48 | 0.05 | 135,000 |
| Hall 13 | 3,200-4,500 | 80 | 111 | 0.36 | 0.05 | 100,000 |
| Hall 18 | 3,300-5,200 | 60 | 102 | 0.25 | 0.058 | 95,000 |
| Hall 20 | 3,300-4,400 | 70 | 107 | 0.23 | 0.047 | 130,000 |
| Hall 22 | 3,300-4,400 | 70 | 103 | 0.39 | 0.061 | 85,000 |
| Hall 23 | 3,200-4,700 | 80 | 105 | 0.31 | 0.046 | 130,000 |
| Hall 19 | 3,400-4,400 | 60 | 99 | 0.22 | 0.054 | 120,000 |
| Hansford 7 | 3,300-5,000 | 110 | 103 | 0.52 | 0.039 | 160,000 |
| Hansford 33 | 3,400-5,100 | 90 | 117 | 0.2 | 0.033 | 180,000 |
| Hansford 35 | 3,400-5,100 | 110 | 116 | 0.45 | 0.035 | 160,000 |

52

*Table C-1 (cont.)*

| County, log no. | Interval considered (ft) | SP (mV) | T (°F) | Rmf (ohm-m) | Rw (ohm-m) | Estimated TDS (ppm) as NaCl |
|---|---|---|---|---|---|---|
| Hansford 43 | 3,400-5,200 | 100 | 101 | 0.6 | 0.05 | 120,000 |
| Hansford 44 | 3,400-5,200 | 110 | 103 | 0.57 | 0.039 | 160,000 |
| Hansford 53 | 3,800-5,300 | 110 | 103 | 0.58 | 0.04 | 160,000 |
| Hansford 56 | 3,800-5,300 | 100 | 117 | 0.35 | 0.036 | 160,000 |
| Hansford 58 | 3,200-5,200 | 100 | 115 | 0.42 | 0.04 | 140,000 |
| Hansford 94 | 3,550-5,000 | 90 | 105 | 0.43 | 0.047 | 130,000 |
| Hansford 95 | 3,500-5,000 | 90 | 104 | 0.39 | 0.045 | 140,000 |
| Hansford 101 | 3,500-5,100 | 90 | 99 | 0.47 | 0.05 | 130,000 |
| Hansford 110 | 3,400-5,100 | 120 | 102 | 0.68 | 0.038 | 170,000 |
| Hansford 124 | 3,400-5,000 | 90 | 104 | 0.35 | 0.041 | 150,000 |
| Hansford 138 | 3,400-5,200 | 90 | 104 | 0.6 | 0.056 | 100,000 |
| Hartley 1 | 3,600-5,100 | 90 | 118 | 0.64 | 0.06 | 80,000 |
| Hartley 7 | 3,600-5,600 | 100 | 108 | 0.58 | 0.045 | 130,000 |
| Hartley 12 | 3,500-5,400 | 100 | 113 | 0.42 | 0.039 | 145,000 |
| Hartley 13 | 3,400-5,400 | 100 | 116 | 0.46 | 0.041 | 140,000 |
| Hartley 17 | 3,600-5,800 | 115 | 122 | 0.43 | 0.033 | 160,000 |
| Hartley 20 | 3,700-5,450 | 80 | 113 | 0.47 | 0.059 | 85,000 |
| Hartley 21 | 3,600-5,200 | 90 | 97 | 0.57 | 0.055 | 120,000 |
| Hartley 24 | 4,100-6,000 | 110 | 121 | 0.46 | 0.035 | 160,000 |
| Hartley 28 | 3,900-5,500 | 110 | 125 | 0.55 | 0.039 | 135,000 |
| Hartley 33 | 4,100-6,300 | 115 | 103 | 0.6 | 0.038 | 170,000 |
| Hartley 34 | 4,100-6,300 | 110 | 126 | 0.37 | 0.032 | 170,000 |
| Hartley 35 | 4,000-6,200 | 100 | 128 | 0.53 | 0.046 | 100,000 |
| Hartley 38 | 3,750-5,400 | 100 | 108 | 0.45 | 0.037 | 160,000 |
| Hartley 40 | 4,000-5,900 | 120 | 125 | 0.36 | 0.029 | 190,000 |
| Hartley 41 | 4,000-5,500 | 110 | 118 | 0.46 | 0.035 | 160,000 |
| Hartley 42 | 3,700-5,300 | 125 | 121 | 0.4 | 0.029 | 190,000 |
| Hartley 44 | 3,900-5,600 | 100 | 109 | 0.5 | 0.042 | 140,000 |
| Hartley 51 | 3,900-5,800 | 70 | 115 | 0.32 | 0.056 | 85,000 |
| Hartley 95 | 3,800-5,900 | 40 | 117 | 0.028 | 0.028 | 225,000 |
| Hartley 97 | 3,800-5,900 | 130 | 120 | 0.53 | 0.03 | 190,000 |
| Hemphill 2 | 3,800-5,400 | 40 | 120 | 0.095 | 0.045 | 120,000 |
| Hemphill 8 | 4,000-6,000 | 80 | 115 | 0.21 | 0.037 | 160,000 |
| Hemphill 9 | 4,100-5,800 | 50 | 118 | 0.12 | 0.045 | 120,000 |
| Hemphill 10 | 3,900-5,200 | 110 | 109 | 0.49 | 0.038 | 160,000 |
| Hemphill 11 | 3,800-5,200 | 115 | 108 | 0.5 | 0.035 | 180,000 |
| Hemphill 20 | 4,000-5,900 | 120 | 113 | 0.55 | 0.034 | 170,000 |
| Hemphill 21 | 4,000-5,800 | 60 | 116 | 0.14 | 0.042 | 130,000 |
| Hemphill 31 | 4,300-6,000 | 110 | 113 | 0.53 | 0.038 | 150,000 |
| Hemphill 32 | 4,000-6,000 | 110 | 113 | 0.49 | 0.036 | 160,000 |
| Hemphill 34 | 4,300-6,400 | 110 | 113 | 0.15 | 0.024 | 300,000+ |
| Hemphill 38 | 4,300-6,000 | 110 | 131 | 0.33 | 0.03 | 170,000 |
| Hemphill 41 | 4,400-6,200 | 100 | 115 | 0.55 | 0.045 | 120,000 |
| Hemphill 42 | 4,500-6,100 | 110 | 117 | 0.4 | 0.035 | 160,000 |
| Hemphill 44 | 4,500-6,200 | 110 | 115 | 0.57 | 0.04 | 140,000 |
| Hockley 9 | 7,500-8,800 | 80 | 110 | 0.4 | 0.055 | 95,000 |
| Hockley 199 | 7,200-8,500 | 130 | 151 | 0.34 | 0.024 | 190,000 |
| Hockley 202 | 7,500-8,700 | 130 | 164 | 0.2 | 0.019 | 250,000 |
| Hockley 204 | 7,300-9,400 | 100 | 163 | 0.32 | 0.033 | 120,000 |
| Hockley 236 | 7,800-9,200 | 80 | 148 | 0.4 | 0.055 | 70,000 |
| Hockley 469 | 7,700-9,100 | 80 | 147 | 0.34 | 0.05 | 75,000 |
| Hockley 474 | 7,200-9,100 | 110 | 158 | 0.22 | 0.024 | 180,000 |
| Hockley 498 | 4,500-5,000 | 110 | 114 | 0.66 | 0.043 | 130,000 |
| Hutchinson 10 | 3,300-4,800 | 120 | 113 | 0.49 | 0.031 | 180,000 |
| Hutchinson 11 | 3,400-4,800 | 90 | 109 | 0.25 | 0.035 | 180,000 |
| Hutchinson 13 | 3,400-4,800 | 80 | 109 | 0.46 | 0.058 | 90,000 |

53

Table C-1 (cont.)

| County, log no. | Interval considered (ft) | SP (mV) | T (°F) | Rmf (ohm-m) | Rw (ohm-m) | Estimated TDS (ppm) as NaCl |
|---|---|---|---|---|---|---|
| Hutchinson 16 | 3,300-4,400 | 110 | 111 | 0.32 | 0.031 | 200,000 |
| Hutchinson 18 | 3,300-4,500 | 110 | 111 | 0.41 | 0.035 | 170,000 |
| Hutchinson 23 | 3,300-5,100 | 110 | 111 | 0.44 | 0.036 | 160,000 |
| Hutchinson 28 | 3,500-5,000 | 110 | 111 | 0.62 | 0.04 | 140,000 |
| Hutchinson 33 | 3,300-4,800 | 120 | 108 | 0.57 | 0.035 | 160,000 |
| Hutchinson 62 | 3,300-5,100 | 120 | 110 | 0.55 | 0.035 | 180,000 |
| Lipscomb 4 | 3,300-4,700 | 110 | 102 | 0.69 | 0.05 | 120,000 |
| Lipscomb 8 | 3,300-4,900 | 110 | 105 | 0.52 | 0.044 | 135,000 |
| Lipscomb 31 | 3,400-5,000 | 100 | 106 | 0.39 | 0.04 | 155,000 |
| Lipscomb 43 | 3,500-5,000 | 110 | 110 | 0.46 | 0.038 | 150,000 |
| Lipscomb 47 | 3,700-5,200 | 80 | 106 | 0.35 | 0.055 | 95,000 |
| Lipscomb 48 | 3,800-5,700 | 110 | 115 | 0.4 | 0.037 | 150,000 |
| Lipscomb 49 | 3,900-5,900 | 90 | 116 | 0.26 | 0.041 | 130,000 |
| Lipscomb 53 | 3,700-5,200 | 110 | 114 | 0.44 | 0.036 | 155,000 |
| Lipscomb 58 | 3,800-5,400 | 110 | 115 | 0.38 | 0.032 | 180,000 |
| Lipscomb 59 | 4,000-5,500 | 115 | 113 | 0.43 | 0.032 | 185,000 |
| Lubbock 41 | 4,100-6,000 | 110 | 107 | 0.41 | 0.038 | 160,000 |
| Moore 14 | 2,800-5,100 | 105 | 119 | 0.55 | 0.038 | 140,000 |
| Moore 16 | 3,700-4,100 | 110 | 108 | 0.54 | 0.039 | 150,000 |
| Moore 17 | 3,600-5,100 | 120 | 107 | 0.61 | 0.034 | 180,000 |
| Moore 34 | 3,200-4,200 | 130 | 115 | 0.6 | 0.039 | 140,000 |
| Moore 10 | 2,800-3,600 | 50 | 98 | 0.35 | 0.075 | 70,000 |
| Moore 28 | 2,500-3,400 | 100 | 104 | 0.58 | 0.05 | 115,000 |
| Moore 49 | 2,900-3,500 | 60 | 97 | 0.18 | 0.055 | 110,000 |
| Motley 4 | 3,400-5,300 | 80 | 112 | 0.41 | 0.052 | 95,000 |
| Motley 6 | 3,000-4,800 | 80 | 109 | 0.34 | 0.051 | 100,000 |
| Motley 10 | 4,300-6,600 | 110 | 121 | 0.36 | 0.03 | 185,000 |
| Motley 39 | 3,700-5,400 | 100 | 126 | 0.36 | 0.04 | 125,000 |
| Ochiltree 16 | 3,300-4,600 | 110 | 107 | 0.43 | 0.039 | 150,000 |
| Ochiltree 25 | 3,300-4,500 | 100 | 98 | 0.52 | 0.048 | 130,000 |
| Ochiltree 28 | 3,400-5,100 | 110 | 109 | 0.53 | 0.038 | 155,000 |
| Ochiltree 29 | 3,500-4,800 | 115 | 111 | 0.44 | 0.032 | 185,000 |
| Ochiltree 44 | 3,700-5,000 | 110 | 114 | 0.42 | 0.032 | 180,000 |
| Ochiltree 47 | 3,600-4,800 | 130 | 106 | 0.51 | 0.03 | 220,000 |
| Oldham 8 | 4,500-7,000 | 120 | 108 | 0.46 | 0.036 | 165,000 |
| Oldham 21 | 3,900-5,400 | 90 | 113 | 0.34 | 0.045 | 115,000 |
| Oldham 27 | 2,900-3,200 | 90 | 97 | 0.44 | 0.057 | 100,000 |
| Oldham 24 | 3,300-5,100 | 100 | 102 | 0.6 | 0.048 | 125,000 |
| Oldham 42 | 4,500-6,600 | 115 | 113 | 0.55 | 0.04 | 140,000 |
| Oldham 59 | 4,500-4,900 | 90 | 109 | 0.52 | 0.056 | 90,000 |
| Oldham 62 | 4,900-5,300 | 70 | 116 | 0.36 | 0.061 | 75,000 |
| Oldham 71 | 4,800-6,500 | 110 | 116 | 0.53 | 0.042 | 130,000 |
| Parmer 1 | 6,400-7,800 | 90 | 132 | 0.28 | 0.037 | 125,000 |
| Parmer 9 | 6,700-7,600 | 130 | 135 | 0.56 | 0.026 | 200,000 |
| Potter 14 | 4,000-5,500 | 90 | 105 | 0.25 | 0.038 | 160,000 |
| Potter 34 | 4,100-5,800 | 80 | 107 | 0.48 | 0.056 | 90,000 |
| Potter 43 | 4,900-6,300 | 120 | 115 | 0.45 | 0.03 | 200,000 |
| Randall 15 | 4,700-6,600 | 110 | 121 | 0.6 | 0.04 | 130,000 |
| Roberts 4 | 3,300-4,800 | 60 | 114 | 0.065 | 0.034 | 175,000 |
| Roberts 6 | 3,400-4,800 | 100 | 110 | 0.32 | 0.038 | 150,000 |
| Roberts 17 | 3,600-5,000 | 120 | 116 | 0.37 | 0.03 | 200,000 |
| Roberts 25 | 3,600-4,800 | 120 | 116 | 0.54 | 0.031 | 185,000 |
| Roberts 27 | 3,800-5,100 | 140 | 118 | 0.41 | 0.028 | 225,000 |

Table C-1 (cont.)

| County, log no. | Interval considered (ft) | SP (mV) | T (°F) | Rmf (ohm-m) | Rw (ohm-m) | Estimated TDS (ppm) as NaCl |
|---|---|---|---|---|---|---|
| Roberts 29 | 4,200-5,700 | 110 | 123 | 0.31 | 0.028 | 190,000 |
| Roberts 32 | 4,300-5,700 | 120 | 123 | 0.37 | 0.027 | 200,000 |
| Roberts 44 | 4,200-6,100 | 90 | 111 | 0.36 | 0.035 | 170,000 |
| Sherman 1 | 3,400-4,700 | 60 | 82 | 0.57 | 0.08 | 80,000 |
| Sherman 4 | 2,500-3,300 | 80 | 80 | 0.65 | 0.065 | 110,000 |
| Sherman 16 | 3,000-4,400 | 60 | 82 | 0.79 | 0.09 | 70,000 |
| Sherman 35 | 3,000-4,300 | 100 | 108 | 0.42 | 0.044 | 130,000 |
| Sherman 46 | 2,800-4,200 | 90 | 103 | 0.27 | 0.045 | 135,000 |
| Sherman 47 | 2,600-4,700 | 95 | 98 | 0.33 | 0.038 | 180,000 |
| Sherman 49 | 3,200-4,500 | 100 | 109 | 0.44 | 0.04 | 145,000 |
| Sherman 52 | 3,400-5,000 | 100 | 102 | 0.31 | 0.036 | 180,000 |
| Sherman 60 | 3,300-4,600 | 90 | 106 | 0.28 | 0.04 | 150,000 |
| Swisher 4 | 5,300-6,600 | 110 | 120 | 0.58 | 0.038 | 140,000 |
| Swisher 6 | 5,300-6,500 | 70 | 124 | 0.34 | 0.043 | 110,000 |
| Wheeler 6 | 4,600-6,000 | 110 | 117 | 0.33 | 0.03 | 190,000 |
| Wheeler 31 | 4,100-5,900 | 100 | 119 | 0.33 | 0.034 | 160,000 |
| Wheeler 35 | 4,200-6,200 | 100 | 119 | 0.29 | 0.037 | 170,000 |
| Wheeler 37 | 4,300-6,200 | 100 | 129 | 0.5 | 0.037 | 130,000 |
| Wheeler 51 | 4,500-6,000 | 90 | 121 | 0.33 | 0.035 | 150,000 |
| Wheeler 54 | 4,200-6,500 | 110 | 119 | 0.75 | 0.042 | 125,000 |
| Wheeler 55 | 4,300-6,500 | 110 | 118 | 0.38 | 0.031 | 180,000 |
| Wheeler 57 | 4,600-6,600 | 110 | 121 | 0.7 | 0.042 | 120,000 |
| Wheeler 58 | 4,300-6,500 | 105 | 129 | 0.45 | 0.032 | 155,000 |
| Wheeler 69 | 3,300-6,000 | 90 | 125 | 0.45 | 0.038 | 130,000 |
| Wheeler 81 | 4,400-6,500 | 120 | 130 | 0.42 | 0.027 | 190,000 |

Table C-2. Estimates of TDS (salinity) in the granite-wash deep-basin aquifer obtained from analysis of spontaneous potential logs.

| County, log no. | Interval considered (ft) | SP (mV) | T (°F) | Rmf (ohm-m) | Rw (ohm-m) | Estimated TDS (ppm) as NaCl |
|---|---|---|---|---|---|---|
| Armstrong 8 | 4,600 | 125 | 111 | 0.26 | 0.031 | 200,000 |
| Armstrong 16 | 5,340-5,360 | 98 | 119 | 0.38 | 0.034 | 160,000 |
| Armstrong 21 | 5,700 | 95 | 123 | 0.6 | 0.049 | 90,000 |
| Briscoe 6 | 5,870-5,895 | 103 | 125 | 0.3 | 0.031 | 170,000 |
| Briscoe 7 | 5,650-5,660 | 95 | 122 | 0.33 | 0.035 | 150,000 |
| Briscoe 13 | 7,720-7,740 | 93 | 145 | 0.24 | 0.03 | 150,000 |
| Carson 46 | 5,400 | 105 | 119 | 0.52 | 0.04 | 130,000 |
| Castro 4 | 7,920-7,950 | 70 | 147 | 0.17 | 0.039 | 100,000 |
| Castro 6 | 8,490-8,505 | 115 | 153 | 0.32 | 0.027 | 160,000 |
| Castro 9 | 8,610-8,625 | 110 | 155 | 0.33 | 0.027 | 160,000 |
| Castro 16 | 8,930-8,980 | 120 | 159 | 0.34 | 0.025 | 170,000 |
| Castro 3 | 7,840-7,890 | 92 | 147 | 0.3 | 0.039 | 100,000 |
| Childress 8 | 5,090-5,110 | 80 | 116 | 0.29 | 0.045 | 120,000 |
| Childress 10 | 5,115-5,160 | 55 | 117 | 0.14 | 0.045 | 120,000 |
| Childress 11 | 5,380-5,420 | 75 | 119 | 0.23 | 0.043 | 120,000 |
| Childress 17 | 5,790-5,820 | 95 | 124 | 0.31 | 0.036 | 140,000 |
| Childress 28 | 6,090-6,110 | 80 | 127 | 0.31 | 0.045 | 100,000 |
| Childress 30 | 6,650-6,680 | 110 | 133 | 0.31 | 0.03 | 160,000 |
| Childress 39 | 6,380-6,400 | 80 | 130 | 0.23 | 0.04 | 120,000 |

*Table C-2 (cont.)*

| County, log no. | Interval considered (ft) | SP (mV) | T (°F) | Rmf (ohm-m) | Rw (ohm-m) | Estimated TDS (ppm) as NaCl |
|---|---|---|---|---|---|---|
| Childress 44 | 6,490-6,530 | 65 | 132 | 0.15 | 0.039 | 120,000 |
| Childress 46 | 6,605-6,630 | 60 | 133 | 0.15 | 0.043 | 100,000 |
| Childress 47 | 6,315-6,335 | 70 | 130 | 0.24 | 0.044 | 100,000 |
| Childress 52 | 4,590-4,640 | 65 | 111 | 0.22 | 0.051 | 100,000 |
| Collingsworth 2 | 9,170-9,190 | 110 | 161 | 0.39 | 0.041 | 85,000 |
| Collingsworth 25 | 4,900-4,930 | 73 | 114 | 0.35 | 0.062 | 75,000 |
| Cottle 6 | 6,220-6,250 | 60 | 129 | 0.15 | 0.038 | 130,000 |
| Cottle 9 | 6,760-6,820 | 97 | 135 | 0.3 | 0.034 | 140,000 |
| Cottle 18 | 4,480-4,500 | 65 | 109 | 0.2 | 0.047 | 120,000 |
| Cottle 20 | 6,690-6,720 | 75 | 134 | 0.18 | 0.036 | 130,000 |
| Cottle 25 | 5,150-5,165 | 65 | 117 | 0.26 | 0.052 | 90,000 |
| Cottle 26 | 4,570-4,590 | 105 | 110 | 0.43 | 0.039 | 150,000 |
| Cottle 33 | 5,735-5,775 | 77 | 123 | 0.18 | 0.035 | 150,000 |
| Cottle 34 | 5,670-5,700 | 95 | 123 | 0.3 | 0.035 | 150,000 |
| Cottle 41 | 6,420-6,500 | 80 | 131 | 0.15 | 0.032 | 150,000 |
| Dallam 5 | 4,970-4,990 | 105 | 115 | 0.57 | 0.04 | 140,000 |
| Dallam 20 | 6,500 | 100 | 132 | 0.53 | 0.045 | 95,000 |
| Dallam 22 | 4,735-4,770 | 100 | 112 | 0.53 | 0.042 | 130,000 |
| Dallam 29 | 4,900 | 120 | 114 | 0.63 | 0.037 | 150,000 |
| Dallam 33 | 5,970-5,995 | 130 | 126 | 0.55 | 0.028 | 190,000 |
| Dallam 36 | 5,430-5,455 | 130 | 120 | 0.6 | 0.03 | 180,000 |
| Dallam 39 | 6,180-6,195 | 90 | 128 | 0.31 | 0.038 | 130,000 |
| Dallam 40 | 6,390-6,415 | 84 | 130 | 0.41 | 0.04 | 120,000 |
| Dallam 43 | 6,500-6,550 | 135 | 132 | 0.49 | 0.027 | 190,000 |
| Dallam 44 | 5,410-5,460 | 100 | 120 | 0.4 | 0.036 | 150,000 |
| Dallam 46 | 6,820-6,845 | 140 | 135 | 0.44 | 0.026 | 200,000 |
| Deaf Smith 13 | 8,605-8,635 | 120 | 160 | 0.35 | 0.024 | 170,000 |
| Deaf Smith 15 | 8,820-8,840 | 115 | 162 | 0.36 | 0.026 | 160,000 |
| Dickens 3 | 7,925-7,950 | 70 | 147 | 0.2 | 0.039 | 100,000 |
| Dickens 11 | 6,370-6,380 | 95 | 130 | 0.42 | 0.04 | 120,000 |
| Dickens 31 | 6,770-6,820 | 110 | 135 | 0.33 | 0.03 | 160,000 |
| Donley 3 | 4,200 | 70 | 106 | 0.3 | 0.056 | 95,000 |
| Donley 21 | 3,945-3,960 | 100 | 108 | 0.45 | 0.047 | 120,000 |
| Donley 24 | 5,700 | 120 | 123 | 0.52 | 0.035 | 150,000 |
| Donley 25 | 5,375-5,410 | 110 | 119 | 0.36 | 0.036 | 150,000 |
| Donley 26 | 5,410-5,430 | 90 | 120 | 0.33 | 0.045 | 110,000 |
| Donley 27 | 4,380-4,395 | 60 | 108 | 0.26 | 0.042 | 140,000 |
| Donley 28 | 5,110-5,115 | 75 | 116 | 0.24 | 0.041 | 130,000 |
| Donley 29 | 3,400 | 70 | 98 | 0.4 | 0.062 | 90,000 |
| Donley 31 | 5,125-5,145 | 90 | 116 | 0.4 | 0.045 | 120,000 |
| Donley 32 | 4,825-4,840 | 110 | 113 | 0.57 | 0.04 | 140,000 |
| Donley 36 | 5,125-5,140 | 90 | 116 | 0.3 | 0.036 | 150,000 |
| Donley 38 | 5,425-5,440 | 80 | 120 | 0.18 | 0.034 | 160,000 |
| Floyd 3 | 6,220-6,270 | 115 | 129 | 0.43 | 0.03 | 170,000 |
| Floyd 8 | 9,200 | 40 | 161 | 0.034 | 0.025 | 170,000 |
| Gray 3 | 7,500-7,540 | 40 | 148 | 0.095 | 0.022 | 250,000 |
| Gray 7 | 7,630-7,710 | 133 | 149 | 0.35 | 0.022 | 250,000 |
| Gray 8 | 7,830-7,860 | 95 | 151 | 0.2 | 0.026 | 170,000 |
| Gray 9 | 6,600-6,670 | 110 | 138 | 0.33 | 0.028 | 170,000 |
| Gray 11 | 6,800-6,900 | 100 | 140 | 0.23 | 0.028 | 170,000 |
| Gray 14 | 7,610-7,670 | 100 | 149 | 0.25 | 0.028 | 160,000 |
| Gray 15 | 6,400-6,440 | 130 | 136 | 0.4 | 0.029 | 170,000 |
| Gray 18 | 7,560-7,630 | 120 | 149 | 0.33 | 0.026 | 170,000 |
| Gray 19 | 8,010-8,050 | 110 | 153 | 0.5 | 0.027 | 160,000 |

Table C-2 (cont.)

| County, log no. | Interval considered (ft) | SP (mV) | T (°F) | Rmf (ohm-m) | Rw (ohm-m) | Estimated TDS (ppm) as NaCl |
|---|---|---|---|---|---|---|
| Gray 21 | 8,475-8,500 | 160 | 158 | 0.58 | 0.025 | 170,000 |
| Gray 27 | 6,700-6,770 | 120 | 139 | 0.41 | 0.025 | 200,000 |
| Gray 28 | 8,160-8,230 | 135 | 155 | 0.24 | 0.019 | 300,000 |
| Gray 31 | 6,480-6,650 | 120 | 137 | 0.4 | 0.027 | 180,000 |
| Gray 46 | 8,370-8,430 | 100 | 157 | 0.39 | 0.029 | 140,000 |
| Gray 23 | 6,260-6,320 | 95 | 129 | 0.26 | 0.03 | 170,000 |
| Gray 33 | 8,900-8,990 | 140 | 158 | 0.45 | 0.022 | 200,000 |
| Gray 41 | 6,520-6,670 | 130 | 133 | 0.42 | 0.027 | 190,000 |
| Hall 1 | 4,900-4,945 | 90 | 114 | 0.39 | 0.045 | 120,000 |
| Hall 13 | 6,045-6,075 | 110 | 127 | 0.31 | 0.034 | 150,000 |
| Hall 23 | 6,440-6,490 | 90 | 131 | 0.24 | 0.034 | 140,000 |
| Hall 22 | 5,040-5,120 | 100 | 116 | 0.34 | 0.039 | 140,000 |
| Hansford 26 | 6,190-6,200 | 97 | 128 | 0.35 | 0.036 | 140,000 |
| Hansford 33 | 5,160-5,175 | 90 | 117 | 0.2 | 0.038 | 140,000 |
| Hansford 35 | 5,050-5,090 | 110 | 116 | 0.45 | 0.038 | 140,000 |
| Hansford 38 | 6,095-6,110 | 110 | 127 | 0.28 | 0.029 | 180,000 |
| Hansford 48 | 5,230-5,260 | 100 | 118 | 0.47 | 0.04 | 130,000 |
| Hansford 52 | 4,910-4,980 | 120 | 114 | 0.58 | 0.036 | 160,000 |
| Hansford 58 | 5,500-5,510 | 100 | 121 | 0.4 | 0.038 | 140,000 |
| Hansford 59 | 5,465-5,480 | 90 | 120 | 0.29 | 0.038 | 140,000 |
| Hansford 84 | 4,800-4,910 | 120 | 113 | 0.58 | 0.036 | 160,000 |
| Hansford 85 | 5,010-5,020 | 115 | 115 | 0.55 | 0.039 | 140,000 |
| Hansford 86 | 5,155-5,200 | 110 | 117 | 0.56 | 0.038 | 140,000 |
| Hansford 93 | 5,260-5,310 | 82 | 118 | 0.33 | 0.043 | 120,000 |
| Hansford 94 | 5,200-5,250 | 100 | 117 | 0.38 | 0.036 | 150,000 |
| Hansford 103 | 5,120-5,180 | 105 | 117 | 0.4 | 0.035 | 160,000 |
| Hansford 104 | 5,140-5,210 | 105 | 117 | 0.45 | 0.039 | 140,000 |
| Hansford 105 | 5,175-5,260 | 100 | 117 | 0.26 | 0.033 | 170,000 |
| Hansford 108 | 4,765-4,790 | 100 | 113 | 0.4 | 0.038 | 150,000 |
| Hansford 122 | 4,850-4,870 | 90 | 113 | 0.27 | 0.038 | 150,000 |
| Hansford 124 | 4,930-4,980 | 90 | 115 | 0.31 | 0.04 | 140,000 |
| Hansford 110 | 5,280-5,310 | 120 | 118 | 0.58 | 0.035 | 160,000 |
| Hansford 118 | 5,780-5,800 | 100 | 124 | 0.32 | 0.039 | 130,000 |
| Hansford 119 | 4,750-4,775 | 117 | 112 | 0.52 | 0.034 | 170,000 |
| Hansford 133 | 5,375-5,450 | 100 | 120 | 0.29 | 0.034 | 160,000 |
| Hansford 138 | 5,080-5,110 | 100 | 116 | 0.5 | 0.045 | 120,000 |
| Hartley 1 | 6,470-6,480 | 115 | 136 | 0.6 | 0.032 | 150,000 |
| Hartley 2 | 6,110-6,190 | 110 | 133 | 0.6 | 0.027 | 190,000 |
| Hartley 7 | 7,370-7,400 | 100 | 146 | 0.42 | 0.04 | 100,000 |
| Hartley 10 | 6,500 | 100 | 132 | 0.34 | 0.033 | 150,000 |
| Hartley 16 | 6,610-6,670 | 120 | 138 | 0.37 | 0.028 | 170,000 |
| Hartley 17 | 6,580-6,690 | 120 | 138 | 0.4 | 0.028 | 170,000 |
| Hartley 23 | 6,450-6,570 | 120 | 137 | 0.45 | 0.028 | 170,000 |
| Hartley 24 | 6,780-6,830 | 115 | 132 | 0.41 | 0.031 | 160,000 |
| Hartley 25 | 6,310-6,550 | 110 | 136 | 0.35 | 0.034 | 140,000 |
| Hartley 26 | 6,430-6,680 | 110 | 136 | 0.4 | 0.031 | 160,000 |
| Hartley 33 | 6,400 | 130 | 130 | 0.35 | 0.027 | 200,000 |
| Hartley 34 | 7,660-7,740 | 120 | 149 | 0.55 | 0.031 | 140,000 |
| Hartley 37 | 6,500-6,580 | 115 | 132 | 0.36 | 0.028 | 180,000 |
| Hartley 39 | 6,870-6,900 | 100 | 138 | 0.45 | 0.028 | 170,000 |
| Hartley 61 | 7,540-7,580 | 107 | 148 | 0.37 | 0.029 | 150,000 |
| Hartley 85 | 5,900 | 85 | 125 | 0.29 | 0.041 | 120,000 |
| Hartley 86 | 5,960-6,000 | 80 | 131 | 0.44 | 0.044 | 100,000 |
| Hartley 89 | 6,100 | 100 | 127 | 0.34 | 0.041 | 120,000 |

*Table C-2 (cont.)*

| County, log no. | Interval considered (ft) | SP (mV) | T (°F) | Rmf (ohm-m) | Rw (ohm-m) | Estimated TDS (ppm) as NaCl |
|---|---|---|---|---|---|---|
| Hemphill 11 | 5,500 | 125 | 121 | 0.44 | 0.031 | 180,000 |
| Hemphill 32 | 5,900 | 120 | 125 | 0.42 | 0.031 | 170,000 |
| Hemphill 42 | 9,600 | 135 | 166 | 0.28 | 0.021 | 200,000 |
| Hemphill 43 | 10,000 | 150 | 170 | 0.41 | 0.021 | 200,000 |
| Hutchinson 1 | 5,380-5,400 | 120 | 124 | 0.48 | 0.036 | 140,000 |
| Hutchinson 4 | 5,170-5,210 | 80 | 122 | 0.45 | 0.042 | 120,000 |
| Hutchinson 10 | 5,470-5,490 | 110 | 125 | 0.45 | 0.03 | 180,000 |
| Hutchinson 11 | 5,450-5,470 | 80 | 125 | 0.23 | 0.036 | 140,000 |
| Hutchinson 13 | 6,560-6,580 | 80 | 137 | 0.22 | 0.036 | 130,000 |
| Hutchinson 15 | 6,440-6,470 | 75 | 136 | 0.18 | 0.034 | 140,000 |
| Hutchinson 16 | 6,300-6,320 | 105 | 134 | 0.27 | 0.029 | 170,000 |
| Hutchinson 17 | 6,500 | 90 | 132 | 0.28 | 0.036 | 130,000 |
| Hutchinson 18 | 6,180-6,300 | 115 | 134 | 0.34 | 0.028 | 180,000 |
| Hutchinson 19 | 6,100 | 110 | 127 | 0.36 | 0.03 | 170,000 |
| Hutchinson 23 | 6,180-6,420 | 120 | 134 | 0.35 | 0.03 | 160,000 |
| Hutchinson 25 | 5,490-6,040 | 130 | 128 | 0.51 | 0.036 | 140,000 |
| Hutchinson 28 | 6,320-6,450 | 160 | 135 | 0.51 | 0.026 | 190,000 |
| Hutchinson 29 | 6,360-6,370 | 115 | 135 | 0.4 | 0.028 | 170,000 |
| Hutchinson 30 | 5,190-5,230 | 110 | 122 | 0.43 | 0.037 | 140,000 |
| Hutchinson 31 | 5,340-5,360 | 90 | 124 | 0.26 | 0.034 | 150,000 |
| Hutchinson 32 | 5,950-6,020 | 100 | 131 | 0.34 | 0.03 | 170,000 |
| Hutchinson 33 | 6,880-6,920 | 120 | 141 | 0.45 | 0.028 | 170,000 |
| Hutchinson 40 | 5,910-5,960 | 45 | 131 | 0.09 | 0.04 | 120,000 |
| Hutchinson 60 | 5,750-5,780 | 100 | 128 | 0.41 | 0.036 | 140,000 |
| Hutchinson 62 | 6,210-6,310 | 115 | 134 | 0.45 | 0.029 | 170,000 |
| King 41 | 5,160-5,190 | 98 | 117 | 0.35 | 0.036 | 150,000 |
| Lipscomb 4 | 5,780-5,800 | 120 | 124 | 0.54 | 0.033 | 160,000 |
| Lipscomb 11 | 5,930-6,000 | 80 | 126 | 0.18 | 0.034 | 150,000 |
| Lipscomb 25 | 6,580-6,600 | 105 | 132 | 0.36 | 0.034 | 140,000 |
| Lipscomb 31 | 6,140-6,330 | 105 | 129 | 0.32 | 0.032 | 160,000 |
| Lipscomb 33 | 6,240-6,330 | 120 | 129 | 0.39 | 0.029 | 180,000 |
| Lipscomb 44 | 6,330-6,450 | 130 | 130 | 0.45 | 0.028 | 180,000 |
| Lipscomb 46 | 6,390-6,460 | 103 | 131 | 0.34 | 0.032 | 150,000 |
| Lipscomb 50 | 6,435-6,530 | 90 | 131 | 0.23 | 0.032 | 150,000 |
| Lipscomb 53 | 6,330-6,440 | 110 | 130 | 0.35 | 0.031 | 160,000 |
| Lipscomb 58 | 6,770-6,820 | 120 | 135 | 0.32 | 0.028 | 180,000 |
| Moore 14 | 5,320-5,330 | 110 | 124 | 0.5 | 0.034 | 150,000 |
| Moore 17 | 5,850-5,880 | 130 | 130 | 0.51 | 0.028 | 180,000 |
| Moore 20 | 6,250-6,280 | 130 | 129 | 0.6 | 0.028 | 180,000 |
| Moore 28 | 5,580-5,630 | 95 | 122 | 0.48 | 0.037 | 140,000 |
| Moore 34 | 5,835-5,860 | 105 | 124 | 0.45 | 0.028 | 200,000 |
| Motley 3 | 7,185-7,210 | 105 | 139 | 0.33 | 0.027 | 180,000 |
| Motley 4 | 7,400-7,415 | 100 | 141 | 0.32 | 0.032 | 140,000 |
| Motley 5 | 7,170-7,215 | 105 | 139 | 0.35 | 0.033 | 140,000 |
| Motley 7 | 7,645-7,670 | 83 | 144 | 0.22 | 0.034 | 130,000 |
| Ochiltree 9 | 6,080-6,100 | 128 | 127 | 0.51 | 0.029 | 180,000 |
| Ochiltree 24 | 5,730-5,750 | 67 | 123 | 0.13 | 0.034 | 150,000 |
| Ochiltree 25 | 5,710-5,750 | 92 | 123 | 0.4 | 0.042 | 120,000 |
| Ochiltree 26 | 5,810-5,840 | 78 | 124 | 0.2 | 0.036 | 140,000 |
| Ochiltree 28 | 5,980-6,000 | 110 | 126 | 0.45 | 0.034 | 150,000 |
| Ochiltree 29 | 5,970-6,030 | 110 | 126 | 0.4 | 0.032 | 160,000 |
| Ochiltree 31 | 5,690-5,830 | 120 | 123 | 0.5 | 0.033 | 160,000 |
| Ochiltree 42 | 5,775-5,910 | 130 | 124 | 0.35 | 0.028 | 200,000 |
| Ochiltree 44 | 6,210-6,300 | 120 | 129 | 0.36 | 0.028 | 180,000 |
| Ochiltree 45 | 6,220-6,390 | 120 | 129 | 0.4 | 0.029 | 180,000 |

*Table C-2 (cont.)*

| County, log no. | Interval considered (ft) | SP (mV) | T (°F) | Rmf (ohm-m) | Rw (ohm-m) | Estimated TDS (ppm) as NaCl |
|---|---|---|---|---|---|---|
| Ochiltree 46 | 6,350-6,440 | 120 | 130 | 0.43 | 0.03 | 170,000 |
| Ochiltree 47 | 6,000-6,100 | 125 | 127 | 0.43 | 0.029 | 180,000 |
| Ochiltree 49 | 5,780-5,930 | 120 | 124 | 0.53 | 0.033 | 160,000 |
| Ochiltree 55 | 6,085-6,180 | 100 | 127 | 0.3 | 0.032 | 160,000 |
| Ochiltree 56 | 6,280-6,360 | 120 | 130 | 0.4 | 0.028 | 180,000 |
| Ochiltree 59 | 6,335-6,460 | 120 | 130 | 0.43 | 0.03 | 170,000 |
| Oldham 8 | 6,800 | 125 | 135 | 0.36 | 0.036 | 130,000 |
| Oldham 24 | 5,480-5,510 | 100 | 125 | 0.47 | 0.042 | 120,000 |
| Oldham 36 | 6,280-6,370 | 120 | 130 | 0.34 | 0.027 | 200,000 |
| Oldham 49 | 7,560-7,620 | 95 | 143 | 0.27 | 0.03 | 150,000 |
| Parmer 1 | 8,570-8,750 | 95 | 155 | 0.24 | 0.028 | 150,000 |
| Parmer 9 | 8,450-8,490 | 120 | 153 | 0.45 | 0.028 | 150,000 |
| Potter 12 | 6,370-6,420 | 70 | 128 | 0.29 | 0.06 | 70,000 |
| Potter 14 | 5,710-5,720 | 70 | 123 | 0.21 | 0.046 | 100,000 |
| Potter 27 | 5,500 | 100 | 125 | 0.46 | 0.041 | 120,000 |
| Potter 43 | 6,925-6,940 | 115 | 141 | 0.35 | 0.027 | 180,000 |
| Randall 13 | 7,505-7,525 | 135 | 148 | 0.35 | 0.024 | 200,000 |
| Randall 14 | 7,200 | 130 | 139 | 0.47 | 0.027 | 180,000 |
| Randall 22 | 8,200 | 110 | 150 | 0.26 | 0.025 | 180,000 |
| Randall 23 | 7,705-7,770 | 115 | 150 | 0.25 | 0.025 | 180,000 |
| Roberts 1 | 5,300-5,500 | 65 | 126 | 0.13 | 0.036 | 140,000 |
| Roberts 5 | 6,050-6,170 | 110 | 132 | 0.44 | 0.033 | 150,000 |
| Roberts 6 | 6,090-6,120 | 110 | 132 | 0.27 | 0.028 | 180,000 |
| Roberts 11 | 6,400-6,450 | 90 | 136 | 0.36 | 0.034 | 140,000 |
| Roberts 25 | 7,500-7,560 | 120 | 148 | 0.4 | 0.025 | 180,000 |
| Roberts 27 | 6,010-6,040 | 150 | 131 | 0.25 | 0.022 | 300,000+ |
| Roberts 32 | 8,670-8,690 | 110 | 160 | 0.27 | 0.025 | 170,000 |
| Roberts 34 | 8,380-8,450 | 120 | 158 | 0.32 | 0.024 | 180,000 |
| Roberts 38 | 8,570-8,710 | 120 | 160 | 0.24 | 0.024 | 180,000 |
| Sherman 1 | 4,675-4,725 | 100 | 112 | 0.41 | 0.036 | 160,000 |
| Sherman 4 | 4,920-4,930 | 120 | 114 | 0.45 | 0.032 | 180,000 |
| Sherman 8 | 5,995-6,020 | 102 | 126 | 0.39 | 0.035 | 150,000 |
| Sherman 14 | 5,790-5,805 | 110 | 124 | 0.24 | 0.028 | 200,000 |
| Sherman 16 | 4,400 | 110 | 108 | 0.59 | 0.032 | 200,000 |
| Sherman 17 | 4,220-4,270 | 140 | 107 | 0.65 | 0.03 | 240,000 |
| Sherman 26 | 4,380-4,430 | 130 | 108 | 0.49 | 0.034 | 180,000 |
| Sherman 27 | 4,600 | 90 | 111 | 0.26 | 0.037 | 160,000 |
| Sherman 49 | 5,820-5,840 | 105 | 124 | 0.36 | 0.031 | 170,000 |
| Sherman 50 | 5,200 | 115 | 117 | 0.36 | 0.032 | 180,000 |
| Sherman 59 | 6,000 | 120 | 126 | 0.39 | 0.027 | 200,000 |
| Swisher 3 | 7,580-7,600 | 120 | 148 | 0.27 | 0.024 | 190,000 |
| Swisher 4 | 8,425-8,450 | 125 | 153 | 0.42 | 0.026 | 170,000 |
| Wheeler 1 | 8,730-8,780 | 160 | 161 | 0.4 | 0.018 | 300,000 |
| Wheeler 2 | 7,900-7,970 | 155 | 152 | 0.62 | 0.022 | 220,000 |
| Wheeler 4 | 9,200 | 130 | 161 | 0.32 | 0.021 | 220,000 |
| Wheeler 17 | 9,100 | 140 | 160 | 0.39 | 0.022 | 200,000 |
| Wheeler 20 | 8,900 | 130 | 158 | 0.43 | 0.024 | 180,000 |
| Wheeler 23 | 9,985-10,020 | 108 | 175 | 0.12 | 0.017 | 280,000 |
| Wheeler 31 | 8,300 | 100 | 151 | 0.25 | 0.028 | 150,000 |
| Wheeler 35 | 6,390-6,430 | 90 | 136 | 0.25 | 0.034 | 140,000 |
| Wheeler 40 | 6,900 | 125 | 136 | 0.5 | 0.03 | 160,000 |
| Wheeler 41 | 6,300 | 115 | 129 | 0.5 | 0.034 | 150,000 |
| Wheeler 45 | 6,900 | 105 | 136 | 0.46 | 0.033 | 140,000 |
| Wheeler 54 | 5,700-5,730 | 120 | 128 | 0.68 | 0.038 | 130,000 |
| Wheeler 55 | 7,450-7,490 | 110 | 147 | 0.3 | 0.026 | 180,000 |